UNIVERSIDADE ESTADUAL DO SUDOESTE DA BAHIA
PROGRAMA DE PÓS-GRADUAÇÃO EM ENGENHARIA E CIÊNCIA DE ALIMENTOS
Área de concentração: Engenharia de Alimentos

PRISCILLA AMARAL NASCIMENTO

BIORREATORES COM LIPASE IMOBILIZADA: EFEITO DA MODIFICAÇÃO DOS SUPORTES E SUA APLICAÇÃO NA INDÚSTRIA DE ALIMENTOS

ITAPETINGA – BAHIA
FEVEREIRO, 2024

PRISCILLA AMARAL NASCIMENTO

BIORREATORES COM LIPASE IMOBILIZADA: EFEITO DA MODIFICAÇÃO DOS SUPORTES E SUA APLICAÇÃO NA INDÚSTRIA DE ALIMENTOS

Tese apresentada como parte das exigências para obtenção do título de doutorado em Engenharia e Ciência de Alimentos, área de concentração em Engenharia de Alimentos, da Universidade Estadual do Sudoeste da Bahia – UESB.

Orientadora: Prof.ª Dra. Cristiane Martins Veloso

Coorientadores: Prof.ª Dra. Renata Cristina Ferreira Bonomo

Prof. Dr. Leandro Soares Santos

Prof. Dr. Rafael da Costa Ilhéu Fontan

ITAPETINGA – BAHIA

FEVEREIRO, 2024

660.634
N197b

Nascimento, Priscilla Amaral.

Biorreatores com lipase imobilizada: efeito da modificação dos suportes e sua aplicação na indústria de alimentos. / Priscilla Amaral Nascimento. – Itapetinga-BA: UESB, 2024.

147f.

Tese apresentada como parte das exigências para obtenção do título de doutorado em Engenharia e Ciência de Alimentos, área de concentração em Engenharia de Alimentos, da Universidade Estadual do Sudoeste da Bahia – UESB. Sob a orientação da Prof.ª D. Sc. Cristiane Martins Veloso e coorientação da Prof.ª D. Sc. Renata Cristina Ferreira, Prof. D. Sc. Leandro Soares Santos e Prof. D. Sc. Rafael da Costa Ilhéu Fontan.

1. Enzima imobilizada – Carvão ativado. 2. Carvão ativado – Enzima – Resíduos agroindustriais. 3. Biorreator – Enzima imobilizada. I. Universidade Estadual do Sudoeste da Bahia – Programa de Pós-Graduação de Doutorado em Engenharia e Ciências de Alimentos, C*ampus* de Itapetinga. II. Veloso, Cristiane Martins. III. Bonomo, Renata Cristina Ferreira. IV. Santos, Leandro Soares. V. Fontan, Rafael da Costa Ilhéu. VI. Título.

CDD(21): 660.634

Catalogação na Fonte:
Adalice Gustavo da Silva – CRB 535-5ª Região
Bibliotecária – UESB – Campus de Itapetinga-BA

Índice Sistemático para desdobramentos por Assunto:

1. Indústria de alimentos – Biorreatores – Enzima imobilizada

PPGECAL
ENGENHARIA E CIÊNCIA DE ALIMENTOS
UESB
Universidade Estadual do Sudoeste da Bahia – UESB
Recredenciada pelo Decreto Estadual
N° 16.825, de 04.07.2016

Governo do Estado da Bahia

DECLARAÇÃO DE APROVAÇÃO

Título: "BIORREATORES COM LIPASE IMOBILIZADA: EFEITO DA MODIFICAÇÃO DOS SUPORTES E SUA APLICAÇÃO NA INDÚSTRIA DE ALIMENTOS"

Autor (a): **PRISCILLA AMARAL NASCIMENTO**

Orientador (a): Prof.ª Dr.ª Cristiane Martins Veloso

Coorientador (a): Prof.ª Dr.ª Renata Cristina Ferreira Bonomo

Prof. Dr. Leandro Soares Santos

Prof. Dr. Rafael da Costa Ilhéu Fontan

Aprovada como parte das exigências para obtenção do Título de *DOUTORA EM ENGENHARIA E CIÊNCIA DE ALIMENTOS, ÁREA DE CONCENTRAÇÃO: ENGENHARIA DE ALIMENTOS*, pela Banca Examinadora.

gov.br Documento assinado digitalmente
MATEUS PEREIRA FLORES SANTOS
Data: 04/03/2024 19:21:28-0300
Verifique em https://validar.iti.gov.br

Dr. Mateus Pereira Flores Santos
(PÓS/DOC- UESC)

gov.br Documento assinado digitalmente
MYLENA JUNQUEIRA PINTO BRITO
Data: 04/03/2024 20:36:03-0300
Verifique em https://validar.iti.gov.br

Dr.ª Mylena Junqueira Pinto Brito
(Membro Externo /EMBASA)

gov.br Documento assinado digitalmente
RENATA CRISTINA FERREIRA BONOMO
Data: 05/03/2024 09:51:43-0300
Verifique em https://validar.iti.gov.br

Prof.ª Dr.ª Renata Cristina Ferreira Bonomo
(UESB)

gov.br Documento assinado digitalmente
LEANDRO SOARES SANTOS
Data: 05/03/2024 16:39:25-0300
Verifique em https://validar.iti.gov.br

Prof. Dr. Leandro Soares Santos
(UESB)

gov.br Documento assinado digitalmente
CRISTIANE MARTINS VELOSO
Data: 04/03/2024 19:11:28-0300
Verifique em https://validar.iti.gov.br

Prof.ª Dr.ª Cristiane Martins Veloso
Orientadora - UESB
Presidente da Banca

Itapetinga-BA, 22 de fevereiro de 2024.

“Adventure is worthwhile in itself.”
(Amelia Earhart)

A Deus

Aos meus pais

Aos meus irmãos

Ao meu sobrinho

Dedico!

AGRADECIMENTOS

Agradeço primeiramente a Deus, pela proteção, amparo nos momentos difíceis e por mostrar que sou forte o suficiente para vencer qualquer obstáculo.
Aos meus amados pais, Maria e Ademir, pelo amor incondicional, por não medirem esforços para me ver feliz e sempre acreditarem em mim, mesmo quando nem eu mesma acreditei.
Aos meus irmãos, Artur e Natália, por serem meus melhores amigos e companheiros de vida.
À Emanuel, por ser a luz dos meus dias e transformar tudo desde que chegou. Já não me lembro como era a vida sem você.
À Adolfo, por ser meu porto seguro e maior incentivador. Meu amor, você me dá sorte!
Aos meus cunhados Lis e Celso, pela relação de família construída por opção mútua.
À minha orientadora Cristiane Veloso, pela excelente orientação, ensinamentos, compreensão, confiança e paciência em minhas empreitadas. Foi um prazer ser sua orientada!
À Renata Bonomo, pelo laço criado e fortalecido que ultrapassou as barreiras acadêmicas e contribuiu para que me tornasse a pessoa e profissional que sou hoje.
À Jéssica, por se tornar uma amiga/irmã durante esses anos. Da rotina compartilhada no grupo de pesquisa e na vida, você tornou tudo mais leve e prazeroso! Obrigada por tudo!
Aos amigos de Nanuque e Ouro Branco, em especial à Luiz Henrique, Kalythea, Nathália, Maria Júlia, Alan e meninas da república Pirei, por sempre se fazerem presentes, apoiando e torcendo por cada passo dado. A amizade de vocês é um privilégio!
Aos familiares, pelo carinho e preocupação.
Aos co-orientadores Rafael Fontan e Leandro Soares, pelas sugestões, apoio e incentivo para o desenvolvimento do trabalho.
Aos integrantes da banca examinadora, por aceitarem fazer parte da avalição desse trabalho.
Ao grupo de pesquisa em carvão ativado, pela proatividade e disponibilidade em todos os momentos. Em especial à Mateus, Mylena e Thayná.
Aos colegas do Laboratório de Engenharia de Processos, pela troca de conhecimento, carinho e momentos de descontração. Em especial, à Jonathan, Izabella e Annie.
Ao Programa de Doutorado Sanduíche no Exterior (PDSE-CAPES) e à Deakin University, pela melhor e mais desafiadora experiência da minha vida. Um agradecimento especial aos meus supervisores Wenrong Yang e Motilal Mathesh por todas as contribuições positivas na realização do projeto de pesquisa.

Aos colegas da Escola de Ciências Ambientais e da vida (Deakin University), pelos ensinamentos e acolhimento tão genuínos, em especial à Brendan, Asavari, Dulini, Vahide e Mengchi.

Aos amigos de intercâmbio, por se tornarem minha família do outro lado do oceano, em especial à Arshi, Chanchal, Nina, Glaucimar, Glenda, Luís, Igor, Carol e Karin.

À Universidade Estadual do Sudoeste da Bahia (UESB) e ao Programa de Pós-Graduação em Engenharia e Ciência de Alimentos pela oportunidade e por fornecerem as condições de trabalho necessárias para que a obtenção do título de doutorado.

Ao Conselho Nacional de Desenvolvimento Científico e Tecnológico (CNPq) pela bolsa concedida e à CAPES pelo auxílio ao experimento.

A todos que não foram citados, mas contribuíram de forma significativa para a realização desse trabalho.

MUITO OBRIGADA!

ÍNDICE

LISTA DE FIGURAS

CAPÍTULO 1

CAPÍTULO 2

CAPÍTULO 3

CAPÍTULO 4

LISTA DE TABELAS

CAPÍTULO 1

CAPÍTULO 2

CAPÍTULO 3

CAPÍTULO 4

RESUMO

NASCIMENTO, P.A. **Biorreatores com lipase imobilizada: efeito da modificação dos suportes e sua aplicação na indústria de alimentos.** Itapetinga – BA: UESB, 2024. 147 p. (Tese – Doutorado em Engenharia e Ciência de Alimentos). *

As lipases são enzimas que constituem um importante grupo destinado a aplicações biotecnológicas por catalisar reações de hidrólise, esterificação e transesterificação. No entanto, o emprego de enzimas livres em nível comercial ainda é limitado pela sua baixa estabilidade e reuso, o que dificulta sua aplicação em processos contínuos e no aumento de escala. Uma proposta viável capaz de solucionar tais limitações é a utilização da enzima na forma imobilizada. Nesse sentido, pode-se apontar o carvão ativado como um suporte promissor por possuir elevada área superficial, porosidade e pela possibilidade de síntese a partir de resíduos agroindustriais. Dentro desse contexto, o presente trabalho teve como objetivo produzir biorreatores por meio da imobilização de lipase em carvão ativado sintetizado a partir do resíduo de sisal e submetido a diferentes métodos de modificação, investigando o potencial dos derivados mais promissores em sintetizar lactato de etila e acilgliceróis ricos em ômega-3. As condições ótimas de síntese do carvão ativado foram determinadas utilizando-se o Delineamento Composto Central Rotacional (DCCR), empregando como variáveis independentes o tempo e a temperatura de carbonização, e como variáveis resposta a atividade e recuperação enzimática, onde os maiores valores alcançados foram 42,90 U e 60,59 %, respectivamente. O tempo e a temperatura ótimos de síntese foram definidos a partir da derivada parcial da equação de regressão (86 min e 700 ºC) e aplicados aos experimentos subsequentes. O efeito das modificações de superfície do carvão ativado foi investigado a partir da incorporação de genipina (GAC), ácido iminodiacético + partículas metálicas (MAC) e genipina + partículas metálicas (GMAC) na imobilização de lipases do pâncreas do porco (PPL) e *Candida rugosa* (CRL). Todos os suportes apresentaram alta eficiência de imobilização (E > 87 %), onde os carvões ativados metalizados apresentaram maior atividade de hidrólise (MAC = 47.3 U e GMAC = 51.6 U para CRL). Os derivados apresentaram resultados promissores para a síntese de lactato de etila (Y > 90 %) e o suporte metalizado teve o maior rendimento após os ciclos de reuso (86,16 % para PPL e 88,46 % para CRL). Além disso, o efeito das condições de glicerólise utilizando o derivado produzido foi avaliado de acordo com a concentração enzimática, concentração de suporte, razão molar de substrato e tempo de reação, tendo a conversão de ácido graxo livre como variável resposta. Os parâmetros ótimos foram 15 mg g^{-1} (enzima/suporte), 8 % de derivativo (m/v), 1:5 de glicerol:óleo e 24 h de reação. Foram obtidos 8,08 % de ácidos graxos livres com composição de ácidos graxos n-3 PUFAs de 42,28 %, após o tratamento enzimático do óleo residual de lula. O carvão ativado do resíduo do sisal funcionalizado por diferentes métodos de modificação tem potencial para aplicação em processos de imobilização de lipases para aplicação na obtenção de ingredientes alimentícios, como o lactato de etila e acilgliceróis de ômega-3.

Palavras-chave: Carvão ativado; Esterificação; Glicerólise; Lactato de etila; Ômega-3.

Orientador (a): DSc. UESB. Cristiane Martins Veloso; Co-orientador: DSc. UESB. Renata Cristina Ferreira Bonomo; DSc. UESB. Leandro Soares Santos; DSc. UESB. Rafael da Costa Ilhéu Fontan.

SUMMARY

NASCIMENTO, P.A. **Bioreactors through immobilized lipase: effect of support modification and their application in the food industry.** Itapetinga – BA: UESB, 2024. 147 p. (Thesis – Doctorate in Food Science and Engineering).*

Lipases are enzymes that catalyze hydrolysis, esterification, and transesterification reactions. However, the low stability and reusability of free enzymes make it difficult to use them in continuous processes and scale-up. One strategy that can reduce such limitations is enzyme immobilization. Therefore, activated carbon is a valuable support material due to its high BET surface area, porosity, and synthesis through agro-industrial waste. This work aimed to produce bioreactors through lipase immobilization in activated carbon synthesized from sisal waste and functionalized by different modification methods, investigating the potential of promising derivatives to synthesize ethyl lactate and omega-3 acylglycerols. The optimal conditions were determined by the Central Composite Design (CCD) and Response Surface Methodology (RSM) through carbonization time and temperature as independent variables, and Enzyme activity and Recovery as response variables. The highest Enzyme activity and Recovery were 42.90 U and 60.59 %, respectively. The optimal time and temperature were calculated by the partial derivative of regression equations (86 minutes and 700 ºC) and they were applied in the following experiments. The effect of activated carbon surface modifications was investigated based on the incorporation of genipin (GAC), iminodiacetic acid + metallic particles (MAC), and genipin + metallic particles (GMAC) for lipase immobilization (porcine pancreas lipase (PPL) and *Candida rugosa* lipase (CRL)). All the adsorbents showed high immobilization efficiency (E > 87 %), with the metalized-activated carbons presenting the highest hydrolysis activity (MAC = 46.9 U and GMAC = 48.1 U for PPL and MAC = 47.3 U and GMAC = 51.6 U for CRL). The biocatalysts have reported promising results for the synthesis of ethyl lactate (Y > 90 %). The high ester conversion after five cycles suggested that the immobilization process efficiently protected the lipase from desorption, and the metalized supports had the highest yield in the last cycle (MAC = 86.16 % for PPL and MAC = 88.46 % for CRL). The effect of glycerolysis conditions was evaluated according to enzyme concentration, support concentration, substrate molar ratio, and reaction time with the conversion of Free Fatty Acid as the response variable. The optimal parameters were 15 mg g^{-1} support, 8 % of derivative (w/v), 1:5 of glycerol:oil, and 24 hours. The squid waste oil obtained Free Fatty Acid (%) = 8.08 % and n-3 PUFAs fatty acid composition = 42.28 % after enzymatic treatment. The microcapsules synthesized through microencapsulation by complex coacervation showed unexpectedly high oxidative stability (OSI = 52.35 h) compared to untreated (OSI = 0.04 h) and lipase-treated oil (OSI = 2.46 h). Activated carbon from sisal waste has the potential to immobilize lipases and it can be applied as a biocatalyst to synthesize ethyl lactate and produce omega-3 acylglycerols.

Keywords: Activated carbon; Esterification; Ethyl lactate; Glycerolysis; Omega-3.

Supervisor: DSc. UESB. Cristiane Martins Veloso; Co-supervisor: DSc. UESB. Renata Cristina Ferreira Bonomo; DSc. UESB. Leandro Soares Santos; DSc. UESB. Rafael da Costa Ilhéu Fontan.

CAPÍTULO 1

INTRODUÇÃO

REFERENCIAL TEÓRICO

OBJETIVOS

---

1. INTRODUÇÃO

A busca por processos alternativos aplicáveis na síntese de compostos de interesse industrial intensificou-se nos últimos anos, onde a síntese enzimática oferece grande potencial frente à síntese química por apresentar inúmeros benefícios envolvendo seletividade, biocompatibilidade, biodegradabilidade e aceitabilidade ambiental. Por esse motivo, o uso de enzimas na biocatálise é uma das áreas que apresenta maior crescimento nos últimos anos (MELO et al., 2023; SINGH et al., 2024; WU et al., 2021).

As enzimas são biocatalisadores de origem proteica responsáveis por acelerar a velocidade das reações. Dentre as variedades existentes, a lipase se destaca por catalisar diversos processos produtivos devido à sua versatilidade e especificidade, tanto em meio aquoso quanto em meio orgânico, como na catálise de reações de hidrólise de triacilgliceróis e esterificação (PEREIRA et al., 2022; VERMA et al., 2021). No entanto, o emprego de enzimas livres em nível comercial ainda é limitado pela baixa estabilidade, reuso e elevado custo de isolamento e purificação, o que limita sua aplicação em processos contínuos e no aumento de escala (MONTEIRO et al., 2021; ROMERO-FERNÁNDEZ e PARADISI, 2020; SAMPAIO et al., 2022; SOUSA et al., 2021). Uma proposta viável capaz de solucionar tais limitações é a utilização da enzima na forma imobilizada.

A imobilização consiste no confinamento de biocompostos, com retenção da atividade biológica e estabilidade, destacando como principais características: simplicidade de execução, baixo custo operacional e facilidade de recuperação e reutilização da molécula (ALMEIDA; PRATA; FORTE, 2022; RODRIGUES et al., 2021). Dos métodos de imobilização existentes, a adsorção é apontada como uma técnica vantajosa em função da facilidade de execução, baixo custo e possibilidade de regeneração da matriz. Além disso, exerce poucos efeitos na estrutura conformacional das moléculas e no sítio ativo enzimático por envolverem interações de menor energia e especificidade quando comparadas às ligações irreversíveis, quando empregado o suporte adequado. Dentre os suportes com potencial para aplicação no processo de imobilização, o carvão ativado tem sido bastante estudado devido às suas propriedades físico-químicas (ARANA-PEÑA et al., 2021; SANTOS et al., 2022).

O carvão ativado (CA) é um material carbonáceo de estrutura altamente porosa obtida através da ativação e queima controlada da biomassa precursora de carbono. Dentre as variedades de matérias-primas empregadas, os resíduos agroindustriais apresentam grande potencial para a síntese de carvões ativados devido ao elevado teor de carbono e elevada diversidade e disponibilidade, permitindo produzir suportes com melhor custo-

benefício quando comparados aos suportes convencionais, além de minimizar impactos ambientais por envolver um processamento mais sustentável (ALVEAR-DAZA et al., 2022; GIRELLI et al., 2020; GOMEZ-DELGADO et al., 2022; SANDOVAL-GONZÁLEZ et al., 2022).

A síntese do carvão ativado envolve dois processos principais: ativação química/física e carbonização do material precursor. Tais etapas são responsáveis pelo desenvolvimento das características do adsorvente, como área superficial, distribuição e tamanho de poros. Apesar das diversas vantagens relatadas, a aplicação da técnica demonstra inconvenientes para a imobilização enzimática quanto às restrições difusionais de substrato e dos produtos, aleatoriedade e força da interação enzima-suporte (HASANZADEH et al., 2020; RATHER et al., 2022). Algumas alternativas a essas limitações são a modificação das propriedades texturais a partir da otimização das condições de síntese, como o tempo e temperatura de carbonização, e as funcionalizações de superfície a partir da incorporação de agentes reticulantes e/ou partículas metálicas. Nesse sentido, a utilização de genipina como agente reticulante e partículas metálicas de ferro podem ser apontadas como métodos de modificação dos suportes, onde a ligação covalente e a interação iônica, respectivamente, são os mecanismos de imobilização (BAYRAMOGLU et al., 2022a; OLIVEIRA et al., 2022).

A imobilização enzimática em carvões ativados funcionalizados favorece a aplicação da lipase como catalisadora de diversos processos produtivos, onde uma das vertentes de maior expansão para o setor alimentício nos últimos anos é a sua utilização na síntese de ésteres de aromas (KOVALENKO et al., 2021). Além disso, as enzimas lipolíticas têm sido relatadas recentemente no processamento de óleo de peixe para a síntese de ácidos graxos poli-insaturados de cadeia longa - ômega-3 (n-3 PUFAs) para suplementação nutricional, uma vez que o ômega-3 é um nutriente essencial e, portanto, não pode ser produzido pelo organismo humano (PALACIOS et al., 2022).

Dentro desse contexto, o trabalho em questão teve como objetivo produzir biorreatores por meio da imobilização de lipase em carvão ativado sintetizado a partir do resíduo de sisal e submetido a diferentes métodos de modificação, investigando o potencial dos derivados mais promissores em sintetizar lactato de etila e acilgliceróis ricos em ômega-3.

2. REVISÃO BIBLIOGRÁFICA

2.1. Imobilização enzimática

A aplicação industrial de catalisadores biológicos oferece grande potencial frente aos catalisadores químicos por apresentar inúmeros benefícios envolvendo seletividade, biocompatibilidade, biodegradabilidade e aceitabilidade ambiental. Por esse motivo, o uso de enzimas na biocatálise é uma das áreas que apresenta maior crescimento no mercado de moléculas biologicamente ativas (MELO et al., 2023; SINGH et al., 2024; WU et al., 2021). Entretanto, o emprego de enzimas livres em nível comercial ainda é limitado pela baixa estabilidade, reuso e elevado custo de isolamento e purificação, o que limita sua aplicação em processos contínuos e no aumento de escala. Uma proposta viável capaz de solucionar tais limitações é a utilização da enzima na forma imobilizada (DE SOUSA et al., 2023; NWAGU et al., 2021).

O processo de imobilização consiste no aprisionamento da enzima em uma matriz com preservação de sua atividade, visando a utilização repetida e contínua. A técnica de imobilização busca um melhor desempenho catalítico e a redução do custo global de operação, proporcionando vantagens em relação à enzima na forma livre, tais como (SOUSA et al., 2021):

- maior atividade; estabilidade térmica;
- resistência às variações de pH;
- facilidade de recuperação;
- uso em processos contínuos, o que promove um controle mais preciso das variáveis do processo;
- possibilidade de reutilização.

Dessa forma, a seleção da estratégia de imobilização deve ser baseada em parâmetros que consideram o custo do procedimento, a toxicidade dos reagentes envolvidos, a eficiência de recuperação da atividade enzimática e as propriedades finais desejadas para a enzima (ALMEIDA et al., 2022; MONTEIRO et al., 2021).

Os métodos de imobilização enzimática podem ser divididos em duas categorias principais de acordo com o tipo de interação entre a biomolécula e a matriz (Figura 1): física e química. O método físico consiste na incorporação da enzima por meio de retenção física e interações de menor especificidade. Já a imobilização química envolve a retenção irreversível da enzima por meio de ligações fortes, como a ligação covalente (REMONATTO et al., 2022). A atividade da enzima imobilizada é influenciada pelo método

empregado, condições de reação, características do suporte selecionado (afinidade, área superficial, porosidade e hidrofobicidade), seletividade e especificidade do biocatalisador (ROMERO-FERNÁNDEZ e PARADISI, 2020).

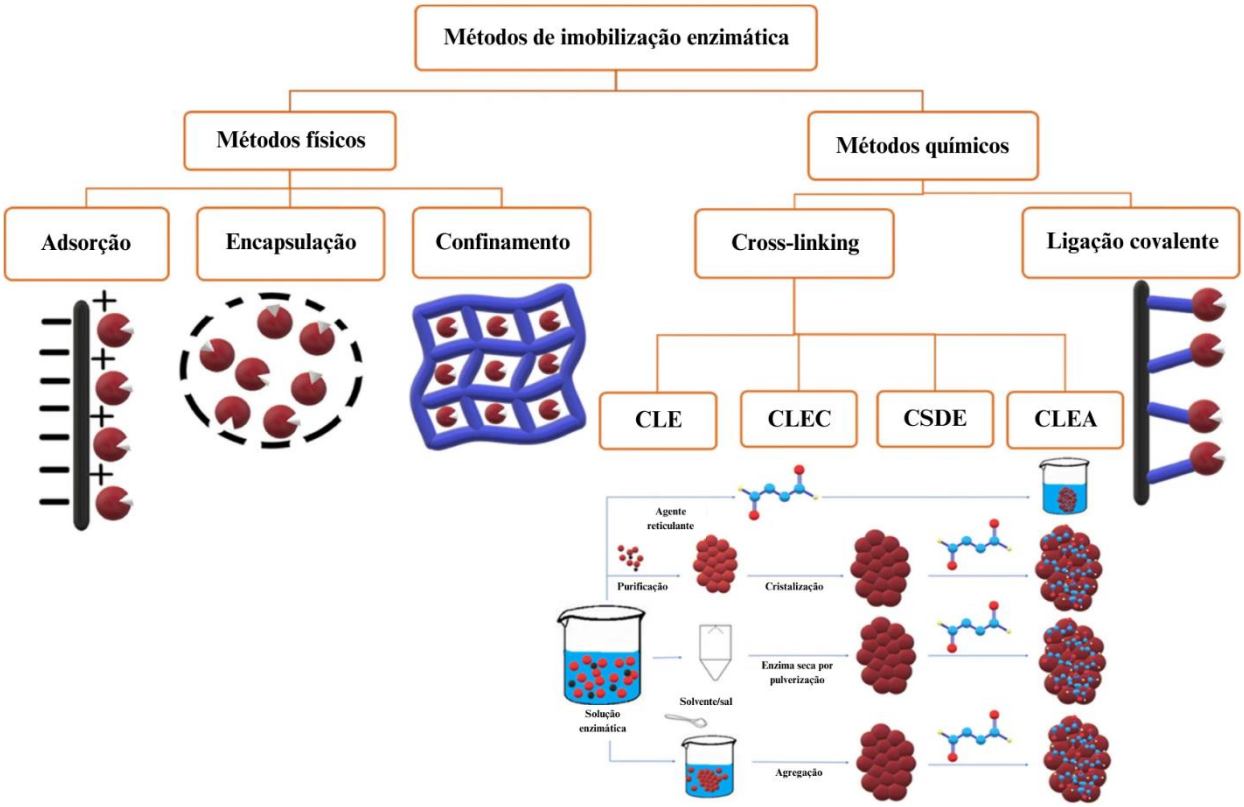

Figura 1. Métodos de imobilização enzimática. Fonte: (FILHO et al., 2019).

2.1.1 Métodos físicos

a. Adsorção

A adsorção física consiste na imobilização reversível da enzima na superfície da matriz. Esse é um dos métodos de imobilização mais utilizados devido à facilidade de execução, baixo custo e possibilidade de regeneração da matriz. Além disso, as interações envolvidas na ligação da enzima à superfície do suporte possuem baixa energia e especificidade (forças de Van der Waals, interações hidrofóbicas, ligações de hidrogênio) quando comparadas às ligações covalentes, permitindo retenção máxima da atividade enzimática uma vez que exercem poucos efeitos na estrutura conformacional e no sítio ativo da enzima. Os suportes mais utilizados são carvão ativado, sílica gel, cerâmica, materiais

naturais como celulose e agarose, além de alguns resíduos industriais (FILHO et al., 2019; ISMAIL e BAEK, 2020; MO et al., 2020a).

Em contrapartida, a técnica demonstra inconvenientes quanto às restrições difusionais de substrato e produtos na estrutura porosa do suporte, aleatoriedade e força da interação enzima-suporte em decorrência da natureza do solvente empregado e da variação dos parâmetros operacionais, como temperatura, pH e força iônica. Tais características podem favorecer a dessorção do composto imobilizado. Sendo assim, a eficiência do método de adsorção física estará associada a esses parâmetros, às características do adsorvente e à relação entre a concentração da enzima e do suporte (FOPASE et al., 2020; RATHER et al., 2022). Algumas alternativas a essas limitações são a otimização das condições de síntese do suporte e o desenvolvimento de modificações de superfície a partir da incorporação de agentes reticulantes (BRITO et al., 2020b; YU et al., 2021b).

b. Encapsulação

A encapsulação envolve a retenção da molécula de interesse de modo irreversível em estruturas poliméricas permeáveis a substratos e produtos. Diferentemente da adsorção, a encapsulação protege a enzima do contato direto com o meio reacional, minimizando os efeitos de inativação que podem ocorrer devido à natureza do solvente. Além disso, o método permite maior estabilidade e facilidade de recuperação frente à enzima livre (SHELDON et al., 2021). No entanto, a atividade da enzima imobilizada, geralmente, é menor do que a da enzima nativa, o que se deve principalmente à limitação à difusão do substrato e/ou à mudança estrutural desfavorável da enzima dentro da matriz (NADAR; RATHOD, 2020). Os mecanismos de encapsulação com maior destaque na literatura são as estruturas orgânicas metálicas (MOF) (DU et al., 2022b), covalentes (COF) (CHAO et al., 2022) e ligadas à hidrogênio (HOF) (LIU; SUN, 2023).

c. Confinamento

O confinamento ou aprisionamento é um método irreversível onde a incorporação da enzima ocorre por meio da sua inclusão em uma matriz, no interior de fibras, em uma estrutura de rede ou em membranas poliméricas. Isso permite com que os substratos e produtos difundam-se através do suporte, enquanto as enzimas permanecem imobilizadas. A imobilização ocorre simultaneamente à polimerização do suporte ao redor da biomolécula,

onde é necessário promover condições operacionais adequadas tanto para a enzima quanto para a matriz (AGGARWAL et al., 2021; IMAM et al., 2021).

Nesse sentido, o confinamento demonstra diversos benefícios, como o baixo custo, facilidade de aplicação em pequena escala e proteção frente ao contato direto com solventes, preservando a estrutura conformacional e atividade catalítica, além de dificultar a inativação proteica. Alguns dos polímeros utilizados como matrizes para imobilização enzimática por aprisionamento são: alginato, carragena, colágeno, poliacrilamida, gelatina, borracha de silicone, poliuretano e álcool polivinílico (ISMAIL e BAEK, 2020; YUAN et al., 2023). Entretanto, o uso prático desta técnica é limitado pela complexa ampliação de escala devido à baixa carga enzimática suportada e a dificuldade em controlar o tamanho dos poros do suporte, o que prejudica a transferência de massa do substrato para o sítio ativo da enzima e pode levar à dessorção (THANGARAJ e SOLOMON, 2019).

2.1.2 Métodos químicos

a. Imobilização por ligação covalente

A imobilização por ligações covalentes é o procedimento irreversível mais aplicado na imobilização enzimática. A retenção da enzima à superfície do suporte ocorre por meio de ligações covalentes entre o suporte e os grupos funcionais da enzima por meio das cadeias laterais dos aminoácidos, como os grupos ε-amino (lisina), tiol (cisteína), carboxílico (ácidos aspártico e glutâmico), fenólico e imidazol (MAGHRABY et al., 2023; RAFIEE e REZAEE, 2021). A eficiência da ligação covalente e a estabilidade do biocatalisador são influenciadas pelas características do suporte e pela orientação de ligação da enzima uma vez que ligações entre os aminoácidos do sítio ativo e a matriz podem desfavorecer a atividade catalítica (LIU et al., 2021). Em geral, o método conta com uma etapa prévia de modificação da superfície ou funcionalização da matriz para inserção de grupos funcionais. Neste método podem ser utilizados como suportes agarose, celulose, quitosana, carvão ativado, cloreto de polivinila, sílica mesoporosa e vidro poroso (LIU et al., 2022).

A principal característica dessa técnica de imobilização é a rigidez imposta à estrutura da enzima devido à força das ligações covalentes, dificultando a dessorção, o desdobramento e a desnaturação proteica, além de proporcionar maior eficiência na imobilização, estabilidade às condições de reação e possibilidade de reutilização. Como desvantagens, podem ser citadas a dificuldade de seleção dos parâmetros de imobilização e

o encarecimento do processo proveniente da adição de agentes funcionalizantes durante a ativação do suporte (LUO et al., 2020; PANDEY et al., 2020).

b. Cross-linking

A imobilização por reticulação ou cross-linking é uma metodologia irreversível baseada na formação de uma estrutura tridimensional. Em geral, a reticulação envolve ligações covalentes entre enzimas usando agentes reticulantes bi ou multifuncionais, como é o caso do glutaraldeído, um reticulante amplamente aplicado devido ao baixo custo e excelente eficiência de operação em escala comercial. Outros agentes conhecidos são poliaminas, polietilenoimina, poliestireno sulfonatos, genipina, polialdeído dextrano e diferentes fosfatos (BOUNEGRU e APETREI, 2023; WANG et al., 2022a; XU et al., 2023).

Os protocolos de reticulação mais utilizados são os agregados enzimáticos reticulados (CLEA), reticulados de enzimas (CLE), cristais de enzima reticulados (CLEC) e enzimas atomizadas reticuladas (CSDE). Os CLEAs destacam-se como um biocatalisador insolúvel em que não é obrigatória a presença de suporte pois a ligação ocorrerá entre enzima e agente reticulante. No entanto, o agente deve conter pelo menos duas extremidades reativas para possibilitar a formação de uma estrutura tridimensional complexa (MULEY et al., 2021; SAMPAIO et al., 2022). Em geral, esse é um processo em que há aumento de estabilidade da estrutura enzimática, possibilidade de co-imobilização e reutilização e não requer moléculas em meios com elevada pureza. No entanto, apresenta baixa reprodutibilidade, baixa estabilidade mecânica, alto custo, possibilidade de alterações na estrutura conformacional e formação de *clusters* com consequente perda de atividade, dificuldades de manuseio devido ao aspecto gelatinoso e o uso excessivo dos reagentes de reticulação pode reduzir a conversão e estabilidade do produto (THANGARAJ e SOLOMON, 2019).

O desenvolvimento de metodologias associadas à imobilização enzimática intensificou-se nos últimos anos, onde as lipases encontram-se em evidência em razão de sua seletividade, especificidade e vasta aplicação industrial (REMONATTO et al., 2022).

2.2 Lipases

Lipases (triacilglicerol hidrolases (E.C. 3.1.1.3)) são enzimas que catalisam a hidrolise de ligações éster dos triacilgliceróis em diacilgliceróis, monoacilgliceróis, ácidos graxos livres e glicerol. Embora sejam pertencentes à família das hidrolases, as lipases também possuem mecanismo de atuação em meio orgânico para a reação de síntese de

ésteres a partir de um álcool e um ácido carboxílico, também conhecida como esterificação (NASCIMENTO et al., 2021a; PEREIRA et al., 2022).

Outras reações podem ser catalisadas de acordo com a composição do meio reacional e da transformação do grupo éster (Figura 2), como é o caso da transesterificação. Essa reação se refere à troca de grupamentos acila entre um éster e outro composto químico em que podem ser citadas: interesterificação, onde há troca entre os substituintes de dois ésteres; acidólise, aminólise e alcóolise, que estão associadas à degradação/síntese na presença de um ácido, amina e álcool como agentes nucleofílicos, respectivamente. Dentre as reações de alcóolise, a glicerólise (troca entre éster e glicerol) possui destaque em aplicações industriais (CHANDRA et al., 2020; VERMA et al., 2021).

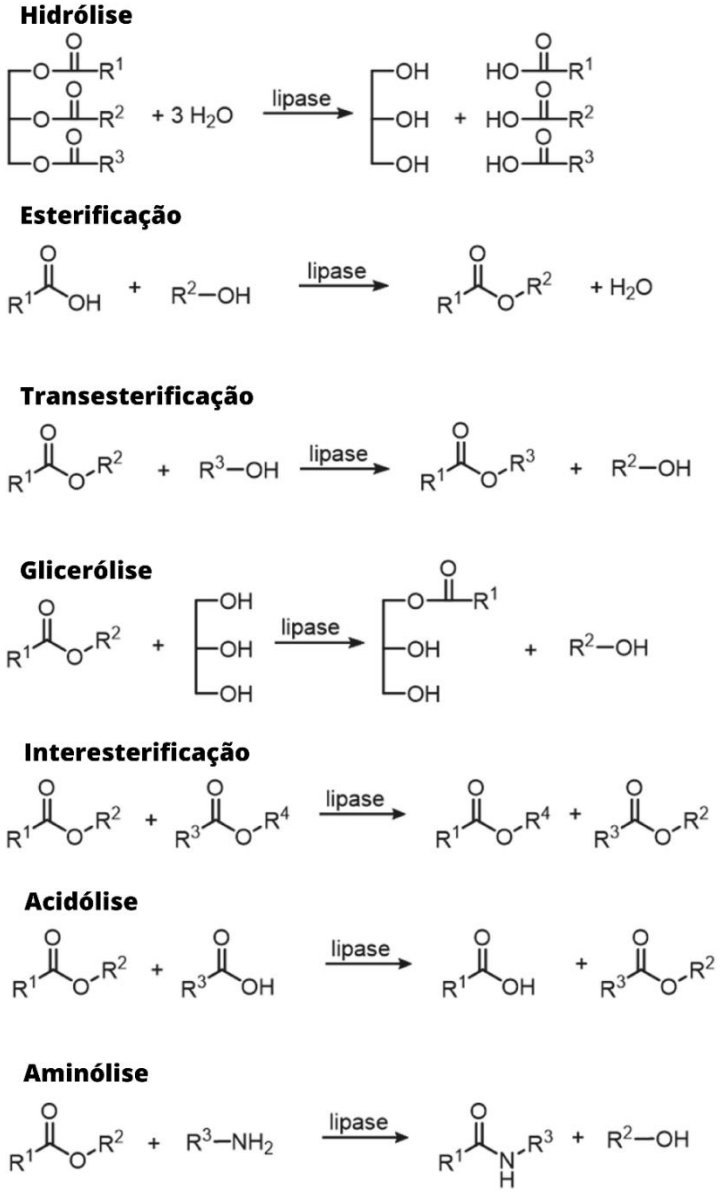

Figura 2. Reações catalisadas por lipases. Fonte: (SALGADO et al., 2022).

Via de regra, enzimas lipolíticas apresentam estabilidade em meio aquoso neutro e temperatura ambiente. De acordo com a fonte enzimática, a massa molecular das lipases está na faixa de 20-75 kDa, o pH de atividade pode variar de 4 a 9, sendo os valores ótimos entre 6 e 8, e a temperatura de atividade está entre 25-70 ºC, onde o valor ideal pode variar entre 30 e 40 ºC (BHARATHI e RAJALAKSHMI, 2019). Conforme relatado por Mortazavi e Aghaei (2020), o sítio ativo das lipases consiste em uma tríade de resíduos de aminoácidos, nomeadamente um resíduo nucleofílico (cisteína, serina ou aspartato), um resíduo catalítico ácido (aspartato ou glutamato) e um resíduo de histidina.

As lipases exibem um mecanismo catalítico específico que ocorre exclusivamente na interface óleo-água e permite que a enzima possua duas conformações: forma fechada e inativa ou forma aberta e ativa. Esse mecanismo é denominado ativação interfacial e está associado à presença de uma cadeia polipeptídica móvel hidrofóbica de α-hélice que atua como uma "tampa" e isola o sítio ativo do meio reacional. No entanto, o contato com uma interface hidrofóbica (ex. gotas de óleo e suportes hidrofóbicos) promove a abertura da tampa e favorece a interação substrato-sítio ativo (REMONATTO et al., 2022; ZHANG et al., 2022a).

As lipases são classificadas quanto à sua regioespecificidade, ou seja, à capacidade de hidrolisar ácidos graxos em posições específicas da cadeia de glicerol na estrutura dos triglicerídeos. Tais biomoléculas podem ser divididas em específicas para sn-1,3, específicas para sn-2 ou inespecíficas. As lipases específicas sn-1,3 (ex: lipases de *Aspergillus niger, Mucor miehei, Bacillus thermocatenulatus, Candida antarctica B, Rhizomucor miehei, Thermomyces lanuginosus* e pâncreas do porco) são as mais comuns e hidrolisam ligações éster nas posições sn-1 e sn-3. As lipases específicas sn-2 hidrolisam ligações éster na posição sn-2 e as lipases inespecíficas (ex: lipases de *Pseudomonas cepacia, Pseudomonas fluorescens, Candida rugosa, Candida cylindracea* e *Chromobacterium viscosum*) hidrolisam aleatoriamente todas as posições dos triglicerídeos. Além disso, algumas lipases apresentam maior preferência por alguns tipos de ácidos graxos, como é o caso das lipases de *Candida rugosa* e *Rhizomucor miehei* que reconhecem preferencialmente substratos contendo ácidos oleico ou elaínico (MONTEIRO et al., 2021; REMONATTO et al., 2022).

As lipases podem ser obtidas a partir de animais, plantas e microrganismos com diferente especificidade de substrato, seletividade e propriedades bioquímicas. As enzimas vegetais apresentam processos de extração de baixo custo e purificação a partir de técnicas simples, uso de fontes renováveis, possibilidade de reaproveitamento de resíduos e

características específicas ao seu mecanismo de funcionamento (ALVES et al., 2022). Algumas fontes vegetais a serem citadas são: amêndoa do pequi (NASCIMENTO et al., 2021b), azeite de dendê (DIN et al., 2021), farelo de arroz (YU et al., 2021a), látex de mamão (VB et al., 2022), semente de mamona (TAVARES et al., 2021) e semente de seringueira (FATIHA et al., 2020). No entanto, os baixos níveis de lipase normalmente encontrados nas fontes nativas limitam a produção em larga escala.

Nesse sentido, grande parte das lipases utilizadas em pesquisas e processos industriais são de origem microbiana devido à elevada estabilidade, baixo custo de produção, biodisponibilidade e versatilidade. O mercado de lipases microbianas tem crescido continuamente ao longo dos anos, com projeção de alcançar 5,59 bilhões de dólares em 2023 e taxa de crescimento anual de 6,8 % (CHANDRA et al., 2020; FASIM et al., 2021; SALGADO et al., 2022). Como citado anteriormente, o emprego de enzimas livres em nível comercial ainda é limitado pela baixa estabilidade em determinados meios, reuso e elevado custo de isolamento e purificação. Sendo assim, entende-se como necessário o desenvolvimento de técnicas que otimizem a eficiência catalítica e industrial da lipase, onde a imobilização pode ser destacada.

2.2.1 Imobilização de lipases

O método mais comum de imobilização lipolítica é a adsorção. Devido ao mecanismo de ativação interfacial das lipases (Figura 3), suportes com características hidrofóbicas são preferenciais por potencializarem a imobilização desse biocatalisador na conformação aberta e ativa, sendo um desses materiais o carvão ativado (BRITO et al., 2020a).

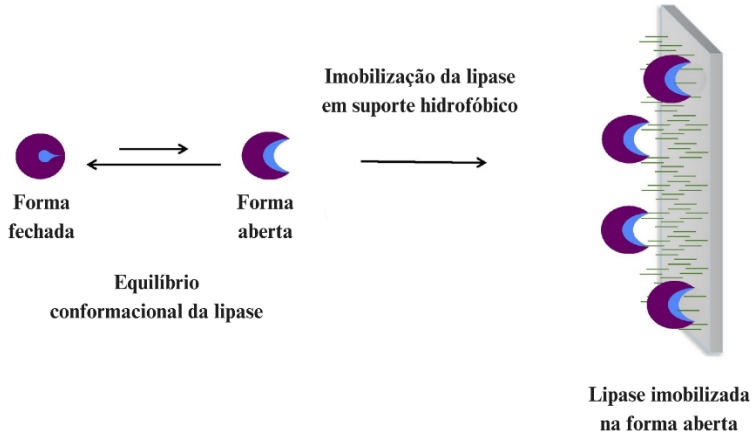

Figura 3. Mecanismo de ativação interfacial das lipases em suportes hidrofóbicos. Fonte: (RODRIGUES et al., 2021).

Entretanto, as limitações associadas ao processo adsortivo ampliaram a variedade de estudos com diferentes suportes e métodos de imobilização de lipases, como é reportado na Tabela 1.

Tabela 1. Desempenho de lipases imobilizadas em diferentes suportes e métodos de imobilização.

Suporte	Método	Fonte	Atividade/ Reuso	Referência
Estrutura zeolítica de imidazolato (ZIF-8) (MOF)	Encapsulação	*Aspergillus niger*	72 % de hidrólise após 6 ciclos	(NADAR e RATHOD, 2020)
LentiKats (Gel de álcool polivinílico (PVA))	Agregados reticulados e confinamento	*Candida antarctica B*	60 % de rendimento de glicerólise após 6 ciclos	(GUAJARDO et al., 2020)
Nanopartículas de sílica (SiO_2)	Reticulação com glutaraldeído e adsorção	*Candida antarctica B*	53 % de hidrólise após 5 ciclos	(QIAN et al., 2023)
Nanotubos de carbono	Adsorção	rPichia/lip	80-85 % da hidrólise após 36 ciclos	(NURULLINA et al., 2020)
Óxido de grafeno	Adsorção	Suco pancreático	71 % de rendimento de transesterificação após 5 ciclos	(KUMAR; PAL, 2021)
Novozym 435 (resina Lewatit VP OC 1600)	Adsorção	*Candida antarctica*	40 % de rendimento de esterificação após 3 ciclos	(DE MENESES et al., 2020a)
Lipozyme TL-IM (sílica catiônica)	Adsorção	*Thermomyces lanuginosus*	58 % de rendimento de esterificação após 3 ciclos	(DE MENESES et al., 2020a)
Lipozyme RM-IM (resina de troca aniônica)	Adsorção	*Rhizomucor miehei*	54 % de rendimento de esterificação após 3 ciclos	(DE MENESES et al., 2020a)

Carvão ativado	Adsorção	Pâncreas do porco	92 % de rendimento de esterificação após 5 ciclos	(BRITO et al., 2020b)
Carvão ativado	Ligação covalente – modificação com glutaraldeído	Pâncreas do porco	90 % de rendimento de esterificação após 5 ciclos	(BRITO et al., 2020b)
Superpartículas magnéticas de Fe_3O_4	Ligação covalente	*Rhizopus oryzae*	45 % de rendimento de transesterificação após 5 ciclos	(NEMATIAN et al., 2020)
Nanopartículas de Fe_3O_4-COF	Ligação covalente	*Rhizomucor miehei*	70 % de rendimento de transesterificação após 8 ciclos	(ZHOU et al., 2021)
Esferas magnéticas de quitosana	Ligação covalente – modificação com polidopamina	*Candida rugosa*	69 % de rendimento de esterificação após 10 ciclos	(BAYRAMOGLU et al., 2022a)
Carvão ativado	Ligação covalente – modificação com partículas metálicas	Pâncreas do porco	80 % de rendimento de esterificação após 5 ciclos	(DE OLIVEIRA et al., 2022)
Biomassa da borra de café	Ligação covalente – modificação com glutaraldeído	*Candida rugosa*	60 % de hidrólise após 3 ciclos	(GIRELLI et al., 2023)
Palha de arroz magnética	Ligação covalente	*Thermomyces lanuginosus*	82 % de rendimento de transesterificação após 5 ciclos	(OTARI et al., 2020)

2.3 Carvão Ativado

O carvão ativado (CA) (Figura 4) é um material carbonáceo de estrutura altamente porosa composta por micro (< 2 nm), meso (2–50 nm) e/ou macroporos (> 50 nm). É desenvolvido através da queima controlada do material precursor e apresenta forma microcristalina não grafítica com pequenas quantidades de heteroátomos (principalmente oxigênio, nitrogênio e hidrogênio) ligados aos átomos de carbono. O CA possui elevadas área superficial específica e porosidade, conferindo-lhe a capacidade de adsorver moléculas líquidas ou gasosas no interior dos seus poros (BENÍTEZ et al., 2022; ZHU e XU, 2020). A

capacidade adsortiva do carvão ativado é orientada por sua porosidade interna, área superficial, distribuição de tamanho e volume de poros e presença de grupos funcionais ligados à superfície, características afetadas significativamente pelas propriedades físicas e químicas do precursor, pelo método de síntese e pelas condições de ativação (BRITO et al., 2020; WANG et al., 2022).

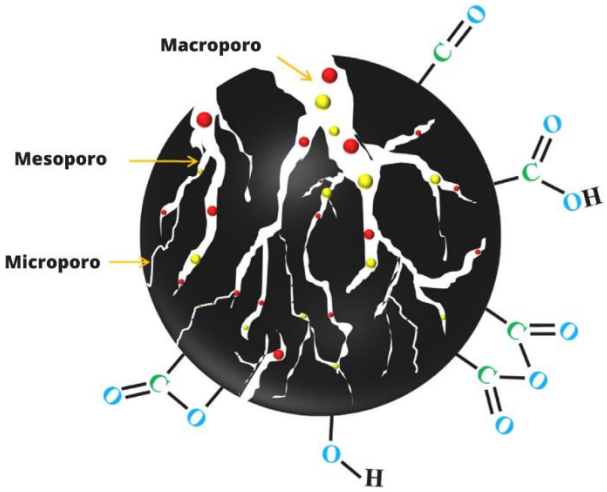

Figura 4. Representação esquemática da estrutura dos poros e grupos funcionais de superfície do carvão ativado. Fonte: (SULTANA et al., 2022).

Os carvões ativados são amplamente utilizados em processos de clarificação, purificação, desodorização e descoloração de materiais, além de servirem como suporte catalítico. Por esse motivo, esses adsorventes são de interesse do ponto de vista econômico e possuem uma diversidade de aplicações na indústria, como no processamento de alimentos, fármacos, petróleo, produtos químicos, tratamento de efluentes e setor automobilístico. Os CA podem ser encontrados na forma granular, fibrosa e pó, o que promove aplicabilidade específica para cada uma dessas estruturas (ADELEYE et al., 2021a; PATHAK e MANDAVGANE, 2023; THONGPAT et al., 2021).

A superfície de um carvão ativado apresenta características químicas ácidas e/ou básicas, sendo as ácidas associadas a grupos funcionais como as carboxilas, lactonas e fenóis; e as básicas associadas a grupos como hidroxilas, carbonilas, piranos e éter. Além disso, o carvão pode ter capacidade oxidante, redutora, hidrofílica ou hidrofóbica (BARROSO-BOGEAT et al., 2019; SANDOVAL-GONZÁLEZ et al., 2022).

O CA pode ser obtido a partir de uma infinidade de materiais ricos em carbono de origem animal, vegetal e mineral. As matérias-primas mais utilizadas são minerais,

madeiras, serragens, ossos de animais, resíduos agroindustriais, algas, entre outros. As fontes minerais são encontradas em abundância, porém não são renováveis. Já as fontes vegetais são renováveis, encontradas em abundância e possuem baixo custo. A escolha do material precursor depende da sua disponibilidade e composição lignocelulósica, visto que as propriedades do carvão serão influenciadas pela natureza do material utilizado e pelo processo de síntese (ABED et al., 2022; ABUELNOOR et al., 2021; ALVEAR-DAZA et al., 2022; GOMEZ-DELGADO et al., 2022).

2.3.1 Síntese do carvão ativado

A síntese do carvão ativado está associada a dois processos conhecidos como ativação e carbonização do material precursor, podendo ocorrer simultaneamente ou não. A carbonização é definida como o tratamento térmico (pirólise) do precursor em atmosfera inerte e elevadas temperaturas que podem variar entre 300°C e 900ºC. Nessa etapa, é removida a umidade, os componentes voláteis (H, N e O) e gases leves (CO, H_2, CO_2 e CH_4), responsáveis pela formação de uma estrutura porosa e pelo aumento da concentração de carbono na amostra, resultando em um material rico em carbono (JIANG et al., 2020; REZA et al., 2020).

A ativação promove reações secundárias no material carbonizado a fim de aumentar sua porosidade através do aumento do diâmetro dos poros e da criação de novos poros, o que consequentemente altera a área superficial. Em alguns casos, há a modificação superficial a partir de diferentes grupos químicos adicionados. Esse processo atribui as características básicas do carvão como distribuição de poros, área superficial específica, atividade química da superfície e resistência mecânica de acordo com a configuração requerida para a aplicação tecnológica do material carbonáceo (HASANZADEH et al., 2020; ZHU e XU, 2020).

A ativação pode ocorrer pelo método físico ou químico. A ativação física envolve um processo de duas etapas térmicas distintas, onde o material precursor é primeiramente carbonizado sob temperatura elevada (entre 700 °C e 900 ºC) e atmosfera inerte a fim de evitar a combustão da estrutura carbonácea. Nessa etapa, há a remoção dos heteroátomos e liberação dos voláteis, o que implica na obtenção de um carvão com elevado teor de carbono. Entretanto, o material obtido exibe uma baixa área superficial e porosidade. Sendo assim, a segunda etapa da ativação física consiste na remoção seletiva dos átomos de carbono mais reativos por meio de reações controladas de gaseificação, gerando a porosidade característica dos carvões ativados (ADELEYE et al., 2021b; DUAN et al., 2021).

A temperatura de gaseificação depende do agente de gaseificação empregado, normalmente dióxido de carbono, vapor d'água, oxigênio ou uma mistura desses gases. Temperaturas entre 700 e 900 °C são usadas para vapor d'água ou CO_2. Por outro lado, a temperatura de gaseificação deve ser muito mais baixa (300-450 °C) ao usar O_2 devido à sua maior reatividade e exotermicidade de reação. Nesse sentido, vapor e dióxido de carbono são os agentes ativadores preferenciais utilizados (LEWOYEHU, 2021).

A ativação química baseia-se na impregnação do material precursor com agentes químicos seguida de tratamento térmico sob atmosfera inerte em faixas de temperatura entre 300 e 900 ºC. Nessa etapa, os compostos químicos auxiliam no aumento da porosidade por meio da despolimerização, desidratação, condensação e degradação da estrutura do precursor. Além disso, há formação de ligações cruzadas no material, reduzindo a susceptibilidade à volatilização durante o processamento em elevadas temperaturas. Alguns dos principais agentes empregados na ativação química são o ácido fosfórico (H_3PO_4), ácido sulfúrico (H_2SO_4), cloreto de zinco ($ZnCl_2$), hidróxido de potássio (KOH) e hidróxido de sódio (NaOH). Por fim, é realizada a lavagem para remoção do agente ativador remanescente e dos subprodutos da reação que podem obstruir os poros formados (BENÍTEZ et al., 2022; HEIDARINEJAD et al., 2020a; LEWOYEHU, 2021).

O ácido fosfórico é um aditivo alimentar aprovado pela Food and Drug Administration (FDA), tornando-o o principal agente ativante químico na síntese de carvões ativados com aplicações na indústria de alimentos (DUNFORD et al., 2023). A ativação química com ácido fosfórico apresenta algumas vantagens frente à ativação física, destacando-se o emprego de temperaturas mais baixas (em torno de 400 a 500 ºC) e, consequentemente, menor tempo de ativação, o que promove maior rendimento por prevenir a queima excessiva, formação de alcatrão e outros produtos voláteis (IWANOW et al., 2020; MONTALVO ANDIA et al., 2020).

Além disso, tal método permite um controle mais preciso sobre o desenvolvimento de microporosidade e distribuição das dimensões dos poros em comparação ao método físico devido ao seu mecanismo de degradação da estrutura lignocelulósica. Durante o processo de ativação, o precursor sofre condensação catalisada pelo H_3PO_4, favorecendo a quebra de ligações. Por serem estruturas amorfas e estarem localizadas na fração mais externa na fibra, as porções de lignina e hemicelulose são mais susceptíveis à degradação e formação de microporos. Por outro lado, a celulose (estrutura cristalina) possui maior reatividade com o ácido fosfórico e forma ligações éster acrescentando grupos polifosfato/fosfato ao longo da

estrutura, o que promove sua expansão. Por esse motivo, a decomposição da celulose está associada ao desenvolvimento de mesoporos. Em geral, o desenvolvimento de microporosidade é observado em faixas de temperatura entre 150 e 300 ºC. Acima dessa faixa, os mesoporos passam a ser desenvolvidos, especialmente pelo enlarguecimento dos microporos existentes (HEIDARINEJAD et al., 2020; HU et al., 2021; PALURI e DURBHA, 2023; BRITO et al., 2020a).

2.4 Utilização de compostos lignocelulósicos como precursores de carbono

A agroindústria é um setor de grande relevância na economia e abastecimento da população brasileira. Entretanto, esse segmento contribui significativamente na geração e descarte indevido de grandes quantidades de resíduos sólidos e líquidos, desencadeando inúmeras problemas ambientais, como a poluição da água e do solo, emissão de gases de efeito estufa e mudanças climáticas, gerando um impacto negativo na saúde humana e animal. Diante disso, o reaproveitamento desse material para a obtenção de diferentes tipos de produtos se tornou uma alternativa lucrativa e sustentável, com destaque para o uso da biomassa lignocelulósica na síntese de carvões ativados (NAIR et al., 2022; SONU et al., 2023; SRIVASTAVA et al., 2023).

Os compostos lignocelulósicos são os materiais mais disponíveis da biosfera com estimativa de que sejam produzidas 181,5 bilhões de toneladas por ano mundialmente. No entanto, apenas cerca de 8,2 bilhões de toneladas de biomassa são utilizadas, sendo 1,2 bilhões de toneladas provenientes de resíduos agrícolas (ASHOKKUMAR et al., 2022). A biomassa lignocelulósica (Figura 5) é encontrada na parede celular vegetal e composta por um conjunto de tecidos celulósicos que podem ser divididos em três frações poliméricas principais, unidas entre si por uma rede complexa de ligações covalentes, sendo elas: celulose (40-60 %), lignina (10-25 %) e hemicelulose (20-40 %), onde a variação na concentração de cada um desses elementos estará associada às características da matéria-prima, estado de maturação e condições climáticas. Além desses componentes, a biomassa vegetal possui constituintes extrativos e inorgânicos (CHAKHTOUNA et al., 2022; GÜLEÇ et al., 2021; ZHANG et al., 2021).

A celulose é um homopolímero integral e estrutural da biomassa lignocelulósica com uma cadeia linear de unidades repetidas de β-D-glucopiranose ligadas covalentemente por ligações β-(1,4) glicosídicas que conferem rigidez e estabilidade à parede celular. As ligações de hidrogênio e as interações de van der Waals ligam as cadeias de celulose

vizinhas, reforçando o alinhamento paralelo e formando uma estrutura cristalina com uma conformação helicoidal dupla plana estendida denominada microfibrila (BAIG, 2020). A hemicelulose é uma estrutura curta de baixo grau de polimerização, aleatória e amorfa que consiste em pentoses altamente ramificadas (xilose e arabinose), hexoses (manose, glicose, galactose), sacarídeos de baixo teor (ramnose e frutose), ácidos urônicos e grupos acetil em quantidades variadas ligados entre si por ligações de hidrogênio e ligações covalentes (SPEIGHT, 2020). A lignina é uma macromolécula fenólica irregular não cristalina sem estrutura primária definida formada pela polimerização por radicais livres de precursores de álcool que fornece resistência mecânica à biomassa e reforça a compactação das fibras entre a parede celular (SCELSI et al., 2021).

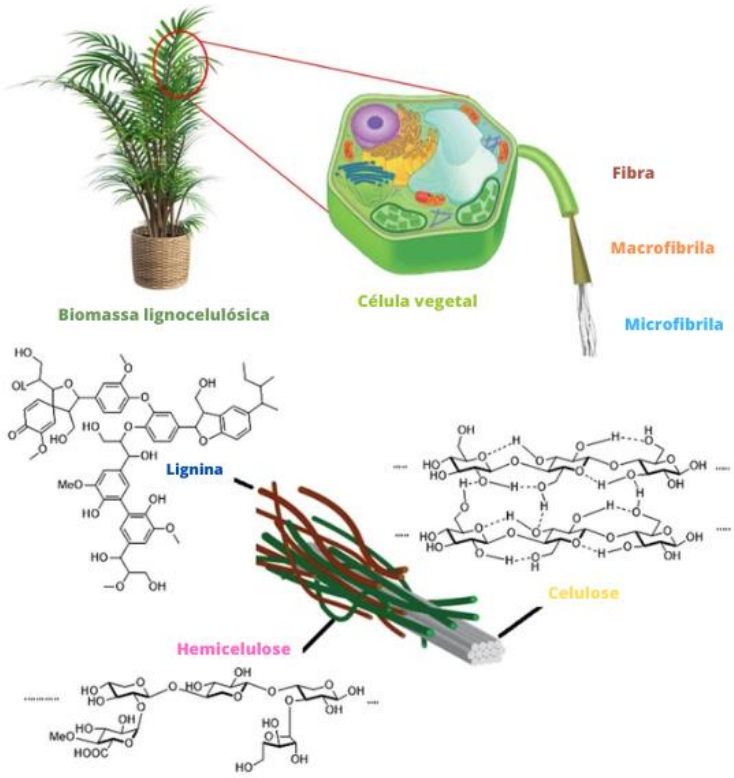

Figura 5. Estrutura da biomassa lignocelulósica. Fonte: (CHAKHTOUNA et al., 2022).

De modo geral, celulose e hemicelulose são constituintes voláteis, enquanto a lignina é o material que proporciona rigidez à biomassa e possui complexa volatilização. A decomposição da estrutura e quebra de ligações ocorre entre 180-260 ºC para a hemicelulose, 240-350 ºC para a celulose e 280-500 ºC para a lignina. Nesse sentido, a composição do material precursor empregado será fator determinante para as propriedades do produto final,

incluindo a distribuição e o tamanho de poros (CHAKHTOUNA et al., 2022; LU et al., 2020; ZHANG et al., 2021).

Os resíduos agroindustriais apresentam grande potencial para a síntese de carvões ativados por serem uma fonte abundante de biomassa. Diversos estudos têm sido realizados a fim de converter tais materiais em produtos de alto valor agregado, uma vez que possuem em sua composição elevado teor de carbono e compostos voláteis, permitindo desenvolver uma estrutura altamente porosa (IMAM et al., 2021). Dentre os resíduos utilizados como precursores de carbono, podem ser citados: casca de cacau (LEÓN et al., 2022), fibra de bambu (RAHMAN e KARACAN, 2022), casca de coco (SUJIONO et al., 2022), casca de laranja e limão (RAMUTSHATSHA-MAKHWEDZHA et al., 2022), casca de palma (HUSSIN et al., 2021), casca de arroz (CHAROENSOOK et al., 2021), casca de castanha de caju (SAMIYAMMAL et al., 2022) e casca de amendoim (CAMPOS et al., 2022). Estudos relatam que o resíduo do processamento do sisal é uma fonte ainda pouco explorada na síntese de carvões ativados (DIZBAY-ONAT et al., 2018).

2.4.1 Sisal (*Agave sisalana*)

O sisal (*Agave sisalana*) (Figura 6) é uma planta originária do México com características morfológicas e fisiológicas que conferem resistência a diferentes condições ambientais, incluindo climas quentes e regiões que sofrem com secas prolongadas. Por esse motivo, o Brasil é o maior produtor e exportador de fibra de sisal do mundo, onde estima-se que 39 % das 220 mil toneladas de fibra de sisal produzidas anualmente sejam oriundas do Brasil (COLLEY et al., 2021). Seu cultivo é predominante em regiões semiáridas, mais especificamente no estado da Bahia, responsável por 95 % da produção de sisal no país (CRUZ-MAGALHÃES et al., 2020). Além disso, o sisal também é cultivado em regiões como Tanzânia, China, Índia, Sul da África e Indonésia (VEIT, 2023).

Figura 6. Planta (a) e fibra de sisal (b). Fonte: EMBRAPA, 2023.

A *Agave sisalana* é uma importante produtora de fibras naturais duras. A fibra extraída ocupa a sexta colocação em relevância, representando cerca de 2 % da produção mundial de fibras vegetais e 75 % da produção global de fibras duras (SHAHZAD et al., 2022). No entanto, apenas 3-5 % da massa total da planta de sisal é utilizada adequadamente na produção de fibras, sendo a porcentagem restante descartada como resíduo de sisal, levando à perda excessiva de matéria-prima e geração de impactos negativos ao meio ambiente (MELO et al., 2020). Nesse sentido, o uso desse resíduo acompanha a tendência de crescimento mundial que favorece a aplicação de recursos naturais sustentáveis com redução de impactos ambientais.

A fibra de sisal é composta por diferentes porcentagens de celulose (47–78 %), hemicelulose (10–24 %) e lignina (7–14 %) (CHOUDHARY et al., 2023). Já o resíduo do desfibramento do sisal possui composição lignocelulósica subdividida em aproximadamente 43,6 % de celulose, 18,8 % de hemicelulose e 18,7 % de lignina (LI et al., 2021). Dessa forma, o resíduo de sisal é um recurso potencialmente valioso com destaque para a sua conversão em carvões ativados.

2.5 Aplicações do carvão ativado

O avanço no desenvolvimento de novas tecnologias ao longo dos últimos anos proporcionou a obtenção de materiais com características adsorventes e de baixo custo, como é o caso dos diferentes tipos de carvões ativados encontrados no mercado. Além disso, o uso de resíduos agroindustriais como fonte de carbono pode reduzir ainda mais os custos de produção por serem abundantes e muitas vezes não possuírem um aproveitamento adequado, o que atribui valor agregado ao produto final (KAUR et al., 2023). Tais características aliadas a propriedades químicas e texturais específicas dos CA, como elevada área superficial e porosidade, estabilidade a variações nas condições operacionais, hidrofilicidade e insolubilidade, têm influenciado em sua aplicação em diversas vertentes (WANG et al., 2022b). De acordo com Mariana et al. (2021), a demanda global por carvões ativados está avaliada em 3 bilhões de dólares anualmente.

O carvão ativado é amplamente empregado em escala industrial na separação e purificação de líquidos e gases, podendo ser apontado como uma das técnicas mais eficientes na remoção de compostos orgânicos e inorgânicos de um meio. Dessa forma, pode-se destacar sua utilização no tratamento de efluentes, águas residuárias e gases; recuperação de solventes e metais; clarificação, descoloração e desodorização de produtos da indústria

alimentícia, química e farmacêutica; e como suporte para a imobilização de enzimas (KAYA et al., 2023; PANAHI et al., 2020; SALGADO et al., 2022).

2.5.1 Modificações em carvões ativados

Nos últimos anos, diversas pesquisas têm sido relatadas sobre modificação de superfície das matrizes para imobilização enzimática, sendo que o carvão ativado se tornou objeto de estudo devido aos inconvenientes observados durante a adsorção e à possibilidade de desenvolvimento de um material heterofuncional (Figura 7). A funcionalização implica em aumento de atividade, estabilidade e seletividade por promover a quimissorção (ligações covalentes) e fisissorção (forças de Van der Waals, interações hidrofóbicas, ligações de hidrogênio, interações iônicas e interações específicas) (LAKSHIMI et al., 2024).

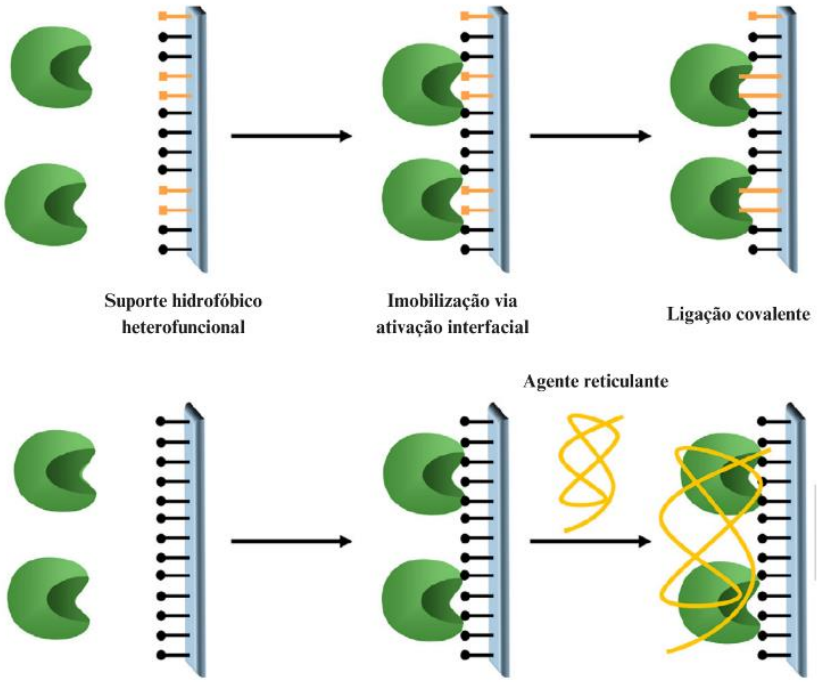

Figura 7. Estratégias de retenção das lipases em suportes hidrofóbicos através dos mecanismos de imobilização por ligação covalente e reticulação. Fonte: (MONTEIRO et al., 2021).

O glutaraldeído é o reagente multifuncional mais utilizado na modificação para imobilização de enzimas por ligação covalente por apresentar baixo custo, facilidade de execução e promover estabilidade através da formação de interações rígidas entre a molécula de interesse e o suporte. Os suportes ativados por glutaraldeído reagem principalmente com

os grupos amino primários da estrutura proteica, embora possam reagir com outros grupos funcionais como tióis, fenóis e imidazóis. O método consiste na aminação da superfície carbonácea seguida da incorporação do glutaraldeído pela formação de bases de Schiff entre os grupamentos amina e aldeído, levando à formação de ligações aminas secundárias estáveis e promovendo a imobilização enzimática por ligações covalentes devido à sua elevada força iônica. As maiores desvantagens ao uso dessa técnica são a toxicidade do glutaraldeído e sua capacidade de polimerização em meio aquoso (MO et al., 2020b; SANTOS et al., 2019; THANGARAJ e SOLOMON, 2019).

Nesse sentido, novos métodos estão sendo desenvolvidos como alternativas ao glutaraldeído, onde a genipina é apontada como uma abordagem verde promissora (toxicidade até 10000 vezes menor) devido à biocompatibilidade, biodegradabilidade e por formar produtos reticulados estáveis. A genipina é um composto natural obtido do glicosídeo iridoide (geniposídeo) comumente utilizada na medicina alternativa por possuir propriedades antimicrobianas, antitumorais e anti-inflamatórias (YU et al., 2021b). Sua atividade reticulante é proveniente da reação espontânea com aminas primárias de diferentes materiais formando ligações covalentes. O uso de genipina como agente de reticulação já é amplamente difundido na imobilização enzimática em quitosana (BAYRAMOGLU et al., 2022b), gelatina (SUN et al., 2022) e colágeno (ADAMIAK e SIONKOWSKA, 2020). Contudo, há uma carência de estudos reportados para a modificação de carvões ativados, podendo ser citada apenas a aplicação na imobilização de proteases (SANTOS et al., 2022). Sendo assim, a imobilização de lipases em carvões ativados funcionalizados com genipina deve ser investigada com o objetivo de aumentar a eficiência do processo.

A funcionalização de matrizes utilizando partículas metálicas também vem ganhando destaque por apresentar diversos benefícios como biocompatibilidade, baixa toxicidade, propriedades magnéticas vantajosas, facilidade de execução, estabilidade em diferentes condições e possibilidade de reutilização da solução. Dentre os compostos empregados, as partículas magnéticas de óxido de ferro (Fe_3O_4) possuem grande destaque. O óxido de ferro (II, III) é produzido pela co-precipitação de íons Fe^{2+} e Fe^{3+} e têm as interações iônicas como mecanismo de imobilização (DARWESH et al., 2020; OLIVEIRA et al., 2022; GRACIDA et al., 2019; RUSU et al., 2022).

Diante do exposto, diversos estudos têm sido desenvolvidos a fim de avaliar a eficiência dos carvões ativados como suportes catalíticos em processos de imobilização de enzimas, conforme mostrado na Tabela 2.

Tabela 2. Estudos desenvolvidos com carvão ativado como suporte para imobilização enzimática.

Enzima	Método	Aplicação	Referência
Lipase	Adsorção	Hidrólise da emulsão de azeite de oliva	(BRITO et al., 2020)
	Adsorção Ligação covalente	Esterificação de acetato de isoamila	(OLIVEIRA et al., 2022)
	Adsorção	Transesterificação de óleo de palma em biodiesel	(QUAYSON et al., 2020)
	Ligação covalente	Interesterificação entre óleo de cânfora e perilla	(ZHAO et al., 2022)
Lacase	Adsorção	Oxidação de ABTS	(BORGES et al., 2023)
Pepsina	Adsorção Ligação covalente	Hidrólise da caseína bovina	(SANTOS et al., 2022)
Amilo glucosidase	Ligação covalente	Hidrólise da maltodextrina	(ASLAN et al., 2020)
Tripsina	Adsorção Ligação covalente	Hidrólise de caseína de cabra, búfalo e bovina	(SOUZA JÚNIOR et al., 2020)
Celulase	Ligação covalente	Hidrólise de celulose	(MO et al., 2020b)

2.6 Aplicações de lipases

Devido à versatilidade das reações catalisadas por lipases, essa biomolécula é considerada um catalisador valioso para a biotecnologia por ser uma alternativa limpa frente aos métodos químicos enquanto fornece alta especificidade e seletividade ao substrato,

atividade sob condições operacionais amenas e formação reduzida de subprodutos e intermediários, o que aumenta o rendimento da reação (ISMAIL e BAEK, 2020). Por esse motivo, as enzimas lipolíticas são empregadas em diversas áreas, como na síntese de biossensores para detecção de poluentes ambientais, como os pesticidas. Na indústria alimentícia, os biossensores podem ser utilizados para controlar a qualidade dos alimentos, principalmente a presença de triacilgliceróis. Já na medicina, sensores de lipase e fosfolipase são usados como ferramentas de diagnóstico para detectar níveis de triglicerídeos, colesterol e fosfolipídios em amostras de sangue (CHEN et al., 2022b; THAKKAR et al., 2023).

O uso de lipases na produção de biodiesel é uma das metodologias mais conhecidas e difundidas do mercado através da transesterificação de óleos e gorduras (WANCURA et al., 2023). Lipases são apontadas como a enzima mais importante para a indústria de cosméticos devido ao seu uso como ingrediente ativo em formulações de cosméticos e na síntese de ésteres utilizados nesses materiais. Além disso, pode ser usada na produção de medicamentos (BALOGH-WEISER et al., 2023), detergentes (SAFDAR et al., 2023), desengorduramento de efluentes industriais (NIMKANDE et al., 2023) e matérias-primas têxteis (TALEB et al., 2022).

Na indústria de alimentos, as lipases são amplamente aplicadas em laticínios através da hidrólise da gordura do leite e na catálise da maturação de queijos (CHEN et al., 2021; GUAN et al., 2021). Também existe uma grande demanda de enzimas lipolíticas na síntese de ésteres flavorizantes (GONÇALVES et al., 2021), na redução do nível de gordura de carnes (MOHAMMED et al., 2023) e na panificação (XIANG et al., 2021). Por fim, a modificação de óleos e gorduras é uma das principais áreas do processamento de alimentos que requer novas tecnologias econômicas e verdes. As lipases modificam as propriedades dos lipídeos e os convertem em produtos de alto valor agregado, como na transesterificação de lipídeos estruturados e de óleos ricos em PUFAs ômega-3 (ALI et al., 2023). As aplicações empregadas no presente trabalho são apresentadas a seguir.

2.7 Ésteres flavorizantes

O aroma é o aditivo responsável por determinar as propriedades sensoriais e a identidade de um produto, sendo considerado um parâmetro chave associado à aceitação do consumidor. Estima-se que o mercado de flavorizantes de alimentos tenha alcançado US$12,8 bilhões em 2023 (SANTOS et al., 2023; PAULINO et al., 2021). Entretanto, a produção de aromas naturais atualmente não é capaz de atender a demanda comercial,

fazendo-se necessária a utilização de ferramentas biotecnológicas para oferecer processos eficientes e sustentáveis (PEREIRA et al., 2022; SOUSA et al., 2021).

Tradicionalmente, ésteres flavorizantes são isolados de fontes naturais por extração ou produzidos por meio de reações químicas. No entanto, esses métodos possuem algumas limitações, como a baixa concentração dos componentes ativos desejados presentes na matéria-prima e/ou sua dificuldade de remoção da matriz, o que demanda etapas adicionais de purificação e eleva os custos do processo; influência das condições climáticas e de processamento; toxicidade de reagentes químicos e catalisadores; e possibilidade de formação de subprodutos (BAYRAMOGLU et al., 2022; VILAS BÔAS e DE CASTRO, 2022). Dessa forma, a catálise enzimática é capaz de reduzir várias dessas limitações com características específicas de seletividade e pureza, atuação em condições de reação moderadas, além de ser considerada uma alternativa mais sustentável que a catálise química e conferir ao éster o rótulo de produto natural (MELO et al., 2023).

Uma importante vertente que se encontra em constante expansão nos últimos anos é a aplicação da lipase como catalisador da síntese de ésteres de aromas, obtidos a partir da reação de esterificação de um ácido carboxílico de cadeia curta ou média e um álcool, produzindo normalmente aromas frutados e florais (Tabela 3). Por esse motivo, tais compostos são imprescindíveis para os setores de limpeza, alimentos, cosméticos e higiene pessoal (BAYOUT et al., 2020; KOVALENKO et al., 2021; ZAPPATERRA et al., 2021).

Tabela 3. Tipos de ésteres de aromas produzidos por lipases.

Éster de aroma	Aroma	Conversão (%)	Referência
Acetato de cinamila	Canela, floral, adocicado, apimentado, balsâmico	99 % de rendimento	(DONG et al., 2020)
Acetato de isoamila	Frutado (banana)	93 % de rendimento	(OLIVEIRA et al., 2022)
Benzoato de benzila	Balsâmico, herbáceo, oleoso	92 % de rendimento	(MENESES et al., 2020b)
Butirato de benzila	Frutado (ameixa)	90 % de rendimento	(MENESES et al., 2019)
Butirato de butila	Frutado (abacaxi)	82 % de rendimento	(GONÇALVES et al., 2021)

Butirato de citronelila	Floral (rosa)	99 % de rendimento	(GIRÃO NETO et al., 2023)
Lactato de etila	Amanteigado, frutado, vinagre	87 % de rendimento	(MEHTA et al., 2020)
		88 % de rendimento	(KOUTINAS et al., 2018)
		83 % de rendimento	(SUN et al., 2010)
Propionato de benzila	Nozes, adocicado, frutado	99 % de rendimento	(JAWALE e BHANAGE, 2021)

O lactato de etila, ou éster etílico do ácido láctico, é um éster monobásico produzido pela combinação de ácido láctico e etanol. Reconhecido por sua versatilidade e alto desempenho, é amplamente empregado como solvente e agente solubilizante "verde" em inúmeras aplicações industriais, incluindo materiais para revestimentos especiais, tintas e produtos de limpeza (MAJGAONKAR et al., 2021; MEHTA et al., 2020). Além disso, desempenha um papel crucial devido à sua baixa toxicidade, principalmente como agente aromatizante que confere notas amanteigadas a laticínios e vinhos, além de estar associado a diferentes sabores como repolho, ervilha, vinagre, pão, amora, frango assado, abacaxi e framboesa (KOUTINAS et al., 2018).

Por fim, o lactato de etila destaca-se como ingrediente farmacêutico e aditivo alimentar por ser Geralmente Reconhecido como Seguro (GRAS) pela Food and Drug Administration (FDA) e pela European Food Safety Authority (EFSA) (CONG et al., 2019; XUE et al., 2024). Até o momento, a esterificação do lactato de etila via tratamento enzimático a partir de lipase imobilizada em carvão ativado do resíduo do sisal não foi relatada na literatura. Nesse sentido, é interessante explorar a viabilidade comercial do derivado produzido em sintetizar esse flavorizante.

2.8 Ácidos graxos poli-insaturados ômega-3 (PUFAs n-3)

Os ácidos graxos (AG) de ocorrência natural podem ser classificados de acordo com o comprimento da cadeia carbônica, onde AG que contêm mais de 12 átomos de carbono são chamados de AG de cadeia longa. Além disso, com base no número de ligações duplas, os ácidos graxos podem ser divididos em saturados (SFAs, sem ligações duplas),

monoinsaturados (MUFAs, uma ligação dupla única) e poli-insaturados (PUFAs, ≥ 2 ligações duplas). Os PUFAs ainda podem ser classificados em dois grupos, ômega-3 (ω-3 ou n-3) e ômega-6 (ω-6 ou n-6), com base na posição da primeira ligação dupla na extremidade do terminal metila (OLIVER et al., 2020; SAINI et al., 2021).

Os PUFAs ômega-3 são reconhecidos como nutrientes essenciais para a nutrição e saúde humana, de modo que precisam ser introduzidos pela dieta ou outros tipos de suplementação (INNES e CALDER, 2020). Os três principais tipos de ácidos graxos ômega-3 envolvidos na fisiologia humana são o ácido α-linolênico (ALA, 18:3-$\triangle^{9,12,15}$), o ácido eicosapentaenoico (EPA, 20:5-$\triangle^{5,8,11,14,17}$) e o ácido docosaexaenoico (DHA, 22:6-$\triangle^{4,7,10,13,16,19}$), que podem ser encontrados no mercado principalmente na forma de triglicerídeos e ésteres etílicos (MAGONI et al., 2022).

EPA e DHA são compostos valiosos por desempenharem papel crucial na prevenção de diversas doenças, como as doenças coronarianas (SHEN et al., 2022). Esses PUFAs estão envolvidos no desenvolvimento de estruturas de membrana, cérebro e retina, e na regulação da função metabólica e fisiológica, como a redução de triacilgliceróis no sangue e o controle da pressão arterial (ZHANG et al., 2022b). Além disso, as atividades antioxidantes e anti-inflamatórias do EPA e DHA desempenham um efeito preventivo ou paliativo contra doenças neurodegenerativas (KOUSPAROU et al., 2023) e cancerígenas (SIM et al., 2022) e, mais recentemente, COVID 19 (TAHA et al., 2022).

Dentro desse contexto e com base na dose diária recomendada (500 mg/pessoa), a demanda global de ácidos graxos ômega-3 é estimada em mais de 1,27 milhões de toneladas por ano e espera-se que esta procura cresça continuamente (cerca de 11 % entre 2020 e 2025). O mercado de PUFAs ômega-3 está avaliado em USD 2,1 bilhões e foi projetado um crescimento de 7,8 % entre 2020 e 2028 (BENVENGA et al., 2022). A distribuição de ácidos graxos n-3 ocorre na forma de triglicerídeos e ésteres etílicos para diversas aplicações, como suplementos dietéticos e alimentos fortificados. A América do Sul pode ser citada como um mercado crescente impulsionado pelo alto consumo de produtos fortificados (CHOPRA et al., 2022).

2.8.1 Reaproveitamento de resíduos marinhos para produção de PUFAs

A principal fonte de ácidos graxos ômega-3 é marinha, principalmente peixes e crustáceos como o salmão, atum, sardinha, camarão e lula. No entanto, o processamento dessas espécies produz quantidades significativas de subprodutos. Em países ocidentais

como o Brasil e a Austrália, existe um nível considerável de desperdício resultante da subutilização de partes de mariscos, uma vez que apenas a carne é consumida por grande parte das pessoas (ÖZYURT e ÖZKUTUK, 2020). De acordo com a Organização para a Alimentação e Agricultura (FAO), a produção anual de mariscos está estimada em mais de 180 milhões de toneladas, mas cerca de um quarto de sua massa total é descartada (AUBOURG et al., 2023).

Recentemente, tem sido discutida a valorização de espécies marinhas descartadas e subprodutos da indústria de frutos do mar por apresentarem composição constituinte semelhante aos tecidos marinhos comerciais e comestíveis (AUBOURG et al., 2023). Ahmad et al. (2019) reportou altos níveis de PUFAs ricos em ω-3 em extratos lipídicos da cabeça (26 e 29 %), intestino (24 e 27 %) e fígado (23 e 24 %) da sardinha e atum, respectivamente. Nesse sentido, o desenvolvimento de novas tecnologias e estratégias para recuperação e purificação de compostos de alto valor agregado, como os PUFAs ω-3, pode promover um aproveitamento sustentável de resíduos, além da incorporação em formulações nutracêuticas, alimentos funcionais ou aplicações farmacêuticas.

Uma fonte alternativa de matéria-prima para a obtenção de PUFAs são as vísceras da lula. As lulas são consideradas frutos do mar econômicos com elevada qualidade proteica e nutricional que podem trazer inúmeros benefícios às funções fisiológicas humanas. Park (2017) observou um conteúdo significativo de EPA (20,23 %) e DHA (35,50 %) para o óleo de lula. No entanto, o processamento da lula gera uma grande quantidade de subprodutos que representam 35 % da massa total capturada e incluem cabeça, vísceras e pele (WANG et al., 2019b). Estudos têm sido desenvolvidos com o intuito de reaproveitar tais componentes, onde Aubourg et al. (2023) relatou altos níveis de EPA (17,73 %) e DHA (34,67 %) para uma mistura de resíduo de lula. Até o momento, não foi relatada na literatura a reutilização do óleo proveniente do intestino da lula para obtenção de compostos n-3 PUFAs.

Diversas reações podem ser empregadas no processamento de óleos ômega-3 por meio de métodos químicos ou enzimáticos, onde a biotransformação enzimática apresenta vantagens por ser um processo verde com elevada seletividade e especificidade sob condições amenas. Nesse sentido, é possível destacar a glicerólise entre as reações em potencial para o tratamento do óleo residual de lula.

2.8.2 Glicerólise

A glicerólise é a reação de transesterificação entre ácidos graxos livres (AGL), mono (MAG), di (DAG) ou triacilgliceróis (TAG) e glicerol. A reação entre acilgliceróis e glicerol é uma alternativa ao tratamento de esterificação convencional para a redução do teor de ácidos graxos livres dos óleos (MAMTANI et al., 2021), como é o caso do óleo residual de lula, que apresenta 44,25 % de ácidos graxos livres em sua composição. Os AGLs são compostos mais instáveis e susceptíveis à oxidação frente aos demais componentes lipídicos quando submetidos a variações nas condições operacionais. Por esse motivo, é necessária a conversão eficaz de ácidos graxos livres em lipídeos estruturais, como os mono e diacilgliceróis (NICHOLSON e MARANGONI, 2022).

A composição lipídica de óleos e gorduras é dividida em Etil Ester (EE), Ácido Graxo Livre (AGL), Monoacilglicerol (MAG), Diacilglicerol (DAG) e Triacilglicerol (TAG). As formas mais disponíveis de concentrados de ômega-3 são EE e TAG. No entanto, estudos recentes demonstraram que MAG e DAG (MDG) são mais facilmente utilizados pelo corpo humano devido às diferenças em relação a absorção, digestão e estereoespecificidade (CHEN et al., 2022a; GUNATHILAKE et al., 2021). Além disso, as propriedades de cristalização e fusão dos MDGs também despertam interesse por apresentarem maior ponto de cristalização e fusão que os TAGs (NICHOLSON e MARANGONI, 2022).

Mono e diacilgliceróis são surfactantes não iônicos amplamente utilizados na indústria de alimentos como emulsificantes (Ex. margarinas, molhos, laticínios e panificação) e podem ser considerados ingredientes funcionais por suas propriedades nutricionais. Além disso, são utilizados em cosméticos, fármacos e têxteis devido às suas características plastificantes e texturizantes (AWADALLAK et al., 2020; PALACIOS et al., 2022). Nesse sentido, há um grande interesse de mercado na obtenção de mono e diacilglicerois de ômega-3 uma vez que é sintetizado um produto de alto valor agregado com maior estabilidade à oxidação enquanto fornece absorção e digestão adequadas.

Um esquema simplificado para a reação de esterificação de AGLs em MAG, DAG e TAG através da glicerólise é apresentado na Figura 8.

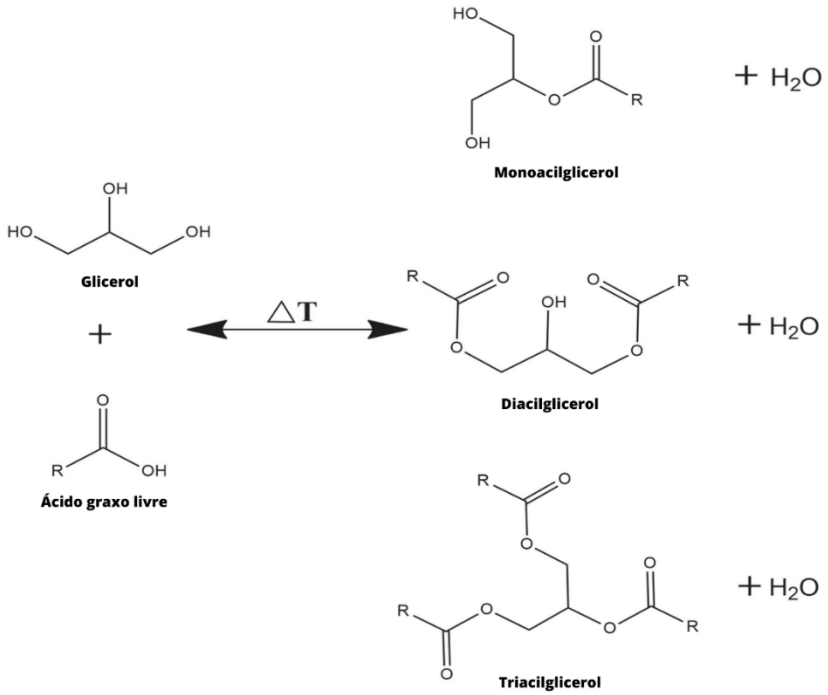

Figura 8. Esquema de reação de glicerólise. Fonte: (MAMTANI et al., 2021).

O glicerol é uma molécula hidrofílica que possui três grupos hidroxila ligados à sua estrutura e, portanto, apresenta baixa solubilidade em soluções orgânicas (4-5 % em gorduras comuns). Essa insolubilidade traz limitações à reação e, a menos que seja realizada na presença de um catalisador ou em elevadas temperaturas, levará longos períodos para ser concluída. A eficiência da reação de glicerólise catalisada por lipases pode ser influenciada pelas condições reacionais, como: concentração enzimática, temperatura, razão molar de substrato, presença de solventes e tempo de reação (LI et al., 2023; PALACIOS et al., 2019). Sendo assim, é importante investigar o efeito dos parâmetros de glicerólise no tratamento enzimático do óleo de lula.

A incorporação de óleos ómega-3 em alimentos é limitada pela elevada susceptibilidade desses óleos altamente insaturados à oxidação, principalmente na exposição ao ar, luz e temperaturas elevadas. Tais limitações podem ser solucionadas a partir do desenvolvimento de metodologias de proteção da estrutura lipídica, onde a microencapsulação pode ser citada.

2.9 Oxidação lipídica dos PUFAs

Nos últimos anos, as tendências de mercado têm se adaptado ao novo perfil dos consumidores em buscar alimentos que ofereçam propriedades benéficas a saúde. Espera-se

que os produtos auxiliem na saúde e bem-estar para além da sua função básica de fornecer os nutrientes necessários ao funcionamento do corpo humano. Assim, o conceito de alimentos funcionais é ativamente promovido por governos, indústria e população (WANG et al., 2019a). Os óleos ricos em PUFAs ômega-3 são um importante exemplo dessa tendência de consumo. No entanto, a aplicação desses óleos na indústria de alimentos é limitada por sua susceptibilidade à oxidação durante a produção e armazenamento. A oxidação dos PUFAs compromete as propriedades funcionais dos produtos e produz características sensoriais desagradáveis (XIA et al., 2020).

A oxidação lipídica é um fenômeno complexo relacionado à uma série de reações químicas indesejáveis que afetam a qualidade de alimentos, cosméticos e fármacos. As reações envolvem a degradação de lipídeos que resultam na formação de sabores e aromas desagradáveis (*off-flavors*) e produtos potencialmente tóxicos, além de outros efeitos negativos como a descoloração, destruição de vitaminas, perdas nutricionais e polimerização (GARCIA-OLIVEIRA et al., 2021). Dentro das vias químicas, a oxidação lipídica pode ocorrer por oxidação enzimática, foto-oxidação ou auto-oxidação, que podem ser induzidas por diferentes fatores, incluindo temperatura, exposição à luz, teor de oxigênio, grau de insaturação dos lipídeos formulados e presença de espécies pró-oxidantes (fotossensibilizadores, metais pró-oxidantes, espécies radicais). Além disso, a composição, estrutura e propriedades de um produto também influenciam na sensibilidade à oxidação lipídica, incluindo o teor de umidade, atividade de água, organização estrutural, reologia e estado físico (QIU et al., 2019; VILLENEUVE et al., 2021).

A microencapsulação pode proteger o composto ativo contra a oxidação durante o armazenamento, processamento ou incorporação em alimentos e medicamentos (MU et al., 2022; ŠAVIKIN et al., 2021). Dentre as metodologias de encapsulamento aplicadas ao óleo de peixe, podem ser citadas as emulsões, lipossomas, hidrogéis e coacervados complexos. A coacervação complexa tem sido amplamente utilizada nos últimos anos por apresentar características únicas como baixo custo, alta estabilidade, estrutura compacta, alta densidade de carga e processamento em condições moderadas (XIA et al., 2019).

2.9.1 Microencapsulação por coacervação complexa

A coacervação complexa ocorre a partir do revestimento do composto de interesse utilizando duas macromoléculas biológicas de cargas opostas que são responsáveis por formar um invólucro complexo por interação eletrostática e outras forças motrizes. Uma

ampla gama de biopolímeros, especialmente proteínas e carboidratos, pode ser combinada para a formação dos coacervados complexos. Na indústria alimentícia moderna, a gelatina é a principal proteína usada nessa técnica, enquanto outras moléculas aniônicas podem ser empregadas, como a goma arábica, dodecil sulfato de sódio (SDS), quitosana, pectina e hexametafosfato de sódio (SHMP) (DU et al., 2022a; MA et al., 2019; XIA et al., 2020).

O processo de microencapsulação por coacervação complexa envolve quatro etapas principais: 1) Preparação de emulsões óleo-água e definição do tamanho das estruturas internas das cápsulas; 2) Coacervação, onde gotículas de óleo na emulsão são revestidas pelos coacervados através do ajuste de pH da emulsão. Durante essa etapa, as gotículas de óleo revestidas tendem a se aglomerar para formar partículas de tamanho definido, onde espera-se que as partículas estejam dentro do limiar sensorial (entre 10–25 μm) para que sejam imperceptíveis pela boca; 3) Resfriamento, que irá favorecer a formação da camada externa ao redor dos aglomerados; 4) Enrijecimento do invólucro da microcápsula por reticulação enzimática ou química, de modo que as partículas não possam ser redissolvidas (WANG et al., 2014). Vários parâmetros operacionais podem influenciar a coacervação complexa através de interações eletrostáticas, como força iônica, pH, proporção, distribuição de carga e hidrofobicidade relativa dos polímeros empregados, além das propriedades físicas e químicas das microcápsulas (MA et al., 2019).

Nesse sentido, é interessante explorar a estabilidade oxidativa do método de microencapsulação por coacervação complexa de acilgliceróis ricos em PUFAs ômega-3 obtidos da reação de glicerólise do óleo proveniente do intestino da lula utilizando lipases imobilizadas em carvão ativado do resíduo do sisal.

3. OBJETIVOS

3.1 Objetivo Geral

Produzir biorreatores por meio da imobilização de lipase em carvão ativado sintetizado a partir do resíduo de sisal e submetido a diferentes métodos de modificação, investigando o potencial dos derivados mais promissores em sintetizar lactato de etila e acilgliceróis ricos em ômega-3.

3.2 Objetivos Específicos

- Sintetizar carvões ativados através da ativação química com ácido fosfórico utilizando o resíduo do processamento do sisal como precursor de carbono;

- Modificar a superfície do carvão por meio da incorporação da genipina como agente reticulante;
- Modificar a superfície do carvão por meio da incorporação do ácido iminodiacético (IDA) como agente quelante + partículas metálicas;
- Modificar a superfície do carvão por meio da incorporação da genipina como agente reticulante + partículas metálicas;
- Caracterizar os carvões ativados produzidos;
- Avaliar a eficiência das funcionalizações dos carvões na imobilização de lipases;
- Investigar o potencial dos derivados em sintetizar o éster lactato de etila (aroma amanteigado);
- Avaliar a estabilidade operacional da lipase imobilizada de acordo com os ciclos de esterificação;
- Investigar o potencial dos derivados em converter o elevado teor de ácidos graxos livres do óleo residual de lula em acilglicerois ricos em PUFAs Ômega-3;
- Avaliar a estabilidade à oxidação dos acilglicerois de Ômega-3 encapsulados por coacervação complexa;
- Caracterizar as microcápsulas de acordo com as propriedades físico-químicas e morfológicas.

4. REFERÊNCIAS

ABED, K. M. et al. Palm Raceme as a Promising Biomass Precursor for Activated Carbon to Promote Lipase Activity with the Aid of Eutectic Solvents. **Molecules**, v. 27, n. 24, 1 dez. 2022.

ABUELNOOR, N. et al. **Activated carbons from biomass-based sources for CO2 capture applications**. **Chemosphere**Elsevier Ltd, , 1 nov. 2021.

ADAMIAK, K.; SIONKOWSKA, A. **Current methods of collagen cross-linking: Review**. **International Journal of Biological Macromolecules**Elsevier B.V., , 15 out. 2020.

ADELEYE, A. T. et al. **Efficient synthesis of bio-based activated carbon (AC) for catalytic systems: A green and sustainable approach**. **Journal of Industrial and Engineering Chemistry**Korean Society of Industrial Engineering Chemistry, , 25 abr. 2021a.

ADELEYE, A. T. et al. **Efficient synthesis of bio-based activated carbon (AC) for catalytic systems: A green and sustainable approach**. **Journal of Industrial and Engineering Chemistry**Korean Society of Industrial Engineering Chemistry, , 25 abr. 2021b.

AGGARWAL, S.; CHAKRAVARTY, A.; IKRAM, S. **A comprehensive review on incredible renewable carriers as promising platforms for enzyme immobilization & thereof strategies**. **International Journal of Biological Macromolecules**Elsevier B.V., , 15 jan. 2021.

AHMAD, T. B. et al. Correlation between fatty acid profile and anti-inflammatory activity in common Australian seafood by-products. **Marine Drugs**, v. 17, n. 3, 6 mar. 2019.

ALI, S. et al. **The Recent Advances in the Utility of Microbial Lipases: A Review**. **Microorganisms**MDPI, , 1 fev. 2023.

ALMEIDA, F. L. C.; PRATA, A. S.; FORTE, M. B. S. **Enzyme immobilization: what have we learned in the past five years? Biofuels, Bioproducts and Biorefining**John Wiley and Sons Ltd, , 1 mar. 2022.

ALVEAR-DAZA, J. J. et al. Removal of diclofenac and ibuprofen on mesoporous activated carbon from agro-industrial wastes prepared by optimized synthesis employing a central composite design. **Biomass Conversion and Biorefinery**, 1 set. 2022.

ALVES, A. N. et al. Extraction of protease from ora-pro-nobis (Pereskia aculeata Miller) and partial purification in polyethylene glycol + sodium phosphate aqueous two-phase system. **Journal of Food Processing and Preservation**, v. 46, n. 2, 1 fev. 2022.

ARANA-PEÑA, S. et al. **Enzyme co-immobilization: Always the biocatalyst designers' choice…or not? Biotechnology Advances**Elsevier Inc., , 1 nov. 2021.

ASHOKKUMAR, V. et al. **Recent advances in lignocellulosic biomass for biofuels and value-added bioproducts - A critical review**. **Bioresource Technology**Elsevier Ltd, , 1 jan. 2022.

ASLAN, Y.; SHARIF, Y. M.; ŞAHIN, Ö. Covalent immobilization of Aspergillus niger amyloglucosidase (ANAG) with ethylenediamine-functionalized and glutaraldehyde-activated active carbon (EFGAAC) obtained from sesame seed shell. **International Journal of Biological Macromolecules**, v. 142, p. 222–231, 1 jan. 2020.

AUBOURG, S. P. et al. Yield Enhancement of Valuable Lipid Compounds from Squid (Doryteuthis gahi) Waste by Ethanol/Acetone Extraction. **Foods**, v. 12, n. 14, p. 2649, 9 jul. 2023.

AWADALLAK, J. A.; DA SILVA, E. A.; DA SILVA, C. Production of linseed diacylglycerol-rich oil by combined glycerolysis and esterification. **Industrial Crops and Products**, v. 145, 1 mar. 2020.

BAIG, K. S. **Interaction of enzymes with lignocellulosic materials: causes, mechanism and influencing factors**. **Bioresources and Bioprocessing**Springer Science and Business Media Deutschland GmbH, , 1 dez. 2020.

BALOGH-WEISER, D. et al. Combined Nanofibrous Face Mask: Co-Formulation of Lipases and Antibiotic Agent by Electrospinning Technique. **Pharmaceutics**, v. 15, n. 4, 1 abr. 2023.

BARROSO-BOGEAT, A. et al. Activated carbon surface chemistry: Changes upon impregnation with Al(III), Fe(III) and Zn(II)-metal oxide catalyst precursors from NO3− aqueous solutions. **Arabian Journal of Chemistry**, v. 12, n. 8, p. 3963–3976, 1 dez. 2019.

BAYOUT, I. et al. Natural flavor ester synthesis catalyzed by lipases. **Flavour and Fragrance Journal**, v. 35, n. 2, p. 209–218, 1 mar. 2020.

BAYRAMOGLU, G. et al. Immobilization of Candida rugosa lipase on magnetic chitosan beads and application in flavor esters synthesis. **Food Chemistry**, v. 366, 1 jan. 2022a.

BAYRAMOGLU, G. et al. Immobilization of Candida rugosa lipase on magnetic chitosan beads and application in flavor esters synthesis. **Food Chemistry**, v. 366, 1 jan. 2022b.

BENÍTEZ, A. et al. **Recent advances in lithium-sulfur batteries using biomass-derived carbons as sulfur host**. **Renewable and Sustainable Energy Reviews**Elsevier Ltd, , 1 fev. 2022.

BENVENGA, S. et al. **Fish and the Thyroid: A Janus Bifrons Relationship Caused by Pollutants and the Omega-3 Polyunsaturated Fatty Acids**. **Frontiers in Endocrinology**Frontiers Media S.A., , 27 maio 2022.

BHARATHI, D.; RAJALAKSHMI, G. **Microbial lipases: An overview of screening, production and purification**. **Biocatalysis and Agricultural Biotechnology**Elsevier Ltd, , 1 nov. 2019.

Biorefinery: A Sustainable Approach for the Production of Biomaterials, Biochemicals and Biofuels. [s.l.] Springer Nature Singapore, 2023.

BORGES, J. F. et al. Laccase Immobilization on Activated Carbon from Hydrothermal Carbonization of Corn Cob. **Waste and Biomass Valorization**, 2023.

BOUNEGRU, A. V.; APETREI, C. **Tyrosinase Immobilization Strategies for the Development of Electrochemical Biosensors—A Review**. **Nanomaterials**MDPI, , 1 fev. 2023.

CAMPOS, N. F. et al. Adsorption of naphthenic acids on peanut shell activated carbon: Batch and fixed-bed column study of the process. **Chemical Engineering Research and Design**, v. 188, p. 633–644, 1 dez. 2022.

CHAKHTOUNA, H. et al. **Recent advances in eco-friendly composites derived from lignocellulosic biomass for wastewater treatment**. **Biomass Conversion and Biorefinery**Springer Science and Business Media Deutschland GmbH, , 2022.

CHANDRA, P. et al. **Microbial lipases and their industrial applications: A comprehensive review**. **Microbial Cell Factories**BioMed Central Ltd, , 26 ago. 2020.

CHAO, H. et al. Template-Free in Situ Encapsulation of Enzymes in Hollow Covalent Organic Framework Capsules for the Electrochemical Analysis of Biomarkers. **ACS Applied Materials and Interfaces**, 2022.

CHAROENSOOK, K. et al. Preparation of porous nitrogen-doped activated carbon derived from rice straw for high-performance supercapacitor application. **Journal of the Taiwan Institute of Chemical Engineers**, v. 120, p. 246–256, 1 mar. 2021.

CHEN, W. et al. Encapsulation of lipases by nucleotide/metal ion coordination polymers: enzymatic properties and their applications in glycerolysis and esterification studies. **Journal of the Science of Food and Agriculture**, v. 102, n. 10, p. 4012–4024, 15 ago. 2022a.

CHEN, X. et al. Lipase-catalyzed modification of milk fat: A promising way to alter flavor notes of goat milk products. **LWT**, v. 145, 1 jun. 2021.

CHEN, Y. et al. Hollow Hierarchical Cu-BTC as Nanocarriers to Immobilize Lipase for Electrochemical Biosensor. **Journal of Inorganic and Organometallic Polymers and Materials**, v. 32, n. 11, p. 4401–4411, 1 nov. 2022b.

CHOPRA, A. S. et al. **The current use and evolving landscape of nutraceuticals**. **Pharmacological Research**Academic Press, , 1 jan. 2022.

CHOUDHARY, S. et al. Advantages and applications of sisal fiber reinforced hybrid polymer composites in automobiles: A literature review. **Materials Today: Proceedings**, 2023.

COLLEY, T. A. et al. Addressing nutrient depletion in Tanzanian sisal fiber production using life cycle assessment and circular economy principles, with bioenergy co-production. **Sustainability (Switzerland)**, v. 13, n. 16, 2 ago. 2021.

CONG, S. et al. Synthesis of flavor esters by a novel lipase from Aspergillus niger in a soybean-solvent system. **3 Biotech**, v. 9, n. 6, 1 jun. 2019.

DARWESH, O. M. et al. Enzymes immobilization onto magnetic nanoparticles to improve industrial and environmental applications. Em: **Methods in Enzymology**. [s.l.] Academic Press Inc., 2020. v. 630p. 481–502.

DE MENESES, A. C. et al. Benzyl butyrate esterification mediated by immobilized lipases: Evaluation of batch and fed-batch reactors to overcome lipase-acid deactivation. **Process Biochemistry**, v. 78, p. 50–57, 1 mar. 2019.

DE MENESES, A. C. et al. Enzymatic synthesis of benzyl benzoate using different acyl donors: Comparison of solvent-free reaction techniques. **Process Biochemistry**, v. 92, p. 261–268, 1 maio 2020a.

DE MENESES, A. C. et al. Enzymatic synthesis of benzyl benzoate using different acyl donors: Comparison of solvent-free reaction techniques. **Process Biochemistry**, v. 92, p. 261–268, 1 maio 2020b.

DE OLIVEIRA, T. P. et al. Incorporation of metallic particles in activated carbon used in lipase immobilization for production of isoamyl acetate. **Journal of Chemical Technology and Biotechnology**, v. 97, n. 7, p. 1736–1746, 1 jul. 2022.

DE SOUSA, I. G. et al. Renewable processes of synthesis of biolubricants catalyzed by lipases. **Journal of Environmental Chemical Engineering**, v. 11, n. 1, 1 fev. 2023.

DIN, M. H. M. et al. Heterologous expression and characterization of plant lipase lip2 from elaeis guineensis jacq. Oil palm mesocarp in escherichia coli. **Catalysts**, v. 11, n. 2, p. 1–20, 1 fev. 2021.

DIZBAY-ONAT, M. et al. Applicability of industrial sisal fiber waste derived activated carbon for the adsorption of volatile organic compounds (VOCs). **Fibers and Polymers**, v. 19, n. 4, p. 805–811, 1 abr. 2018.

DONG, F. et al. Facile One-Pot Immobilization of a Novel Esterase and Its Application in Cinnamyl Acetate Synthesis. **Catalysis Letters**, v. 150, n. 9, p. 2517–2528, 1 set. 2020.

DOS SANTOS, M. M. O. et al. Synthesis of hexyl butyrate (apple and citrus aroma) by Candida rugosa lipase immobilized on Diaion HP-20 using the Box-Behnken design. **Food Science and Biotechnology**, v. 32, n. 5, p. 689–696, 1 abr. 2023.

DU, Q. et al. **Omega-3 polyunsaturated fatty acid encapsulation system: Physical and oxidative stability, and medical applications**. **Food Frontiers**John Wiley and Sons Inc, , 1 jun. 2022a.

DU, Y. et al. **Metal-organic frameworks with different dimensionalities: An ideal host platform for enzyme@MOF composites**. **Coordination Chemistry Reviews**Elsevier B.V., , 1 mar. 2022b.

DUAN, D. et al. **Activated carbon from lignocellulosic biomass as catalyst: A review of the applications in fast pyrolysis process**. **Journal of Analytical and Applied Pyrolysis**Elsevier B.V., , 1 set. 2021.

DUNFORD, E. K.; MILES, D. R.; POPKIN, B. Food Additives in Ultra-Processed Packaged Foods: An Examination of US Household Grocery Store Purchases. **Journal of the Academy of Nutrition and Dietetics**, p. 889–901, 2023.

FASIM, A.; MORE, V. S.; MORE, S. S. **Large-scale production of enzymes for biotechnology uses**. **Current Opinion in Biotechnology**Elsevier Ltd, , 1 jun. 2021.

FATIHA, N. et al. The guideline for author in preparing manuscript for the Malaysian Journal of Chemical Engineering and Technology. **Malaysian Journal of Chemical Engineering & Technology Journal Homepage**, v. 3, n. 2, p. 45–50, 2020.

FERREIRA GONÇALVES, G. R. et al. Immobilization of porcine pancreatic lipase on activated carbon by adsorption and covalent bonding and its application in the synthesis of butyl butyrate. **Process Biochemistry**, v. 111, p. 114–123, 1 dez. 2021.

FILHO, D. G.; SILVA, A. G.; GUIDINI, C. Z. **Lipases: sources, immobilization methods, and industrial applications**. **Applied Microbiology and Biotechnology**Springer Verlag, , 1 set. 2019.

FOPASE, R. et al. Strategies, challenges and opportunities of enzyme immobilization on porous silicon for biosensing applications. **Journal of Environmental Chemical Engineering**, v. 8, n. 5, 1 out. 2020.

GARCIA-OLIVEIRA, P. et al. **Evolution of flavors in extra virgin olive oil shelf-life**. **Antioxidants**MDPI, , 1 mar. 2021.

GIRÃO NETO, C. A. C. et al. Enzymatic synthesis of citronellyl butyrate by lipase B from Candida antarctica immobilized on magnetic cashew apple bagasse lignin. **Process Biochemistry**, v. 131, p. 244–255, 1 ago. 2023.

GIRELLI, A. M.; ASTOLFI, M. L.; SCUTO, F. R. **Agro-industrial wastes as potential carriers for enzyme immobilization: A review**. **Chemosphere**Elsevier Ltd, , 1 abr. 2020.

GIRELLI, A. M.; CHIAPPINI, V.; AMADORO, P. Immobilization of lipase on spent coffee grounds by physical and covalent methods: A comparison study. **Biochemical Engineering Journal**, v. 192, 1 mar. 2023.

GOMEZ-DELGADO, E. et al. Agroindustrial waste conversion into ultramicroporous activated carbons for greenhouse gases adsorption-based processes. **Bioresource Technology Reports**, v. 18, 1 jun. 2022.

GRACIDA, J. et al. Improved Thermal and Reusability Properties of Xylanase by Genipin Cross-Linking to Magnetic Chitosan Particles. **Applied Biochemistry and Biotechnology**, v. 188, n. 2, p. 395–409, 15 jun. 2019.

GUAJARDO, N.; AHUMADA, K.; DOMÍNGUEZ DE MARÍA, P. Immobilized lipase-CLEA aggregates encapsulated in lentikats® as robust biocatalysts for continuous processes in deep eutectic solvents. **Journal of Biotechnology**, v. 310, p. 97–102, 20 fev. 2020.

GUAN, T. et al. The enhanced fatty acids flavor release for low-fat cheeses by carrier immobilized lipases on O/W Pickering emulsions. **Food Hydrocolloids**, v. 116, 1 jul. 2021.

GÜLEÇ, F. et al. Hydrothermal conversion of different lignocellulosic biomass feedstocks – Effect of the process conditions on hydrochar structures. **Fuel**, v. 302, p. 121166, 15 out. 2021.

GUNATHILAKE, T.; AKANBI, T. O.; BARROW, C. J. Lipase-produced omega-3 acylglycerols for the fortification and stabilization of extra virgin olive oil using hydroxytyrosyl palmitate. **Future Foods**, v. 4, 1 dez. 2021.

HASANZADEH, M.; SIMCHI, A.; SHAHRIYARI FAR, H. Nanoporous composites of activated carbon-metal organic frameworks for organic dye adsorption: Synthesis, adsorption mechanism and kinetics studies. **Journal of Industrial and Engineering Chemistry**, v. 81, p. 405–414, 25 jan. 2020.

HEIDARINEJAD, Z. et al. **Methods for preparation and activation of activated carbon: a review**. **Environmental Chemistry Letters**Springer, , 1 mar. 2020a.

HEIDARINEJAD, Z. et al. **Methods for preparation and activation of activated carbon: a review**. **Environmental Chemistry Letters**Springer, , 1 mar. 2020b.

HU, S. C. et al. Structural changes and electrochemical properties of lacquer wood activated carbon prepared by phosphoric acid-chemical activation for supercapacitor applications. **Renewable Energy**, v. 177, p. 82–94, 1 nov. 2021.

HUSSIN, F.; AROUA, M. K.; YUSOFF, R. Adsorption of CO2on palm shell based activated carbon modified by deep eutectic solvent: Breakthrough adsorption study. **Journal of Environmental Chemical Engineering**, v. 9, n. 4, 1 ago. 2021.

IMAM, A. et al. Application of laccase immobilized rice straw biochar for anthracene degradation. **Environmental Pollution**, v. 268, 1 jan. 2021.

IMAM, H. T.; MARR, P. C.; MARR, A. C. **Enzyme entrapment, biocatalyst immobilization without covalent attachment**. **Green Chemistry**Royal Society of Chemistry, , 21 jul. 2021.

INNES, J. K.; CALDER, P. C. **Marine omega-3 (N-3) fatty acids for cardiovascular health: An update for 2020**. **International Journal of Molecular Sciences**MDPI AG, , 2 fev. 2020.

ISMAIL, A. R.; BAEK, K. H. **Lipase immobilization with support materials, preparation techniques, and applications: Present and future aspects**. **International Journal of Biological Macromolecules**Elsevier B.V., , 15 nov. 2020.

IWANOW, M. et al. **Activated carbon as catalyst support: Precursors, preparation, modification and characterization**. **Beilstein Journal of Organic Chemistry**Beilstein-Institut Zur Forderung der Chemischen Wissenschaften, , 2 jun. 2020.

JAWALE, P. V.; BHANAGE, B. M. Synthesis of propyl benzoate by solvent-free immobilized lipase-catalyzed transesterification: Optimization and kinetic modeling. **Bioprocess and Biosystems Engineering**, v. 44, n. 2, p. 369–378, 1 fev. 2021.

JIANG, C. et al. Activated carbons prepared by indirect and direct CO2 activation of lignocellulosic biomass for supercapacitor electrodes. **Renewable Energy**, v. 155, p. 38–52, 1 ago. 2020.

KAZEMI SHARIAT PANAHI, H. et al. **A comprehensive review of engineered biochar: Production, characteristics, and environmental applications**. **Journal of Cleaner Production**Elsevier Ltd, , 10 out. 2020.

KOUSPAROU, C. et al. DHA/EPA (Omega-3) and LA/GLA (Omega-6) as Bioactive Molecules in Neurodegenerative Diseases. **International Journal of Molecular Sciences**, v. 24, n. 13, p. 10717, 27 jun. 2023.

KOUTINAS, M. et al. Application of commercial and non-commercial immobilized lipases for biocatalytic production of ethyl lactate in organic solvents. **Bioresource Technology**, v. 247, p. 496–503, 2018.

KOVALENKO, G. et al. Lipase-active heterogeneous biocatalysts for enzymatic synthesis of short-chain aroma esters. **Biocatalysis and Agricultural Biotechnology**, v. 36, 1 set. 2021.

KUMAR, R.; PAL, P. Lipase immobilized graphene oxide biocatalyst assisted enzymatic transesterification of Pongamia pinnata (Karanja) oil and downstream enrichment of biodiesel by solar-driven direct contact membrane distillation followed by ultrafiltration. **Fuel Processing Technology**, v. 211, 1 jan. 2021.

LEÓN, A. Y. et al. Optimization of the preparation conditions for cocoa shell-based activated carbon and its evaluation as salts adsorbent material. **International Journal of Environmental Science and Technology**, v. 19, n. 8, p. 7777–7790, 1 ago. 2022.

LEWOYEHU, M. **Comprehensive review on synthesis and application of activated carbon from agricultural residues for the remediation of venomous pollutants in wastewater**. **Journal of Analytical and Applied Pyrolysis**Elsevier B.V., , 1 out. 2021.

LI, L. et al. Insight into the influence of plant oils on the composition of diacylglycerol fabricated by glycerolysis and esterification. **Industrial Crops and Products**, v. 204, 15 nov. 2023.

LI, W. et al. Production and characterization of lignocellulosic fractions from sisal waste. **Industrial Crops and Products**, v. 160, 1 fev. 2021.

LIU, D. et al. **Immobilization of Biomass Materials for Removal of Refractory Organic Pollutants from Wastewater**. **International Journal of Environmental Research and Public Health**MDPI, , 1 nov. 2022.

LIU, S. et al. **Smart chemistry of enzyme immobilization using various support matrices – A review**. **International Journal of Biological Macromolecules**Elsevier B.V., , 1 nov. 2021.

LIU, S.; SUN, Y. Co-encapsulating Cofactor and Enzymes in Hydrogen-Bonded Organic Frameworks for Multienzyme Cascade Reactions with Cofactor Recycling. **Angewandte Chemie International Edition**, 12 set. 2023.

LU, Y. et al. Selective conversion of lignocellulosic biomass into furan compounds using bimetal-modified bio-based activated carbon: Analytical Py-GC×GC/MS. **Journal of the Energy Institute**, v. 93, n. 6, p. 2371–2380, 1 dez. 2020.

LUO, J. et al. **Biocatalytic membrane: Go far beyond enzyme immobilization**. **Engineering in Life Sciences**Wiley-VCH Verlag, , 1 nov. 2020.

MA, T. et al. Effect of processing conditions on the morphology and oxidative stability of lipid microcapsules during complex coacervation. **Food Hydrocolloids**, v. 87, p. 637–643, 1 fev. 2019.

MAGHRABY, Y. R. et al. **Enzyme Immobilization Technologies and Industrial Applications**. **ACS Omega**American Chemical Society, , 14 fev. 2023.

MAGONI, C. et al. **Could microalgae be a strategic choice for responding to the demand for omega-3 fatty acids? A European perspective**. **Trends in Food Science and Technology**Elsevier Ltd, , 1 mar. 2022.

MAJGAONKAR, P. et al. Chemical Recycling of Post-Consumer PLA Waste for Sustainable Production of Ethyl Lactate. **Chemical Engineering Journal**, v. 423, 1 nov. 2021.

MAMTANI, K.; SHAHBAZ, K.; FARID, M. M. **Glycerolysis of free fatty acids: A review**. **Renewable and Sustainable Energy Reviews**Elsevier Ltd, , 1 mar. 2021.

MARIANA, M. et al. **Recent advances in activated carbon modification techniques for enhanced heavy metal adsorption**. **Journal of Water Process Engineering**Elsevier Ltd, , 1 out. 2021.

MEHTA, A. et al. Application of lipase purified from aspergillus fumigatus in the syntheses of ethyl acetate and ethyl lactate. **Journal of Oleo Science**, v. 69, n. 1, p. 23–29, 2020.

MELO, K. et al. **Experimental Analysis of Styrene, Particle Size, and Fiber Content in the Mechanical Properties of Sisal Fiber Powder Composites**. [s.l: s.n.].

MELO, R. L. F. et al. **Recent applications and future prospects of magnetic biocatalysts**. **International Journal of Biological Macromolecules**Elsevier B.V., , 31 dez. 2023.

MO, H. et al. Preparation and characterization of magnetic polyporous biochar for cellulase immobilization by physical adsorption. **Cellulose**, v. 27, n. 9, p. 4963–4973, 1 jun. 2020a.

MO, H. et al. Porous biochar/chitosan composites for high performance cellulase immobilization by glutaraldehyde. **Enzyme and Microbial Technology**, v. 138, 1 ago. 2020b.

MOHAMMED, A. B. A.; HEGAZY, A. E.; SALAH, A. Predigested high-fat meats based on Lactobacillus fermentum lipase enzyme immobilized on silver-alginate nanoparticle matrix. **Applied Nanoscience (Switzerland)**, v. 13, n. 1, p. 641–649, 1 jan. 2023.

MONTALVO ANDIA, J. et al. Synthesis and characterization of chemically activated carbon from Passiflora ligularis, Inga feuilleei and native plants of South America. **Journal of Environmental Chemical Engineering**, v. 8, n. 4, 1 ago. 2020.

MONTEIRO, R. R. C. et al. **Liquid lipase preparations designed for industrial production of biodiesel. Is it really an optimal solution? Renewable Energy**Elsevier Ltd, , 1 fev. 2021.

MORTAZAVI, S.; AGHAEI, H. Make proper surfaces for immobilization of enzymes: Immobilization of lipase and α-amylase on modified Na-sepiolite. **International Journal of Biological Macromolecules**, v. 164, p. 1–12, 1 dez. 2020.

MU, H. et al. Microencapsulation of algae oil by complex coacervation of chitosan and modified starch: Characterization and oxidative stability. **International Journal of Biological Macromolecules**, v. 194, p. 66–73, 1 jan. 2022.

MULEY, A. B. et al. Preparation of cross-linked enzyme aggregates of lipase from Aspergillus niger: process optimization, characterization, stability, and application for epoxidation of lemongrass oil. **Bioprocess and Biosystems Engineering**, v. 44, n. 7, p. 1383–1404, 1 jul. 2021.

NADAR, S. S.; RATHOD, V. K. Immobilization of proline activated lipase within metal organic framework (MOF). **International Journal of Biological Macromolecules**, v. 152, p. 1108–1112, 1 jun. 2020.

NAIR, L. G.; AGRAWAL, K.; VERMA, P. An overview of sustainable approaches for bioenergy production from agro-industrial wastes. **Energy Nexus**, v. 6, 16 jun. 2022.

NASCIMENTO, P. A. et al. Optimization of lipase extraction from pequi seed (Caryocar brasiliense Camb.). **Journal of Food Processing and Preservation**, v. 45, n. 7, 1 jul. 2021a.

NASCIMENTO, P. A. et al. Partitioning of pequi seed (Caryocar brasiliense Camb.) lipase in aqueous two-phase systems composed of PEG/2-propanol + ammonium sulfate + water. **Brazilian Journal of Chemical Engineering**, v. 38, n. 4, p. 957–965, 1 dez. 2021b.

NEMATIAN, T.; SALEHI, Z.; SHAKERI, A. Conversion of bio-oil extracted from Chlorella vulgaris micro algae to biodiesel via modified superparamagnetic nano-biocatalyst. **Renewable Energy**, v. 146, p. 1796–1804, 1 fev. 2020.

NICHOLSON, R. A.; MARANGONI, A. G. **Glycerolysis structured oils as natural fat replacements**. **Current Opinion in Food Science**Elsevier Ltd, , 1 fev. 2022.

NIMKANDE, V. D.; KRISHNAMURTHI, K.; BAFANA, A. Potential of Antarctic lipase from Acinetobacter johnsonii Ant12 for treatment of lipid-rich wastewater: screening, production, properties and applications. **Biodegradation**, 2023.

NURULLINA, P. V.; PERMINOVA, L. V.; KOVALENKO, G. A. Catalytic Properties of rPichia/lip Lipase Adsorbed on Carbon Nanotubes in the Low-Temperature Synthesis of Esters. **Moscow University Chemistry Bulletin**, v. 75, n. 2, p. 110–114, 1 mar. 2020.

NWAGU, T. N.; OKOLO, B.; AOYAGI, H. Immobilization of raw starch saccharifying amylase on glutaraldehyde activated chitin flakes increases the enzyme operation range. **Bioresource Technology Reports**, v. 13, 1 fev. 2021.

OLIVER, L. et al. **Producing omega-3 polyunsaturated fatty acids: A review of sustainable sources and future trends for the EPA and DHA market**. **Resources**MDPI AG, , 1 dez. 2020.

OTARI, S. V. et al. One-step hydrothermal synthesis of magnetic rice straw for effective lipase immobilization and its application in esterification reaction. **Bioresource Technology**, v. 302, 1 abr. 2020.

PALACIOS, D. et al. Lipase-catalyzed glycerolysis of anchovy oil in a solvent-free system: Simultaneous optimization of monoacylglycerol synthesis and end-product oxidative stability. **Food Chemistry**, v. 271, p. 372–379, 15 jan. 2019.

PALACIOS, D. et al. Synthesis and oxidative stability of monoacylglycerols containing polyunsaturated fatty acids by enzymatic glycerolysis in a solvent-free system. **LWT**, v. 154, 15 jan. 2022.

PALURI, P.; DURBHA, K. S. Equilibrium, kinetic, and thermodynamic study for the adsorption of methylene blue onto activated carbons prepared from the banana root through chemical activation with phosphoric acid. **Biomass Conversion and Biorefinery**, v. 13, n. 12, p. 10575–10594, 1 ago. 2023.

PANDEY, D.; DAVEREY, A.; ARUNACHALAM, K. **Biochar: Production, properties and emerging role as a support for enzyme immobilization**. **Journal of Cleaner Production**Elsevier Ltd, , 10 maio 2020.

PARK, J. H. Quality Characteristics of Refined Squid (Todarodes pacificus) Oil as an Alternative Resource for Omega-3 Fatty Acids. **Journal of Food Processing and Preservation**, v. 41, n. 2, 1 abr. 2017.

PAULINO, B. N. et al. **Recent advances in the microbial and enzymatic production of aroma compounds**. **Current Opinion in Food Science**Elsevier Ltd, , 1 fev. 2021.

PEREIRA, A. DA S. et al. **Lipases as Effective Green Biocatalysts for Phytosterol Esters' Production: A Review**. **Catalysts**MDPI, , 1 jan. 2022.

PINTO BRITO, M. J. et al. Development of activated carbon from pupunha palm heart sheaths: Effect of synthesis conditions and its application in lipase immobilization. **Journal of Environmental Chemical Engineering**, v. 8, n. 5, 1 out. 2020a.

PINTO BRITO, M. J. et al. Lipase immobilization on activated and functionalized carbon for the aroma ester synthesis. **Microporous and Mesoporous Materials**, v. 309, 15 dez. 2020b.

QIAN, J. et al. Immobilization of lipase on silica nanoparticles by adsorption followed by glutaraldehyde cross-linking. **Bioprocess and Biosystems Engineering**, v. 46, n. 1, p. 25–38, 1 jan. 2023.

QIU, X.; CHEN, S.; LIN, H. **Oxidative Stability of Dried Seafood Products during Processing and Storage: A Review**. **Journal of Aquatic Food Product Technology**Taylor and Francis Inc., , 16 mar. 2019.

QUAYSON, E. et al. Valorization of palm biomass waste into carbon matrices for the immobilization of recombinant Fusarium heterosporum lipase towards palm biodiesel synthesis. **Biomass and Bioenergy**, v. 142, 1 nov. 2020.

RAFIEE, F.; REZAEE, M. **Different strategies for the lipase immobilization on the chitosan based supports and their applications**. **International Journal of Biological Macromolecules**Elsevier B.V., , 15 maio 2021.

RAMUTSHATSHA-MAKHWEDZHA, D. et al. Activated carbon derived from waste orange and lemon peels for the adsorption of methyl orange and methylene blue dyes from wastewater. **Heliyon**, v. 8, n. 8, 1 ago. 2022.

RATHER, A. H. et al. **Overview on immobilization of enzymes on synthetic polymeric nanofibers fabricated by electrospinning**. **Biotechnology and Bioengineering**John Wiley and Sons Inc, , 1 jan. 2022.

REMONATTO, D. et al. **Applications of immobilized lipases in enzymatic reactors: A review**. **Process Biochemistry**Elsevier Ltd, , 1 mar. 2022.

REZA, M. S. et al. **Preparation of activated carbon from biomass and its' applications in water and gas purification, a review**. **Arab Journal of Basic and Applied Sciences**Taylor and Francis Ltd., , 1 jan. 2020.

RODRIGUES, R. C. et al. **Stabilization of enzymes via immobilization: Multipoint covalent attachment and other stabilization strategies**. **Biotechnology Advances**Elsevier Inc., , 15 nov. 2021.

ROMERO-FERNÁNDEZ, M.; PARADISI, F. **Protein immobilization technology for flow biocatalysis**. **Current Opinion in Chemical Biology**Elsevier Ltd, , 1 abr. 2020.

RUSU, A. G. et al. Synthesis and Comparative Studies of Glucose Oxidase Immobilized on Fe3O4 Magnetic Nanoparticles Using Different Coupling Agents. **Nanomaterials**, v. 12, n. 14, 1 jul. 2022.

SAFDAR, A.; ISMAIL, F.; IMRAN, M. Characterization of Detergent-Compatible Lipases from *Candida albicans* and *Acremonium sclerotigenum* under Solid-State Fermentation. **ACS Omega**, 23 ago. 2023.

SAINI, R. K. et al. **Omega−3 polyunsaturated fatty acids (PUFAs): Emerging plant and microbial sources, oxidative stability, bioavailability, and health benefits—A review**. **Antioxidants**MDPI, , 1 out. 2021.

SALGADO, C. A.; DOS SANTOS, C. I. A.; VANETTI, M. C. D. **Microbial lipases: Propitious biocatalysts for the food industry**. **Food Bioscience**Elsevier Ltd, , 1 fev. 2022.

SAMIYAMMAL, P. et al. Adsorption of brilliant green dye onto activated carbon prepared from cashew nut shell by KOH activation: Studies on equilibrium isotherm. **Environmental Research**, v. 212, 1 set. 2022.

SAMPAIO, C. S. et al. **Lipase immobilization via cross-linked enzyme aggregates: Problems and prospects – A review**. **International Journal of Biological Macromolecules**Elsevier B.V., , 31 ago. 2022.

SANDOVAL-GONZÁLEZ, A. et al. **Removal of anti-inflammatory drugs using activated carbon from agro-industrial origin: current advances in kinetics, isotherms, and thermodynamic studies**. **Journal of the Iranian Chemical Society**Springer Science and Business Media Deutschland GmbH, , 1 out. 2022.

SANTOS, M. P. F. et al. Pepsin immobilization on biochar by adsorption and covalent binding, and its application for hydrolysis of bovine casein. **Journal of Chemical Technology and Biotechnology**, v. 94, n. 6, p. 1982–1990, 1 jun. 2019.

SANTOS, M. P. F. et al. Pepsin immobilization: Influence of carbon support functionalization. **International Journal of Biological Macromolecules**, v. 203, p. 67–79, 1 abr. 2022.

ŠAVIKIN, K. et al. Effect of Type and Concentration of Carrier Material on the Encapsulation of Pomegranate Peel Using Spray Drying Method. 2021.

SCELSI, E.; ANGELINI, A.; PASTORE, C. Deep Eutectic Solvents for the Valorisation of Lignocellulosic Biomasses towards Fine Chemicals. **Biomass**, v. 1, n. 1, p. 29–59, 12 jul. 2021.

SHAHZAD, S. et al. Proximate composition and spatio-temporal heterogeneity of phytochemicals in Agave sisalana Perrine (sisal) adapted in different agro-ecological zones of Punjab, Pakistan. **Environmental Science and Pollution Research**, v. 29, n. 32, p. 48869–48879, 1 jul. 2022.

SHELDON, R. A.; BASSO, A.; BRADY, D. **New frontiers in enzyme immobilisation: Robust biocatalysts for a circular bio-based economy**. **Chemical Society Reviews**Royal Society of Chemistry, , 1 maio 2021.

SHEN, S. C. et al. **Omega-3 Fatty Acid Supplementation and Coronary Heart Disease Risks: A Meta-Analysis of Randomized Controlled Clinical Trials**. **Frontiers in Nutrition**Frontiers Media S.A., , 3 fev. 2022.

SIM, E. et al. The Effect of Omega,3 Enriched Oral Nutrition Supplement on Nutritional Indices and Quality of Life in Gastrointestinal Cancer Patients: A Randomized Clinical Trial. **Asian Pacific Journal of Cancer Prevention**, v. 23, n. 2, p. 485–494, 2022.

SINGH, S. et al. **Biocatalyst for the synthesis of natural flavouring compounds as food additives: Bridging the gap for a more sustainable industrial future**. **Food Chemistry**Elsevier Ltd, , 1 mar. 2024.

SONU et al. Agro-waste to sustainable energy: A green strategy of converting agricultural waste to nano-enabled energy applications. **Science of the Total Environment**, v. 875, 1 jun. 2023.

SOUSA, R. R. et al. **Solvent-free esterifications mediated by immobilized lipases: A review from thermodynamic and kinetic perspectives**. **Catalysis Science and Technology**Royal Society of Chemistry, , 7 set. 2021.

SOUZA JÚNIOR, E. C. et al. Hydrolysis of casein from different sources by immobilized trypsin on biochar: Effect of immobilization method. **Journal of Chromatography B: Analytical Technologies in the Biomedical and Life Sciences**, v. 1146, 1 jun. 2020.

SPEIGHT, J. G. Non–fossil fuel feedstocks. Em: **The Refinery of the Future**. [s.l.] Elsevier, 2020. p. 343–389.

SRIVASTAVA, R. K. et al. **Valorization of biowastes for clean energy production, environmental depollution and soil fertility**. **Journal of Environmental Management**Academic Press, , 15 abr. 2023.

SUJIONO, E. H. et al. Fabrication and characterization of coconut shell activated carbon using variation chemical activation for wastewater treatment application. **Results in Chemistry**, v. 4, 1 jan. 2022.

SULTANA, M. et al. **A review on experimental chemically modified activated carbon to enhance dye and heavy metals adsorption**. **Cleaner Engineering and Technology**Elsevier Ltd, , 1 fev. 2022.

SUN, G. et al. A Two-Step Cross-Linked Hydrogel Immobilization Strategy for Diacetylchitobiose Deacetylase. **Catalysts**, v. 12, n. 9, 1 set. 2022.

SUN, J. et al. Immobilization of Candida antarctica lipase B by adsorption in organic medium. **New Biotechnology**, v. 27, n. 1, p. 53–58, 31 dez. 2010.

TAHA, A. M. et al. **Effect of Omega-3 fatty acids supplementation on serum level of C-reactive protein in patients with COVID-19: a systematic review and meta-analysis of randomized controlled trials**. **Journal of Translational Medicine**BioMed Central Ltd, , 1 dez. 2022.

TALEB, M. A. et al. Bioscouring of wool fibres using immobilized thermophilic lipase. **International Journal of Biological Macromolecules**, v. 194, p. 800–810, 1 jan. 2022.

TAVARES, F. et al. Rapid enzymatic hydrolysis of crambe oil catalyzed by castor seeds lipases. **Industrial Crops and Products**, v. 171, 1 nov. 2021.

THAKKAR, J. B. et al. Design and characterization of a biosensor with lipase immobilized nanoparticles in polymer film for the detection of triglycerides. **International Journal of Biological Macromolecules**, v. 229, p. 136–145, 28 fev. 2023.

THANGARAJ, B.; SOLOMON, P. R. **Immobilization of Lipases – A Review. Part I: Enzyme Immobilization**. **ChemBioEng Reviews**Wiley-Blackwell, , 1 out. 2019.

THONGPAT, W.; TAWEEKUN, J.; MALIWAN, K. Synthesis and characterization of microporous activated carbon from rubberwood by chemical activation with KOH. **Carbon Letters**, v. 31, n. 5, p. 1079–1088, 1 out. 2021.

VB, A. et al. The Pharma Innovation Journal 2022; 11(9): 838-841 Investigation on enzyme activity of lipase from papaya (Carica papaya) latex. 2022.

VEIT, D. **Fibers: History, Production, Properties, Market**. [s.l.] Springer International Publishing, 2023.

VERMA, S.; MEGHWANSHI, G. K.; KUMAR, R. **Current perspectives for microbial lipases from extremophiles and metagenomics**. **Biochimie**Elsevier B.V., , 1 mar. 2021.

VILAS BÔAS, R. N.; DE CASTRO, H. F. **A review of synthesis of esters with aromatic, emulsifying, and lubricant properties by biotransformation using lipases**. **Biotechnology and Bioengineering**John Wiley and Sons Inc, , 1 mar. 2022.

VILLENEUVE, P. et al. **Lipid oxidation in emulsions and bulk oils: a review of the importance of micelles**. **Critical Reviews in Food Science and Nutrition**Taylor and Francis Ltd., , 2021.

WANCURA, J. H. C. et al. **Demystifying the enzymatic biodiesel: How lipases are contributing to its technological advances**. **Renewable Energy**Elsevier Ltd, , 1 nov. 2023.

WANG, B. et al. Anchovy oil microcapsule powders prepared using two-step complex coacervation between gelatin and sodium hexametaphosphate followed by spray drying. **Powder Technology**, v. 358, p. 68–78, 15 dez. 2019a.

WANG, B.; ADHIKARI, B.; BARROW, C. J. Optimisation of the microencapsulation of tuna oil in gelatin-sodium hexametaphosphate using complex coacervation. **Food Chemistry**, v. 158, p. 358–365, 1 set. 2014.

WANG, B. X. et al. **An Overview on Recent Progress of the Hydrogels: From Material Resources, Properties, to Functional Applications**. **Macromolecular Rapid Communications**John Wiley and Sons Inc, , 1 mar. 2022a.

WANG, C. H. et al. **Reclamation of fishery processing waste: A mini-review**. **Molecules**MDPI AG, , 14 jun. 2019b.

WANG, X. et al. **Key factors and primary modification methods of activated carbon and their application in adsorption of carbon-based gases: A review**. **Chemosphere**Elsevier Ltd, , 1 jan. 2022b.

WU, S. et al. **Biocatalysis: Enzymatic Synthesis for Industrial Applications**. **Angewandte Chemie - International Edition**Wiley-VCH Verlag, , 4 jan. 2021.

XIA, Q. et al. Investigating the mechanism for the enhanced oxidation stability of microencapsulated omega-3 concentrates. **Marine Drugs**, v. 17, n. 3, 28 fev. 2019.

XIA, Q. et al. Investigation of enhanced oxidation stability of microencapsulated enzymatically produced tuna oil concentrates using complex coacervation. **Food and Function**, v. 11, n. 12, p. 10748–10757, 1 dez. 2020.

XIANG, M. et al. Heterologous expression and biochemical characterization of a cold-active lipase from Rhizopus microsporus suitable for oleate synthesis and bread making. **Biotechnology Letters**, v. 43, n. 9, p. 1921–1932, 1 set. 2021.

XU, C. et al. **Cellulase immobilization to enhance enzymatic hydrolysis of lignocellulosic biomass: An all-inclusive review**. **Carbohydrate Polymers**Elsevier Ltd, , 1 dez. 2023.

XUE, D. et al. Ethyl lactate biosynthesis by the cascade of the aerobic process and the anaerobic process with corn stover. **Cellulose**, 2024.

YU, C. WEI et al. Purification, identification, characterization and catalytic mechanism of two lipases from rice bran (Oryza sativa). **LWT**, v. 140, 1 abr. 2021a.

YU, Y. et al. **Genipin-cross-linked hydrogels based on biomaterials for drug delivery: A review**. **Biomaterials Science**Royal Society of Chemistry, , 7 mar. 2021b.

YUAN, Y.; SHEN, J.; SALMON, S. **Developing Enzyme Immobilization with Fibrous Membranes: Longevity and Characterization Considerations**. **Membranes**MDPI, , 1 maio 2023.

ZAPPATERRA, F. et al. Biocatalytic approach for direct esterification of ibuprofen with sorbitol in biphasic media. **International Journal of Molecular Sciences**, v. 22, n. 6, p. 1–18, 2 mar. 2021.

ZHANG, J. et al. Amphiphilic Nanointerface: Inducing the Interfacial Activation for Lipase. **ACS Applied Materials and Interfaces**, v. 14, n. 34, p. 39622–39636, 31 ago. 2022a.

ZHANG, L. et al. Advance in Hydrothermal Bio-Oil Preparation from Lignocellulose: Effect of Raw Materials and Their Tissue Structures. **Biomass**, v. 1, n. 2, p. 74–93, 26 out. 2021.

ZHANG, X. et al. **Omega-3 Polyunsaturated Fatty Acids Intake and Blood Pressure: A Dose-Response Meta-Analysis of Randomized Controlled Trials**. **Journal of the American Heart Association**American Heart Association Inc., , 7 jun. 2022b.

ZHAO, J. et al. Green synthesis of polydopamine functionalized magnetic mesoporous biochar for lipase immobilization and its application in interesterification for novel structured lipids production. **Food Chemistry**, v. 379, 15 jun. 2022.

ZHOU, Z. W. et al. Magnetic COFs as satisfied support for lipase immobilization and recovery to effectively achieve the production of biodiesel by great maintenance of enzyme activity. **Biotechnology for Biofuels**, v. 14, n. 1, 1 dez. 2021.

ZHU, Z.; XU, Z. **The rational design of biomass-derived carbon materials towards next-generation energy storage: A review**. **Renewable and Sustainable Energy Reviews**Elsevier Ltd, , 1 dez. 2020.

CAPÍTULO 2

ARTIGO 1

Optimization of synthesis conditions on activated carbon produced from sisal waste for lipase immobilization and flavoring ester production

---

*Manuscrito será submetido à revista Biomass Conversion and Biorefinery (ISSN: 2190-6823) – Fator de impacto: 4.1.

ABSTRACT

This work aimed to optimize the synthesis conditions (pyrolysis time and temperature) of activated carbon produced from sisal waste by chemical activation for lipase immobilization and ethyl lactate production. The optimal conditions were determined by the Central Composite Design (CCD) and Response Surface Methodology (RSM), through the response variables enzyme activity and yield. The highest enzyme activity and yield were 42.90 U and 60.59%, respectively. The statistical analysis showed a significant quadratic effect for pyrolysis time and a linear effect for pyrolysis temperature for both response variables. The response surface suggested a behavior for increasing enzyme activity and yield as temperature increases and within a time range between 70 and 110 minutes. The optimal time and temperature were 86 minutes and 700 ºC. The coefficient of determination (R^2 = 0.732 and 0.715) verified that the model fits the experimental design. Scanning Electron Microscopy (SEM) confirmed the porous structure, and BET analysis verified a surface area of 433 m^2 g^{-1}, indicating a valuable structure for enzyme immobilization. The derivative was employed in the synthesis of ethyl lactate and achieved high ester conversion after five cycles (Y = 80.68%), suggesting that the immobilization process efficiently protected the lipase from desorption, denaturation, and inactivation under the reaction conditions employed. Therefore, the activated carbon from sisal waste has the potential for lipase immobilization as a low-cost sustainable adsorbent through agro-industrial waste management. It can also be used for catalyzing ethyl lactate esterification for commercial purposes, providing a green alternative to the chemical method.

Keywords: adsorption; enzyme; hydrolysis; response surface; statistical analysis.

1. Introduction

Sisal (*Agave sisalana*) is a plant that originated in Mexico with morphological and physiological characteristics that justify its growth in different conditions, as well as to show adaptation to environments with warm climates, high luminosity, and prolonged droughts. *Agave sisalana* commercial exploitation is based on its fibers, widely used in the automotive industry, ropes, strings, sea cables, carpets, brooms, upholstery, and handicrafts [1]. Brazil is the world's largest producer and exporter of sisal, producing 39 % of the world's 220,363 tonnes of sisal fiber in 2019 [2].

The fiber extracted from sisal is classified as hard natural fiber, extracted from the plant's leaves. This product is ranked the sixth most important fiber crop, representing 2% of the world's production of plant fibers and 75 % of the global production of hard fibers [3]. However, only 3-5 % of the total sisal plant mass is properly used to produce fibers. The remaining percentage is discarded as sisal waste, leading to the loss of plant materials and the generation of environmental wastes [4]. Furthermore, the lignocellulosic content of sisal waste consists of cellulose (44 %), hemicelluloses (19 %), and lignin (19 %) [5]. Considering this content, sisal waste has the potential to be transformed into an added-value product, such as its use as lignocellulosic biomass for activated carbon synthesis.

Activated carbon (AC) is a carbonaceous and porous material obtained by the thermal decomposition of biomass under an inert atmosphere [6]. Biomass includes agricultural, industrial, and household wastes. Nevertheless, agro-industrial waste, such as sisal waste, has great potential for AC synthesis due to its high carbon content, high diversity, and availability of precursor material [7]. Moreover, using these will help in waste management while being economically feasible thereby promoting sustainability on many levels [8].

The production of AC through the chemical method involves two main steps: activation and pyrolysis of the raw material. The synthesis conditions and type of precursor material can influence the AC characteristics, such as surface area, pore size, and distribution [9,10]. For instance, pyrolysis time and temperature are associated with the thermal and chemical decomposition of the lignocellulosic structure, which leads to pore development [11,12]. Accordingly, it is important to evaluate the effect of synthesis variables on activated carbon for different applications, including enzyme immobilization.

Enzyme immobilization was developed to solve issues related to the stability and reusability of free enzymes and enable simpler process control [13]. Among commercial biocatalysts, lipase (triacylglycerol acyl hydrolase, EC 3.1.1.3) can be mentioned as the most prominent biocatalyst in biotechnology. Lipases are biomolecules that hydrolyze triacylglycerols, but they can also carry out ester synthesis via different strategies, such as esterification, transesterification, interesterification, or acidolysis reactions [14,15]. These enzymes have great industrial potential due to their versatility and high selectivity, such as in food [16-19], detergents [20], cosmetics [21], pulp and paper [22], textiles [23], biofuels [24], and pharmaceutical [25] industries. Recently, it has been used to synthesize natural aroma compounds through esters of short-chain carboxylic acid and alcohols such as ethyl lactate.

Ethyl lactate, also known as lactic acid ethyl ester, is a monobasic ester produced by combining lactic acid and ethanol. It is commonly used as a solvent and is considered to be a "green" solubilizing agent, which means that it has several advantages over other organic-based solubilizing agents [26,27]. Ethyl lactate is widely used in industrial applications such as specialty coatings, inks, and cleaners due to its high performance and versatility. Additionally, ethyl lactate is a popular choice due to its low toxicity, particularly as a flavoring agent providing buttery notes to dairy products and wines, as well as being associated with different fruit flavors [28,29].

Although lipolytic enzymes are widely studied, lipase immobilization on activated carbon produced from sisal waste has not been studied, as well as its application in ethyl lactate synthesis. Therefore, the present work aimed to optimize the synthesis conditions (pyrolysis time and temperature) of activated carbon produced from sisal waste for lipase immobilization and ethyl lactate production.

2. Materials and methods

2.1 Materials

The raw material used as the precursor material for activated carbon synthesis was sisal (*Agave sisalana*) waste purchased from a sisal-based products company in Valente, Bahia, Brazil. Lipase from Porcine Pancreas (LPP) type II (CAS number: 9001-62-1) was obtained from Sigma-Aldrich Brazil. Phosphoric acid (85 % P.A-ACS; CAS number: 7664-38-2) was obtained from Synth Brazil. All other chemicals used were of analytical grade.

2.2 Preparation and characterization of precursor material

Sisal waste employed for activated carbon synthesis was dried in an oven at 105 ºC for 24 h, crushed in a blender, and sieved to 20 mesh. The residue was characterized for ash and moisture contents according to the AOAC. Lignocellulosic content (lignin, cellulose, and hemicellulose) was determined using the neutral detergent fiber and acid detergent fiber (NDF and ADF) methodologies described by Van Soest et al. [30]. Fourier Transform Infrared Spectroscopy (FTIR) evaluated functional groups of biomass. The sample was directly analyzed using the attenuated total reflectance (ATR) technique in the 4000-600 cm^{-1} infrared region in an Agilent Cary 630 FTIR spectrophotometer (Agilent Technologies Inc., Santa Clara, CA, USA).

2.3 Activated carbon synthesis

Synthesis of activated carbon was carried out by chemical activation method using phosphoric acid in the impregnation ratio of 2.5:1 (activating agent mass/precursor mass) defined according to preliminary data, followed by drying at 105 °C for 24 h. Then, the samples were carbonized under nitrogen flow (50 mL min $^{-1}$) at different levels of time (min) and temperature (ºC) as reported in Table 1. Finally, the activated carbon was washed with hot water (100 ºC) until it reached pH 7.0. The samples were dried at 105 ºC for 24 h and packaged in airtight packaging.

2.3.1 Optimization of synthesis conditions

The Central Composite Design (CCD) was used as the experimental design. Surface Response Methodology (SRM) was employed to optimize the synthesis conditions of the activated carbon from sisal waste. The independent variables evaluated were carbonization temperature (ºC) and carbonization time (min) with the response variables enzyme activity (U) and enzyme activity yield (%). The experimental design had 11 assays with 4 factorial points, 4 axial points, and triplicate at the central point (Table 1).

Table 1. Factors and levels of the Central Composite Design (CCD).

Factor	Coded factor	Levels				
		-1.41	-1	0	+1	+1.41
Time (min)	X_1	46.14	56.00	82.50	109.00	119.87
Temperature (°C)	X_2	379.97	426.50	540.00	653.50	700.04

The independent parameters were correlated to the response (Y) through a quadratic polynomial model (Equation 1).

$$Y = \beta_0 + \beta_1 X_1 + \beta_2 X_2 + \beta_3 X_1 X_2 + \beta_4 {X_1}^2 + \beta_5 {X_2}^2 \quad (1)$$

Where: β_0 to β_5 are the polynomial coefficients estimated from nonlinear regression following the least square method. The model adequacy was determined by significance ($p < 0.05$), lack of fit ($p > 0.05$), and coefficient of determination (R^2). All statistical analyses were performed using SAS Studio software.

2.4 Activated carbon characterization

The AC was characterized for ash content as reported in the AOAC [86]. Fourier Transform Infrared Spectroscopy (FTIR) evaluated functional groups of material. The sample was directly analyzed using the attenuated total reflectance (ATR) technique in the 4000-600 cm^{-1} infrared region in an Agilent Cary 630 FTIR spectrophotometer (Agilent Technologies Inc., Santa Clara, CA, USA). The point of zero charge (pH_{PZC}) was determined using the methodology reported by Kuśmierek et al. [16]. The morphology of AC was obtained by Scanning Electron Microscopy (SEM). For that, the carbon samples were fixed in appropriate supports (stub) and directly metalized with a thin layer of gold. Then, the samples were subjected to SEM (QUANTA 250, FEI COMPANY, Waltham, MA, USA). The nitrogen adsorption and desorption isotherms were determined on an ASAP 2420 Micrometrics equipment (Micromeritics Instrument Corporation, Norcross, GA, USA) using approximately 0.20 g of sample at -196.15 ºC. Before measurements were taken, the samples were pretreated through heating at 60 ºC. The specific surface area was achieved by the Brunauer–Emmett–Teller (BET) equation [32]. The pore size distribution was determined from the desorption isotherm using the Barrett–Joyner–Halenda (BJH) method [84] and the micropore volume was obtained using the t-plot analysis according to the adsorption isotherms [33].

2.5 Enzyme immobilization

The activated carbons produced according to the CCD were used as supports for lipase immobilization by adsorption. Following Brito et al. [9], 0.1 g of support was added to 5 mL of lipase solution (6000 mg L^{-1}) in sodium acetate buffer (0.1M, pH 5.0) and kept stirring on an orbital shaker at 10 g force, 30 ºC, and 2 h. The derivative was centrifugated at 2000 g force for 5 min, and the supernatant was collected to quantify protein concentration by the Bradford (1976) method. The immobilization capacity was determined according to Equation 2.

$$C_{imo} = \frac{v\,(C_i - C)}{m_a} \quad (2)$$

Where: C_{Imo} is the immobilization capacity (mg g^{-1}); v is the volume of lipase solution (mL); C_i is the initial lipase concentration (mg L^{-1}); C is the lipase concentration at equilibrium (mg L^{-1}); m_a is the adsorbent mass (g).

2.6 Lipase hydrolysis

Hydrolysis was carried out following the olive oil emulsion method [35] with some modifications. The substrate was prepared with 1.25 g of olive oil and 3.75 g of 3 % gum arabic under stirring until reaching a homogenous solution. To this, 5 mL of sodium phosphate buffer (0.1 M, pH 8.0), and the derivative or 1 mL of lipase solution were added in 125 mL erlenmeyer flasks. The samples were incubated in a shaker bath at 37 ºC for 10 min, stirring at 85 g force. The reaction stopped when 10 mL of 92.5 % ethanol was added to the flasks. The liberated fatty acids were titrated with 30 mM NaOH until reaching pH 11. The enzyme activity was calculated by Equation 3, where one unit of activity was defined as the amount of enzyme that releases 1 μmol of fatty acid per minute of reaction under the assay conditions.

$$U\left(\frac{\mu mol}{min}\right) = \frac{(V_a - V_b).M.10^3}{t} \quad (3)$$

Where: V_a is the NaOH volume used in the sample titration (mL), V_b is the NaOH volume used in the control titration (mL), M is the molar concentration of NaOH solution and t is the reaction time (min).

2.7 Enzyme activity yield

The difference in enzyme activity between free enzyme and immobilized enzyme, determined through the method described in 2.6, was measured by enzyme activity yield (%) using Equation 4.

$$Yield(\%) = \frac{U_s}{U_i} 100 \quad (4)$$

Where: U_i is the enzyme activity in the solution before the immobilization process, and U_s is the immobilized enzyme activity.

2.8 Aroma ester synthesis

The ethyl lactate synthesis was performed according to Oliveira et al. [36], with minor modifications. The substrate was prepared by mixing lactic acid (100 mM) and ethanol (300 mM) in hexane solvent. The reaction was carried out in 100 mL Duran flasks containing 5 mL of the reaction mixture and 0.5 g of the derivative. The samples were

incubated in a shaker bath at 40 ºC and 115 g force for 4 hours. The enzyme activity was stopped by freezing the sample for 5 minutes.

After the reaction, the lactic acid content was determined by titration. For this, 500 µL of the reaction mixture was withdrawn, diluted in 10 mL of ethanol-acetone solution (1:1 v/v), and titrated with 30 mM NaOH until reaching pH 11. The yield of esterification for the synthesis of ethyl lactate was calculated through Equation 5.

$$Y(\%) = \frac{(C_0 - C_f)}{C_0} \text{x } 100 \quad (5)$$

Where: C_0 is the initial concentration and C_f is the final concentration of lactic acid (mM).

2.9 Operational stability

The operational stability of the derivative was investigated by conducting successive esterification reactions between lactic acid and ethyl alcohol, as described in 2.8. After each cycle, 20 mL of sodium acetate buffer (0.1M, pH 5.0) was added to the flasks containing the derivative, followed by stirring at 10 g force for 5 min and centrifugation at 2000 g force for 5 min. Subsequently, the derivative was washed with hexane to remove any unconverted substrates, and products adsorbed in their microenvironment. Finally, the derivative was recovered and incubated in a new reaction cycle.

3. Results and discussion

3.1 Chemical composition of precursor material

The chemical characteristics of sisal waste in this study consisted of cellulose, hemicellulose, lignin, and ashes (Table 2).

Table 2. Chemical composition (w/w) of sisal waste.

Sample	Cellulose (%)	Hemicellulose (%)	Lignin (%)	Ash (%)
Sisal waste	41.11 ± 3.68	18.45 ± 0.37	20.83 ± 0.06	5.52 ± 0.01

The chemical composition of lignocellulosic waste varies depending on the climate conditions, maturity, and organizational structure of raw materials, which is essential for the synthesis and yield of carbonaceous material [37]. Precursor sources with high lignin content can yield higher because of their high decomposition temperature (280-500 ºC) [12]. The

lignin in sisal waste agrees with the composition described by Chakhtouna et al. [24], as cellulose (40-60%), lignin (10-25%), and hemicellulose (20-40%).

The sisal waste analyzed in the current work had a high lignocellulosic content (80.39%), with a particularly high cellulosic content (42.11%). These data suggest the potential to synthesize activated carbons with larger surface areas and porosity due to the lower thermal stability of hemicellulose (180-260ºC) and cellulose (240-350ºC) [38,39]. Similar results were reported by Li et al. [5], with 43.6% cellulose, 18.8% hemicellulose, and 18.7% lignin.

The ash content of raw materials refers to their inorganic or mineral composition. Therefore, lignocellulosic biomass contains ash percentages ranging from 0.8% to 15.1% [40]. According to Zhang et al. [28], precursors with low ash content (less than 10%) are generally preferred for activated carbon synthesis due to their ability to enhance texture properties, which has been observed in the current study (ash % = 5.52).

3.2 Optimization of synthesis conditions

To determine the optimum conditions for activated carbon synthesis (pyrolysis time and temperature), the response variables Enzyme activity (U) and Enzyme Activity Yield (%) were evaluated using the Central Composite Design (CCD) (Table 3). The highest Enzyme activity (U = 42.90) and Yield (Y% = 60.59) were achieved at 82.5 minutes and 700 ºC (Assay 8). The enzyme immobilization on activated carbon by adsorption is related to the precursor material, since the activation and pyrolysis can influence the AC characteristics, such as surface area, pore size, and pore distribution. The chemical activation with phosphoric acid improves porosity through dehydration and degradation of the biomass structure [42,43]. While in pyrolysis, volatile components and light gases are removed as the temperature increases [44]. As described in 3.1, the high lignocellulosic content of sisal waste suggests the potential to synthesize carbon-based materials with larger surface area and porosity due to the lower thermal stability of cellulose (240-350 ºC) and hemicellulose (180-260 ºC). Furthermore, the high lignin content of 20.83% explains the need for high temperatures to achieve greater enzyme activity from the biocatalyst. For instance, Assay 3 is among the lowest values for enzyme activity and enzyme activity yield. This may be due to the thermal decomposition of lignin between 280 and 500 ºC, which suggests that the temperature used (426.5 ºC) did not efficiently degrade the structure since lignin is its

external component [12]. The increase in temperature leads to pore development and consequent enzymatic immobilization in its active form, in addition to reducing the substrate diffusion restrictions [45].

Table 3. Central Composite Design (CCD) and values of enzyme activity (U) and enzyme yield (%).

Assay	$(X_1)^a$ $x_1{}^b$	$(X_2)^a$ $x_2{}^b$	Enzyme activity (U)	Immobilization capacity (mg g^{-1})	Enzyme Yield (%)
1	(-1) 56.00	(-1) 426.50	17.40 ± 3.04	271.55 ± 3.26	24.58 ± 4.30
2	(-1) 56.00	(+1) 653.50	26.70 ± 3.60	276.98 ± 2.53	37.71 ± 5.08
3	(+1) 109.00	(-1) 426.50	18.00 ± 3.90	260.83 ± 2.07	25.42 ± 5.51
4	(+1) 109.00	(+1) 653.50	28.00 ± 0.62	272.78 ± 3.77	39.55 ± 0.88
5	(-1.41) 45.14	(0) 540.00	18.60 ± 0.79	263.30 ± 2.71	26.27 ± 1.12
6	(+1.41) 119.87	(0) 540.00	26.70 ± 2.40	276.56 ± 3.83	37.71 ± 3.39
7	(0) 82.50	(-1.41) 379.97	28.10 ± 0.62	252.64 ± 1.89	39.69 ± 0.88
8	(0) 82.50	(+1.41) 700.04	42.90 ± 2.70	279.72 ± 0.96	60.59 ± 3.81
9	(0) 82.50	(0) 540.00	29.25 ± 2.85	264.52 ± 3.40	41.31 ± 4.03
10	(0) 82.50	(0) 540.00	31.60 ± 1.48	275.88 ± 1.55	44.63 ± 2.09
11	(0) 82.50	(0) 540.00	27.80 ± 2.72	270.63 ± 1.17	39.27 ± 3.84

[a] Coded values.
[b] Uncoded values of: x_1 – time (min) and x_2 – pyrolysis temperature (ºC).

Furthermore, the pyrolysis time associated with temperature plays a crucial role in the development of the porous structure. The lowest enzyme activities and yield were observed for assays with very low pyrolysis time (Assays 1 and 5), and this is attributed to the action mechanism of phosphoric acid. According to Brito et al. [9], phosphoric acid degrades hemicellulose and lignin structures before cellulose as they are more accessible to acid hydrolysis. Activation from amorphous polymers (hemicellulose and lignin) creates mainly micropores, while activation from crystalline polymers (cellulose) produces a wider pore size. This is attributed to the greater swelling power from crystalline cellulose when compared to other compounds as it is more susceptible to high esterification with phosphates and polyphosphates. Moreover, cellulose is the most difficult to hydrolyze due to its internal position within the fiber structure [11,46,47]. Since cellulose is the main lignocellulosic

component of sisal waste, more time will be needed during the activation/pyrolysis steps to develop the porous structure.

The pore development begins from the expansion process of the material surface through the phosphate group insertion. The chemical reaction begins at milder temperatures, and significant micropore formation is observed between 150 and 350 ºC. A further increase in temperature creates the mesopores, mainly through the enlargement of existing micropores, leading to a decrease in surface area [9,48]. Therefore, varying carbonization time and temperature will affect the activated carbon texture properties due to the precursor characteristics and activation method, especially for sisal waste which has a high lignocellulosic content. These findings are supported by the immobilization parameters and the behavior observed on the response surface (Figure 1).

Although the enzymatic parameters were affected by synthesis conditions, the Immobilization capacity (mg g^{-1}) was similar for all tests. These results indicate that activated carbon is highly suitable for immobilization, but the lipase may be immobilized in a way that negatively affects its activity. For all assays with low enzymatic activity, low pyrolysis times or temperatures were observed, suggesting that the meso-microporous structure was harmed. Therefore, the micropore development was probably dominant, and the enzyme activity was limited by the lipase immobilization in smaller pores. As a result, there were substrate diffusional restrictions within the pores, steric hindrance, and pore-clogging. Furthermore, the effect of interfacial activation may be reduced [49-51].

The model and factors of experimental design were investigated by analysis of variance (ANOVA) and verified for significance using the F test at a 5% significance level. The independent variables were applied to the regression analysis through their coded values. Non-significant parameters were grouped as errors and a new reduced model was obtained. The low probability ($p < 0.0001$) observed for the F value confirms that the model was significant, as well as the lack of adjustment. The mathematical model is expressed in Table 4.

Table 4. Parameter estimate of the quadratic model adjusted to enzyme activity and yield. X_1 – time (min) and X_2 – temperature (ºC).

Factors	Enzyme activity		Enzyme Yield	
	Parameter estimate	p-Value	Parameter estimate	p-Value
Intercept	32.416	<.0001	45.785	<.0001
X_1	1.670	<.0001	2.359	<.0001
X_2	5.036	<.0001	7.113	<.0001
X_{11}	-6.585	<.0001	-9.301	<.0001

The results of statistical analysis showed a significant quadratic effect for time and a linear effect for temperature on the response variables enzyme activity and yield. The regression equation of the uncoded variables was also determined for their use in the Response Surface Methodology (RSM) (Figure 1), as described in Equations 6 and 7.

$$U = -60.56619 + 1.61018\ t + 0.04437\ T - 0.00938\ t^2 \quad (6)$$

$$Y(\%) = -85.54589 + 2.27427\ t + 0.06267\ T - 0.01324\ t^2 \quad (7)$$

Where: U is the enzyme activity (U); Y(%) is the enzyme yield; t is the pyrolysis time (min); and T is the pyrolysis temperature (°C).

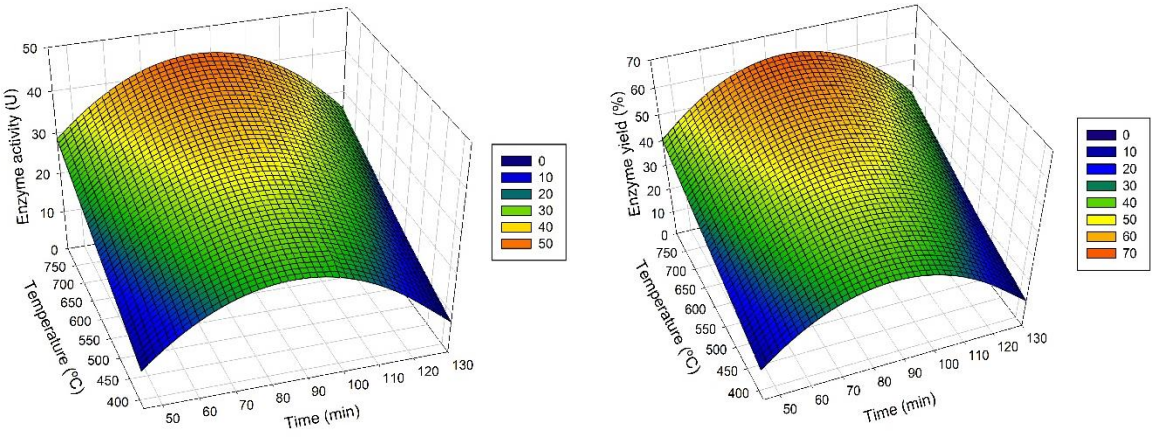

Figure 1. Response surface for enzyme activity and yield: effect of pyrolysis time (min) and temperature (ºC). R^2 = 0.732 and 0.715, respectively.

The response surface suggests a behavior for increasing enzyme activity and yield as temperature increases and within a time range between 70 and 110 minutes. The linear effect for temperature is attributed to the lignocellulosic structure degradation during chemical activation with phosphoric acid. Each component has its thermal stability (lignin > cellulose > hemicellulose), and increasing temperature will completely decompose them since lignin makes up the external layer of the structure. Such compounds have their structure, which develops different pore sizes through activation. Crystalline materials (cellulose) develop mesopores, while amorphous materials (hemicellulose and lignin) develop micropores. As the temperature increases, micropores are formed followed by mesopores. However, very high temperatures cause excessive mass loss with enlargement of pores (macropores) and lower synthesis yield. Therefore, the relationship between the thermal and chemical decomposition of lignocellulosic components will influence the texture properties and the immobilization in a way that enhances catalysis [46,52].

The quadratic effect for time may be due to the complex acid hydrolysis of the cellulolytic crystalline structure that is found inside the fiber. This particular compound constitutes the most significant part of the raw material and promotes mesopore development. Therefore, an intermediate pyrolysis time is required to deteriorate this material. From a commercial perspective, this is an economically promising behavior as it reduces energy costs by using shorter carbonization times. On the other hand, the structure begins to decompose excessively during high pyrolysis periods, causing an increase in pore diameter and a decrease in surface area. This leads to a higher enzyme density within the pores, which can result in the formation of aggregates and inactive enzyme complexes [9,53].

From the partial derivative of regression equations, the optimal conditions to achieve the highest response variables were calculated and described as 86 minutes and 700 ºC, similar to the experimental values. According to Senthilkumar et al. [34], the coefficient of determination (R^2) is a measure of the degree of fit and is defined as the ratio between the explained variance and the total variance. An R^2 of at least 0.7 indicates a satisfactory model fit. In this study, the coefficients of determination $R^2 = 0.732$ and 0.715 confirm that the model fits the experimental design. Therefore, the synthesis conditions were optimized and applied in the subsequent experiments.

3.3 Characterization of activated carbon from optimal conditions

The chemical characterization of activated carbon synthesized from sisal in the optimal condition waste was determined based on yield (45.61%), ash (7.89%), and point of zero charge (pH_{PCZ} = 5.83).

The activated carbon yield obtained under optimal conditions was around 46%, considerably higher than other sisal studies. For instance, Xinping et al. [85] achieved a yield of 35%, Wu et al. [55] verified 27.6%, and Jambeiro et al. [56] had 44%. This might be due to differences between the lignocellulosic composition of the raw materials. Moreover, the activation method and the activating agent applied during synthesis can also contribute to the result. Chemical activation has a greater yield than physical activation by avoiding the formation of tar and other undesirable volatile products [53]. In addition, acidic-activating agents reach higher yields than basic-activating agents, such as phosphoric acid. Although phosphoric acid breaks some bonds in the biomass structure, it provides phosphate cross-links between the polymers of the lignocellulosic structure, which strengthens the internal matrix, prevents excessive burning of precursor material, and reduces the loss of volatiles during heating [42,57-59].

The ash content of activated carbon varies according to the inorganic residues of the raw material and the synthesis conditions, such as the carbonization temperature, as high temperatures lead to greater volatilization of mineral structures. In this work, sisal-activated carbon has a higher ash content compared to sisal waste (7.89 %). This increase is related to the components of the activating agent that were not eliminated in the pyrolysis or desorbed in the washing step, such as phosphate groups from phosphoric acid. Typically, high ash content has a negative effect on adsorption efficiency since the mineral material can block the adsorbent pores [37,60]. As mentioned previously, the ash content of AC is expected to be less than 10%.

The point of zero charge (pH_{PCZ}) or charge density of the adsorbent is the pH at which the surface has zero surface electrical charge density. When the pH of the reaction medium is lower than the pH_{PCZ}, the material surface becomes positively charged and preferentially adsorbs anionic compounds. On the other hand, for solutions with a pH higher than the pH_{PCZ}, the carbonaceous surface becomes negatively charged and presents greater efficiency for adsorbing cationic materials [61]. The point of zero charge of the AC from this study was 5.83, verifying a slightly positively charged surface at the pH of lipase immobilization (pH = 5.0). As the isoelectric point of porcine pancreas lipase is close to 4.9 [62], its surface has

a neutral charge at the pH of immobilization. Therefore, it can be concluded that the hydrophobic effect is predominant in the immobilization process.

Acidic pH_{PCZ} is related to using phosphoric acid as an activating agent and dissociating acidic surface oxygen complexes, such as carboxyl and phenolic groups [57]. The functional groups from this AC responsible for the low pHpcz were C-O-C (1997 cm^{-1}), C=O (1563 cm^{-1}), C–O (1162 cm^{-1}), P^{+}–O^{-} and P–O–P (1070 cm^{-1}), as shown in the FTIR spectra (Figure 2).

Regarding the sisal waste, characteristic wavelengths of lignocellulosic materials were observed (Figure 2), such as the band at 3283 cm^{-1}, which is attributed to the stretching vibrations of the hydroxyl group (OH) and the lignocellulosic structure; the band at 2922 cm^{-1} refers to the axial deformation present in cellulose, hemicellulose, and lignin (C–H group); 1597 cm^{-1} is related to the C=O bond in carboxymethyl cellulose; the band at 1241 cm^{-1} corresponds to the vibration of the guaiacyl groups from lignin; and the band at 1027 cm^{-1} is assigned to the stretching of the glycosidic bonds (C–O–C) in the lignocellulosic structure [63,64].

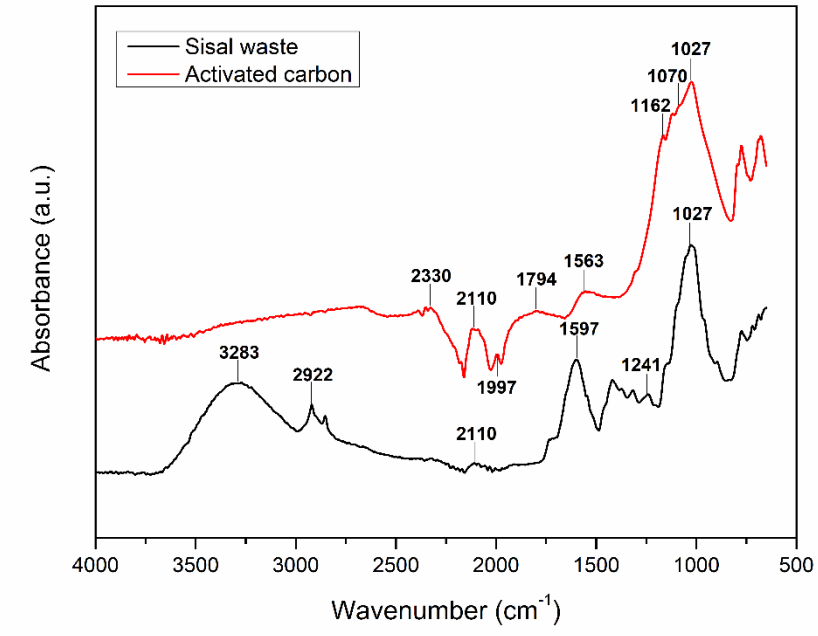

Figure 2. FTIR of sisal waste and activated carbon.

After the chemical activation and pyrolysis, some functional groups disappeared (3283 cm^{-1}, 2922 cm^{-1}, and 1241 cm^{-1}) due to the thermal decomposition, and new compounds were verified. The spectra of activated carbon from sisal waste showed the band

at 2330 $cm^{-1,}$ which is associated with the methyl group; the band at 2110 cm^{-1} represents the carbon-oxygen bond; the bands at 1794 cm^{-1} and 1563 cm^{-1} are attributed to the stretching of C=O and C=C from carbon-based materials; the band at 1162 cm^{-1} is assigned to C–O vibrations; and the band at 1070 cm^{-1} refers to the phosphate ester bonds from the activation with phosphoric acid [65,66].

In Figure 3, the isotherms and pore size distribution of activated carbon from sisal waste are presented. According to the IUPAC classification [67], the support showed a hysteresis loop characteristic of Type IV isotherm. This phenomenon can be defined as the capillary condensation in mesopore structures, exhibiting different shapes described between Type I-IV of the hysteresis loop. Type I found for this work refers to porous materials that feature agglomerates or compacts of regular array and narrow pore size distributions. Furthermore, the first nitrogen slope (low-pressure region) indicates monolayer adsorption, while the second slope implies multilayer adsorption. Such behavior suggests a significant development of carbon mesoporosity, and it can be confirmed by analyzing the pore size distribution (Figure 3 b) and texture properties of the adsorbents (Table 5).

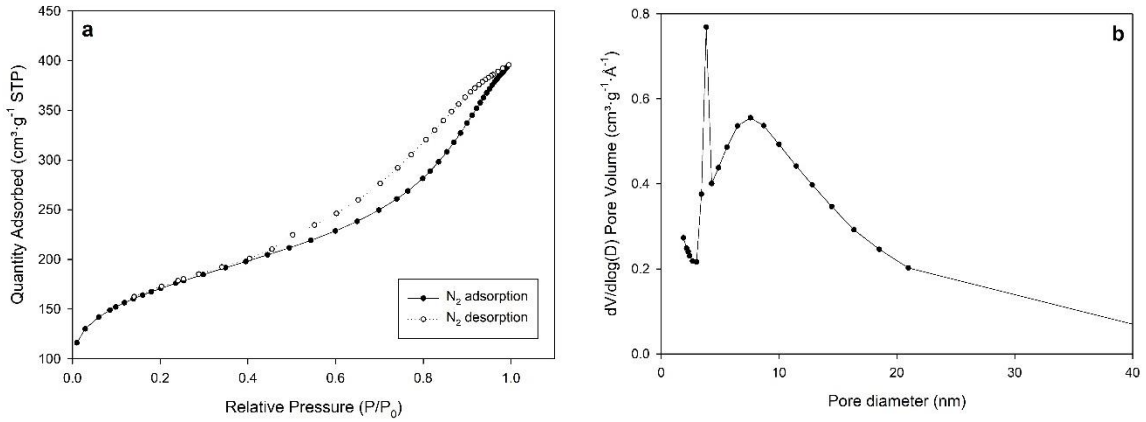

Figure 3. Nitrogen adsorption-desorption isotherms (a) and pore distribution (b) of activated carbon from sisal waste.

The pore distribution exhibits a narrow peak at 3.8 nm diameter and a larger peak at around 10 nm, which can improve the diffusion restrictions. Additionally, the texture properties of activated carbon produced from sisal waste are shown in Table 5. The results confirm the formation of pores, categorizing the material as micro-mesoporous. In adsorption processes, a good relationship between mesopores and micropores of the adsorbent is expected, as the mesopore allows for rapid diffusion of molecules inside it, with

access to the micropores where the adsorption effectively occurs. The high mesopore volume in this material results from the chemical activation with phosphoric acid and the pyrolysis of precursor material containing high cellulose content [9,68]. Furthermore, the optimal conditions for activated carbon synthesis (pyrolysis time and temperature) helped in the efficient decomposition of the lignocellulosic structure to develop the desired texture properties. This is supported by the high immobilization efficiency and enzyme activity.

Table 5. Texture properties of activated carbon produced from sisal waste.

Sample	S_g (m^2 g^{-1})	D_p (nm)[a]	V_{meso} (cm^3 g^{-1})	V_{micro} (cm^3 g^{-1})	V_{total} (cm^3 g^{-1})
Activated carbon	600	5.68	0.4738	0.0888	0.6024

Sg – BET surface area; Dp – average pore diameter; a – maximum pore size distribution; Vmeso – mesopore volume; Vmicro – micropore volume; Vtotal – total pore volume.

The BET surface area is one of the most important parameters for enzyme immobilization by adsorption as it provides a greater available area for bonding between biomolecule and support. A good relationship between surface area and porosity is required as it allows for different types of interaction with the matrix, both on the surface and inside the pores. The surface area (Sg) from our work is similar to other activated carbon from sisal waste under similar synthesis conditions, such as Dizbay-Onat et al. [69] (BET = 674 m^2 g^{-1}).

However, this surface area is lower compared to other studies using lipase immobilized on activated carbon. Oliveira et al. [36] reported a surface area of 1135 m^2 g^{-1} for corn cob-activated carbon using phosphoric acid as a chemical activating agent and Almeida et al. [70] reported a surface area of 1491 m^2 g^{-1} for guava seed AC chemically activated with potassium hydroxide. This can be attributed to sisal stiffness, which is known as a hard natural fibre. Furthermore, sisal waste is obtained from the extraction of sisal fiber, leading to a decrease in lignocellulosic content and changes in the adsorbent texture properties depending on the processing method applied [3].

Despite this, the carbon-based material in our work reached great immobilization parameters and hydrolytic activity similar to Oliveira et al. [36] under the same immobilization conditions (U = 42,5). This can be explained by the pore diameter (Dp) verified, which is larger than lipase dimensions (around 4 nm) and enables its adsorption [62]. Moreover, the surface functional groups observed in the FTIR spectra may have

influenced the affinity of the enzyme for the support, resulting in efficient immobilization by strong interactions [37].

The derivative may also be viable for other lipolytic reactions, such as esterification. This is supported by the results observed in section 3.4. Buchori et al. [71] verified Sg = 61.64 $m^2 g^{-1}$ and a high yield (> 90%) for biodiesel production, and Ramani et al. [72] obtained twice the conversion efficiency into an oily waste when compared to the free enzyme even with BET = 411 $m^2 g^{-1}$.

Scanning Electron Microscope (SEM) was employed to observe the structure of activated carbon from sisal waste (Figure 4). The surface morphology of AC presents a spongy appearance and porous structure with different pore sizes and shapes, containing both micropores and mesopores. Thus, the support from sisal waste provides desirable properties for its application on enzyme immobilization by adsorption once this is a surface mechanism and depends mainly on the surface characteristics of the carbonaceous material.

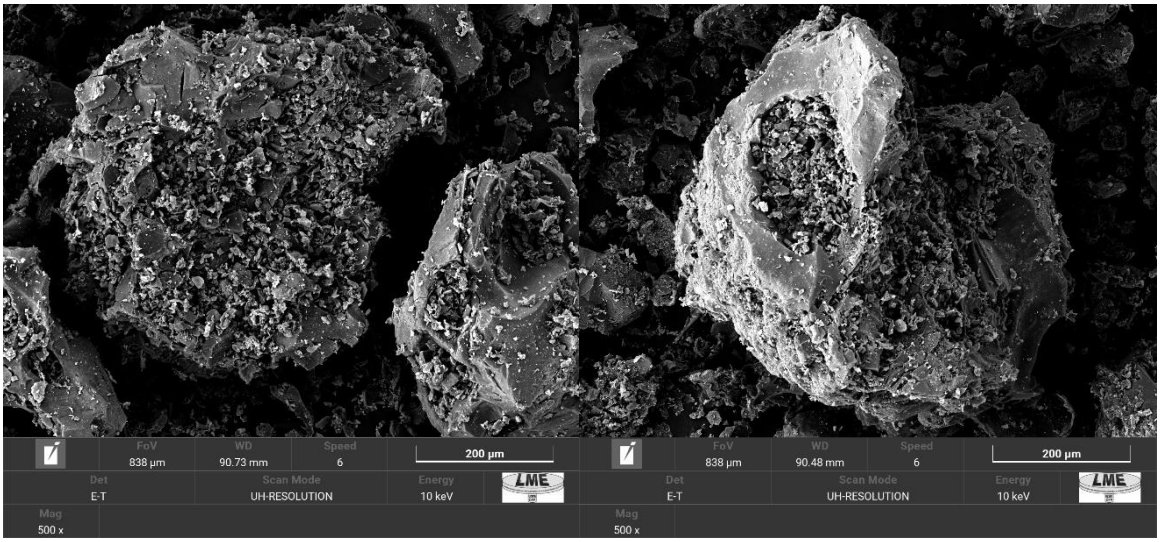

Figure 4. Scanning Electron Microscopy (SEM) of activated carbon from sisal waste.

3.4 Aroma ester synthesis

After successfully optimizing the lipase immobilization, the derivative was explored for commercial purposes such as the esterification of aromas. The esterification yield of ethyl lactate (Y%) for immobilized lipase on activated carbon from sisal waste was 91.290 ± 0.099%, and it may be due to the greater specificity of PPL in anhydrous medium for short- and medium-chain compounds, such as ethyl alcohol and lactic acid, rather than complex triglyceride structures like olive oil [78]. Regarding free enzyme (94.968 ± 0.959%), a

slightly lower yield was observed, but this is expected as PPL-AC has lower mobility and access to the substrate [79]. Furthermore, this is a promising result since pancreatic lipase is a low-cost enzyme when compared to other sources [80]. Subsequently, the operational stability of the derivative was investigated based on the reuse cycles (Figure 5).

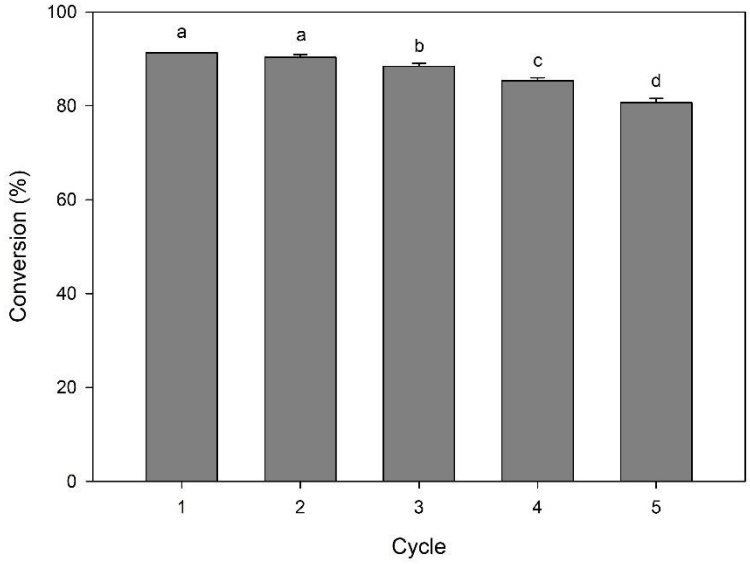

Figure 5. Conversion of ethyl lactate ester catalyzed by porcine pancreas lipase immobilized on activated carbon from sisal waste as a function of the number of reuse cycles.

PPL-AC achieved 80.677 ± 0.888% of ester conversion after five cycles, which is 11.62% lower than the first cycle. This decrease is caused by the biocatalyst desorbing from biochar structure due to the weak forces involved in physical immobilization methods, such as Van der Waals, hydrophobic, and hydrogen interactions [87]. To overcome this problem, binding agents can be incorporated into the activated carbon surface to increase the interaction strength between enzyme and support [81].

However, these findings agree with other studies on lipase-mediated ethyl lactate synthesis, suggesting that the immobilization process efficiently protected the lipase from desorption, denaturation, and inactivation under the reaction conditions employed. Mehta et al. [28] reported Y% = 87.32% in the first cycle, Sun et al. [82] found Y% = 83.3% in the first cycle, and Koutinas et al. [83] reported Y% = 85% after five cycles. Therefore, the derivative synthesized has the potential to catalyze the esterification of ethyl lactate for use in industry and replace the chemical method as a green alternative.

4. Conclusion

The Central Composite Design (CCD) and Response Surface Methodology (RSM) were applied successfully to optimize the synthesis conditions of activated carbon derived from sisal waste for lipase immobilization and ethyl lactate production. The coefficient of determination verified that the model fits the experimental design. Morphological and texture analysis confirmed the porous structure and surface area of activated carbon synthesized under optimal conditions, indicating a valuable structure for enzyme immobilization. The high ester conversion after five cycles suggested that the immobilization process efficiently protected the lipase from desorption, denaturation, and inactivation under the reaction conditions employed. Therefore, the activated carbon from sisal waste has the potential for lipase immobilization as a low-cost sustainable adsorbent through agro-industrial waste management for industrial-scale application. It can also be used for catalyzing ethyl lactate esterification for commercial purposes, providing a green alternative to the chemical method.

Acknowledgments

The authors gratefully acknowledge the financial support provided for this work by the National Council for Scientific and Technological Development (CNPq) and Coordination for the Improvement of Higher Education Personnel (CAPES). We are also thankful for the support in analyses by CETENE and LME (UFLA).

References

[1] S. Wachiye *et al.*, “Soil greenhouse gas emissions from a sisal chronosequence in Kenya”, *Agric For Meteorol*, vol. 307, set. 2021, doi: 10.1016/j.agrformet.2021.108465.

[2] T. A. Colley, J. Valerian, M. Z. Hauschild, S. I. Olsen, e M. Birkved, “Addressing nutrient depletion in Tanzanian sisal fiber production using life cycle assessment and circular economy principles, with bioenergy co-production”, *Sustainability (Switzerland)*, vol. 13, nº 16, ago. 2021, doi: 10.3390/su13168881.

[3] S. Shahzad, M. Hussain, H. Munir, e M. Arfan, “Proximate composition and spatio-temporal heterogeneity of phytochemicals in Agave sisalana Perrine (sisal) adapted in different agro-ecological zones of Punjab, Pakistan”, *Environmental Science and Pollution Research*, vol. 29, nº 32, p. 48869–48879, jul. 2022, doi: 10.1007/s11356-022-19260-5.

[4] K. Melo, T. Santos, C. Santos, R. Fonseca, N. Dantas, e M. Aquino, “Experimental Analysis of Styrene, Particle Size, and Fiber Content in the Mechanical Properties of Sisal Fiber Powder Composites”, 2020.

[5] W. Li, J. Cao, J. Yang, Z. Wang, e Y. Yang, “Production and characterization of lignocellulosic fractions from sisal waste”, *Ind Crops Prod*, vol. 160, fev. 2021, doi: 10.1016/j.indcrop.2020.113109.

[6] D. Pandey, A. Daverey, e K. Arunachalam, “Biochar: Production, properties and emerging role as a support for enzyme immobilization”, *Journal of Cleaner Production*, vol. 255. Elsevier Ltd, 10 de maio de 2020. doi: 10.1016/j.jclepro.2020.120267.

[7] A. Imam, S. K. Suman, R. Singh, B. P. Vempatapu, A. Ray, e P. K. Kanaujia, “Application of laccase immobilized rice straw biochar for anthracene degradation”, *Environmental Pollution*, vol. 268, jan. 2021, doi: 10.1016/j.envpol.2020.115827.

[8] G. Bijoy, R. Rajeev, L. Benny, S. Jose, e A. Varghese, “Enzyme immobilization on biomass-derived carbon materials as a sustainable approach towards environmental applications”, *Chemosphere*, vol. 307, nov. 2022, doi: 10.1016/j.chemosphere.2022.135759.

[9] M. J. Pinto Brito *et al.*, “Development of activated carbon from pupunha palm heart sheaths: Effect of synthesis conditions and its application in lipase immobilization”, *J Environ Chem Eng*, vol. 8, nº 5, out. 2020, doi: 10.1016/j.jece.2020.104391.

[10] M. Hasanzadeh, A. Simchi, e H. Shahriyari Far, “Nanoporous composites of activated carbon-metal organic frameworks for organic dye adsorption: Synthesis, adsorption mechanism and kinetics studies”, *Journal of Industrial and Engineering Chemistry*, vol. 81, p. 405–414, jan. 2020, doi: 10.1016/j.jiec.2019.09.031.

[11] H. Chakhtouna, H. Benzeid, N. Zari, A. el kacem Qaiss, e R. Bouhfid, “Recent advances in eco-friendly composites derived from lignocellulosic biomass for wastewater treatment”, *Biomass Conversion and Biorefinery*. Springer Science and Business Media Deutschland GmbH, 2022. doi: 10.1007/s13399-022-03159-9.

[12] J. G. Speight, “Non–fossil fuel feedstocks”, em *The Refinery of the Future*, Elsevier, 2020, p. 343–389. doi: 10.1016/b978-0-12-816994-0.00010-5.

[13] R. C. Rodrigues, Á. Berenguer-Murcia, D. Carballares, R. Morellon-Sterling, e R. Fernandez-Lafuente, “Stabilization of enzymes via immobilization: Multipoint covalent attachment and other stabilization strategies”, *Biotechnology Advances*, vol. 52. Elsevier Inc., 15 de novembro de 2021. doi: 10.1016/j.biotechadv.2021.107821.

[14] D. Remonatto, R. H. Miotti, R. Monti, J. C. Bassan, e A. V. de Paula, “Applications of immobilized lipases in enzymatic reactors: A review”, *Process Biochemistry*, vol. 114. Elsevier Ltd, p. 1–20, 1º de março de 2022. doi: 10.1016/j.procbio.2022.01.004.

[15] C. S. Sampaio, J. A. F. Angelotti, R. Fernandez-Lafuente, e D. B. Hirata, “Lipase immobilization via cross-linked enzyme aggregates: Problems and prospects – A review”, *International Journal of Biological Macromolecules*, vol. 215. Elsevier B.V., p. 434–449, 31 de agosto de 2022. doi: 10.1016/j.ijbiomac.2022.06.139.

[16] X. Chen, J. Wang, R. J. Stevenson, X. Ang, Y. Peng, e S. Y. Quek, “Lipase-catalyzed modification of milk fat: A promising way to alter flavor notes of goat milk products”, *LWT*, vol. 145, jun. 2021, doi: 10.1016/j.lwt.2021.111286.

[17] T. Guan, B. Liu, R. Wang, Y. Huang, J. Luo, e Y. Li, “The enhanced fatty acids flavor release for low-fat cheeses by carrier immobilized lipases on O/W Pickering emulsions”, *Food Hydrocoll*, vol. 116, jul. 2021, doi: 10.1016/j.foodhyd.2021.106651.

[18] A. B. A. Mohammed, A. E. Hegazy, e A. Salah, “Predigested high-fat meats based on Lactobacillus fermentum lipase enzyme immobilized on silver-alginate nanoparticle matrix”, *Applied Nanoscience (Switzerland)*, vol. 13, nº 1, p. 641–649, jan. 2023, doi: 10.1007/s13204-021-01879-4.

[19] M. Xiang, L. Wang, Q. Yan, Z. Jiang, e S. Yang, “Heterologous expression and biochemical characterization of a cold-active lipase from Rhizopus microsporus suitable for oleate synthesis and bread making”, *Biotechnol Lett*, vol. 43, nº 9, p. 1921–1932, set. 2021, doi: 10.1007/s10529-021-03167-1.

[20] A. Safdar, F. Ismail, e M. Imran, “Characterization of Detergent-Compatible Lipases from *Candida albicans* and *Acremonium sclerotigenum* under Solid-State Fermentation”, *ACS Omega*, ago. 2023, doi: 10.1021/acsomega.3c03644.

[21] Y. Q. Liu, X. WeiZhuo, e X. Wei, “A review on lipase-catalyzed synthesis of geranyl esters as flavor additives for food, pharmaceutical and cosmetic applications”, *Food Chemistry Advances*, vol. 1. Elsevier Ltd, 1º de outubro de 2022. doi: 10.1016/j.focha.2022.100052.

[22] M. Dixit, G. K. Gupta, P. Pathak, N. K. Bhardwaj, e P. Shukla, “An efficient endoglucanase and lipase enzyme consortium (ELEC) for deinking of old newspaper and ultrastructural analysis of deinked pulp”, *Biomass Convers Biorefin*, 2022, doi: 10.1007/s13399-022-03310-6.

[23] M. A. Taleb *et al.*, “Bioscouring of wool fibres using immobilized thermophilic lipase”, *Int J Biol Macromol*, vol. 194, p. 800–810, jan. 2022, doi: 10.1016/j.ijbiomac.2021.11.128.

[24] J. H. C. Wancura *et al.*, “Demystifying the enzymatic biodiesel: How lipases are contributing to its technological advances”, *Renewable Energy*, vol. 216. Elsevier Ltd, 1º de novembro de 2023. doi: 10.1016/j.renene.2023.119085.

[25] D. Balogh-Weiser *et al.*, “Combined Nanofibrous Face Mask: Co-Formulation of Lipases and Antibiotic Agent by Electrospinning Technique”, *Pharmaceutics*, vol. 15, nº 4, abr. 2023, doi: 10.3390/pharmaceutics15041174.

[26] S. Cong *et al.*, “Synthesis of flavor esters by a novel lipase from Aspergillus niger in a soybean-solvent system”, *3 Biotech*, vol. 9, nº 6, jun. 2019, doi: 10.1007/s13205-019-1778-5.

[27] P. Majgaonkar, R. Hanich, F. Malz, e R. Brüll, “Chemical Recycling of Post-Consumer PLA Waste for Sustainable Production of Ethyl Lactate”, *Chemical Engineering Journal*, vol. 423, nov. 2021, doi: 10.1016/j.cej.2021.129952.

[28] A. Mehta, C. Grover, K. K. Bhardwaj, e R. Gupta, “Application of lipase purified from aspergillus fumigatus in the syntheses of ethyl acetate and ethyl lactate”, *J Oleo Sci*, vol. 69, nº 1, p. 23–29, 2020, doi: 10.5650/jos.ess19202.

[29] D. Xue *et al.*, “Ethyl lactate biosynthesis by the cascade of the aerobic process and the anaerobic process with corn stover”, *Cellulose*, 2024, doi: 10.1007/s10570-023-05729-0.

[30] P. J. Van Soest, J. B. Robertson, e B. A. Lewis, “Methods for Dietary Fiber, Neutral Detergent Fiber, and Nonstarch Polysaccharides in Relation to Animal Nutrition”, *J Dairy Sci*, vol. 74, nº 10, p. 3583–3597, 1991, doi: 10.3168/jds.S0022-0302(91)78551-2.

[31] K. Kuśmierek, M. Szala, e A. Świątkowski, “Adsorption of 2,4-dichlorophenol and 2,4-dichlorophenoxyacetic acid from aqueous solutions on carbonaceous materials obtained by combustion synthesis”, *J Taiwan Inst Chem Eng*, vol. 63, p. 371–378, jun. 2016, doi: 10.1016/j.jtice.2016.03.036.

[32] S. Brunauer, P. H. Emmett, e E. Teller, “Adsorption of Gases in Multimolecular Layers”, 1938. [Online]. Disponível em: https://pubs.acs.org/sharingguidelines

[33] B. C. Lippens, B. G. Linsen, e J. H. De Boer, “Studies on Pore Systems in Catalysts I. The Adsorption of Nitrogen; Apparatus and Calculation”, 1964.

[34] M. M. Bradford, “A Rapid and Sensitive Method for the Quantitation of Microgram Quantities of Protein Utilizing the Principle of Protein-Dye Binding”, 1976.

[35] C. M. F. Soares, H. F. De Castro, F. F. De Moraes, e G. M. Zanin, “Characterization and Utilization of Candida rugosa Lipase Immobilized on Controlled Pore Silica”, 1999.

[36] T. P. de Oliveira, M. P. F. Santos, M. J. P. Brito, e C. M. Veloso, “Incorporation of metallic particles in activated carbon used in lipase immobilization for production of isoamyl acetate”, *Journal of Chemical Technology and Biotechnology*, vol. 97, nº 7, p. 1736–1746, jul. 2022, doi: 10.1002/jctb.7043.

[37] J. F. Borges *et al.*, “Laccase Immobilization on Activated Carbon from Hydrothermal Carbonization of Corn Cob”, *Waste Biomass Valorization*, 2023, doi: 10.1007/s12649-023-02160-1.

[38] N. Abuelnoor, A. AlHajaj, M. Khaleel, L. F. Vega, e M. R. M. Abu-Zahra, “Activated carbons from biomass-based sources for CO2 capture applications”, *Chemosphere*, vol. 282. Elsevier Ltd, 1º de novembro de 2021. doi: 10.1016/j.chemosphere.2021.131111.

[39] L. Zhang, X. Dou, Z. Yang, X. Yang, e X. Guo, “Advance in Hydrothermal Bio-Oil Preparation from Lignocellulose: Effect of Raw Materials and Their Tissue Structures”, *Biomass*, vol. 1, nº 2, p. 74–93, out. 2021, doi: 10.3390/biomass1020006.

[40] R. Shen, J. Lu, Z. Yao, L. Zhao, e Y. Wu, “The hydrochar activation and biocrude upgrading from hydrothermal treatment of lignocellulosic biomass”, *Bioresource*

Technology, vol. 342. Elsevier Ltd, 1º de dezembro de 2021. doi: 10.1016/j.biortech.2021.125914.

[41] Y. Zhang, X. Song, P. Zhang, H. Gao, C. Ou, e X. Kong, "Production of activated carbons from four wastes via one-step activation and their applications in Pb2+ adsorption: Insight of ash content", *Chemosphere*, vol. 245, abr. 2020, doi: 10.1016/j.chemosphere.2019.125587.

[42] M. Lewoyehu, "Comprehensive review on synthesis and application of activated carbon from agricultural residues for the remediation of venomous pollutants in wastewater", *Journal of Analytical and Applied Pyrolysis*, vol. 159. Elsevier B.V., 1º de outubro de 2021. doi: 10.1016/j.jaap.2021.105279.

[43] Z. Heidarinejad, M. H. Dehghani, M. Heidari, G. Javedan, I. Ali, e M. Sillanpää, "Methods for preparation and activation of activated carbon: a review", *Environmental Chemistry Letters*, vol. 18, nº 2. Springer, p. 393–415, 1º de março de 2020. doi: 10.1007/s10311-019-00955-0.

[44] C. Jiang, G. A. Yakaboylu, T. Yumak, J. W. Zondlo, E. M. Sabolsky, e J. Wang, "Activated carbons prepared by indirect and direct CO2 activation of lignocellulosic biomass for supercapacitor electrodes", *Renew Energy*, vol. 155, p. 38–52, ago. 2020, doi: 10.1016/j.renene.2020.03.111.

[45] M. Hasanzadeh, A. Simchi, e H. Shahriyari Far, "Nanoporous composites of activated carbon-metal organic frameworks for organic dye adsorption: Synthesis, adsorption mechanism and kinetics studies", *Journal of Industrial and Engineering Chemistry*, vol. 81, p. 405–414, jan. 2020, doi: 10.1016/j.jiec.2019.09.031.

[46] K. S. Baig, "Interaction of enzymes with lignocellulosic materials: causes, mechanism and influencing factors", *Bioresources and Bioprocessing*, vol. 7, nº 1. Springer Science and Business Media Deutschland GmbH, 1º de dezembro de 2020. doi: 10.1186/s40643-020-00310-0.

[47] S. C. Hu *et al.*, "Structural changes and electrochemical properties of lacquer wood activated carbon prepared by phosphoric acid-chemical activation for supercapacitor applications", *Renew Energy*, vol. 177, p. 82–94, nov. 2021, doi: 10.1016/j.renene.2021.05.113.

[48] E. Scelsi, A. Angelini, e C. Pastore, "Deep Eutectic Solvents for the Valorisation of Lignocellulosic Biomasses towards Fine Chemicals", *Biomass*, vol. 1, nº 1, p. 29–59, jul. 2021, doi: 10.3390/biomass1010003.

[49] O. J. Al-sareji *et al.*, "Removal of emerging pollutants from water using enzyme-immobilized activated carbon from coconut shell", *J Environ Chem Eng*, vol. 11, nº 3, jun. 2023, doi: 10.1016/j.jece.2023.109803.

[50] D. Remonatto, R. H. Miotti, R. Monti, J. C. Bassan, e A. V. de Paula, "Applications of immobilized lipases in enzymatic reactors: A review", *Process Biochemistry*, vol. 114. Elsevier Ltd, p. 1–20, 1º de março de 2022. doi: 10.1016/j.procbio.2022.01.004.

[51] J. Zhang *et al.*, “Amphiphilic Nanointerface: Inducing the Interfacial Activation for Lipase”, *ACS Appl Mater Interfaces*, vol. 14, nº 34, p. 39622–39636, ago. 2022, doi: 10.1021/acsami.2c11500.

[52] J. Montalvo Andia, A. Larrea, J. Salcedo, J. Reyes, L. Lopez, e L. Yokoyama, “Synthesis and characterization of chemically activated carbon from Passiflora ligularis, Inga feuilleei and native plants of South America”, *J Environ Chem Eng*, vol. 8, nº 4, ago. 2020, doi: 10.1016/j.jece.2020.103892.

[53] M. Iwanow, T. Gärtner, V. Sieber, e B. König, “Activated carbon as catalyst support: Precursors, preparation, modification and characterization”, *Beilstein Journal of Organic Chemistry*, vol. 16. Beilstein-Institut Zur Forderung der Chemischen Wissenschaften, p. 1188–1202, 2 de junho de 2020. doi: 10.3762/bjoc.16.104.

[54] T. Senthilkumar, A. Selvakumar, e B. Senthilkumar, “Fabrication and optimization of activated carbon using sisal fiber biomass through Box–Behnken experimental design”, *Biomass Convers Biorefin*, 2023, doi: 10.1007/s13399-023-04185-x.

[55] H. Wu, W. Yuan, Y. Zhao, D. Han, X. Yuan, e L. Cheng, “B, N-dual doped sisal-based multiscale porous carbon for high-rate supercapacitors”, *RSC Adv*, vol. 9, nº 3, p. 1476–1486, 2019, doi: 10.1039/C8RA09663E.

[56] T. A. Jambeiro *et al.*, “Fast Pyrolysis of Sisal Residue in a Pilot Fluidized Bed Reactor”, *Energy and Fuels*, vol. 32, nº 9, p. 9478–9492, set. 2018, doi: 10.1021/acs.energyfuels.8b01718.

[57] M. P. F. Santos, M. C. P. Porfírio, E. C. S. Junior, R. C. F. Bonomo, e C. M. Veloso, “Pepsin immobilization: Influence of carbon support functionalization”, *Int J Biol Macromol*, vol. 203, p. 67–79, abr. 2022, doi: 10.1016/j.ijbiomac.2022.01.135.

[58] Y. Luo, D. Li, Y. Chen, X. Sun, Q. Cao, e X. Liu, “The performance of phosphoric acid in the preparation of activated carbon-containing phosphorus species from rice husk residue”, *J Mater Sci*, vol. 54, nº 6, p. 5008–5021, mar. 2019, doi: 10.1007/s10853-018-03220-x.

[59] A. Benítez, J. Amaro-Gahete, Y. C. Chien, Á. Caballero, J. Morales, e D. Brandell, “Recent advances in lithium-sulfur batteries using biomass-derived carbons as sulfur host”, *Renewable and Sustainable Energy Reviews*, vol. 154. Elsevier Ltd, 1º de fevereiro de 2022. doi: 10.1016/j.rser.2021.111783.

[60] A. H. Jawad *et al.*, “Insights into the modeling, characterization and adsorption performance of mesoporous activated carbon from corn cob residue via microwave-assisted H3PO4 activation”, *Surfaces and Interfaces*, vol. 21, dez. 2020, doi: 10.1016/j.surfin.2020.100688.

[61] A. Fernandez-Sanroman, V. Acevedo-García, M. Pazos, M. A. Sanromán, e E. Rosales, “Removal of sulfamethoxazole and methylparaben using hydrocolloid and fiber industry wastes: Comparison with biochar and laccase-biocomposite”, *J Clean Prod*, vol. 271, out. 2020, doi: 10.1016/j.jclepro.2020.122436.

[62] G. R. Ferreira Gonçalves, O. R. Ramos Gandolfi, M. J. P. Brito, R. C. F. Bonomo, R. da Costa Ilhéu Fontan, e C. M. Veloso, “Immobilization of porcine pancreatic

lipase on activated carbon by adsorption and covalent bonding and its application in the synthesis of butyl butyrate", *Process Biochemistry*, vol. 111, p. 114–123, dez. 2021, doi: 10.1016/j.procbio.2021.10.027.

[63] S. Lu *et al.*, "Facile extraction and characterization of cellulose nanocrystals from agricultural waste sugarcane straw", *J Sci Food Agric*, vol. 102, nº 1, p. 312–321, jan. 2022, doi: 10.1002/jsfa.11360.

[64] J. Zhuang, M. Li, Y. Pu, A. J. Ragauskas, e C. G. Yoo, "Observation of potential contaminants in processed biomass using fourier transform infrared spectroscopy", *Applied Sciences (Switzerland)*, vol. 10, nº 12, jun. 2020, doi: 10.3390/app10124345.

[65] E. M. Mistar, T. Alfatah, e M. D. Supardan, "Synthesis and characterization of activated carbon from Bambusa vulgaris striata using two-step KOH activation", *Journal of Materials Research and Technology*, vol. 9, nº 3, p. 6278–6286, 2020, doi: 10.1016/j.jmrt.2020.03.041.

[66] P. S. Bhandari e P. R. Gogate, "Kinetic and thermodynamic study of adsorptive removal of sodium dodecyl benzene sulfonate using adsorbent based on thermo-chemical activation of coconut shell", *J Mol Liq*, vol. 252, p. 495–505, fev. 2018, doi: 10.1016/j.molliq.2017.12.018.

[67] "INTERNATIONAL UNION OF PURE AND APPLIED CHEMISTRY PHYSICAL CHEMISTRY DIVISION COMMISSION ON COLLOID AND SURFACE CHEMISTRY INCLUDING CATALYSIS* REPORTING PHYSISORPTION DATA FOR GAS/SOLID SYSTEMS with Special Reference to the Determination of Surface Area and Porosity Reporting physisorption data for gas/solid systems-with special reference to the determination of surface area and porosity", 1985.

[68] N. F. Mokhtar, R. N. Z. R. Raja Noor Zaliha, N. D. Muhd Noor, F. Mohd Shariff, e M. S. M. Ali, "The immobilization of lipases on porous support by adsorption and hydrophobic interaction method", *Catalysts*, vol. 10, nº 7. MDPI, p. 1–17, 1º de setembro de 2020. doi: 10.3390/catal10070744.

[69] M. Dizbay-Onat, U. K. Vaidya, e C. T. Lungu, "Preparation of industrial sisal fiber waste derived activated carbon by chemical activation and effects of carbonization parameters on surface characteristics", *Ind Crops Prod*, vol. 95, p. 583–590, jan. 2017, doi: 10.1016/j.indcrop.2016.11.016.

[70] L. C. Almeida, A. S. Barbosa, A. T. Fricks, L. S. Freitas, Á. S. Lima, e C. M. F. Soares, "Use of conventional or non-conventional treatments of biochar for lipase immobilization", *Process Biochemistry*, vol. 61, p. 124–129, out. 2017, doi: 10.1016/j.procbio.2017.06.020.

[71] L. Buchori, W. Widayat, H. Hadiyanto, H. Satriadi, N. Chasanah, e M. R. Kurniawan, "Modification of magnetic nanoparticle lipase catalyst with impregnation of Activated Carbon Oxide (ACO) in biodiesel production from PFAD (Palm Fatty Acid Distillate)", *Bioresour Technol Rep*, vol. 19, set. 2022, doi: 10.1016/j.biteb.2022.101137.

[72] K. Ramani, S. Karthikeyan, R. Boopathy, L. J. Kennedy, A. B. Mandal, e G. Sekaran, "Surface functionalized mesoporous activated carbon for the immobilization of acidic lipase and their application to hydrolysis of waste cooked oil: Isotherm and kinetic studies", *Process Biochemistry*, vol. 47, nº 3, p. 435–445, mar. 2012, doi: 10.1016/j.procbio.2011.11.025.

[73] M. Li, H. Xiao, T. Zhang, Q. Li, e Y. Zhao, "Activated Carbon Fiber Derived from Sisal with Large Specific Surface Area for High-Performance Supercapacitors", *ACS Sustain Chem Eng*, vol. 7, nº 5, p. 4716–4723, mar. 2019, doi: 10.1021/acssuschemeng.8b04607.

[74] M. M. O. dos Santos *et al.*, "Synthesis of hexyl butyrate (apple and citrus aroma) by Candida rugosa lipase immobilized on Diaion HP-20 using the Box-Behnken design", *Food Sci Biotechnol*, vol. 32, nº 5, p. 689–696, abr. 2023, doi: 10.1007/s10068-022-01200-1.

[75] G. Bayramoglu, O. Celikbicak, M. Kilic, e M. Yakup Arica, "Immobilization of Candida rugosa lipase on magnetic chitosan beads and application in flavor esters synthesis", *Food Chem*, vol. 366, jan. 2022, doi: 10.1016/j.foodchem.2021.130699.

[76] G. Kovalenko, L. Perminova, M. Pykhtina, e A. Beklemishev, "Lipase-active heterogeneous biocatalysts for enzymatic synthesis of short-chain aroma esters", *Biocatal Agric Biotechnol*, vol. 36, set. 2021, doi: 10.1016/j.bcab.2021.102124.

[77] I. Bayout *et al.*, "Natural flavor ester synthesis catalyzed by lipases", *Flavour Fragr J*, vol. 35, nº 2, p. 209–218, mar. 2020, doi: 10.1002/ffj.3554.

[78] G. VS e S. KL, "Enzymatic Synthesis of Fatty Esters by Lipase from Porcine Pancreas", *Journal of Thermodynamics & Catalysis*, vol. 07, nº 01, 2016, doi: 10.4172/2157-7544.1000161.

[79] M. Maria Oliveira dos Santos *et al.*, "APPLICATION OF LIPASE IMMOBILIZED ON A HYDROPHOBIC SUPPORT FOR THE SYNTHESIS OF AROMATIC ESTERS RUNNING TITLE: LIPASE IMMOBILIZED IN AROMA ESTERS SYNTHESIS", doi: 10.1002/bab.1959_AM_COPY.

[80] F. Zappaterra, M. E. M. Rodriguez, D. Summa, B. Semeraro, S. Costa, e E. Tamburini, "Biocatalytic approach for direct esterification of ibuprofen with sorbitol in biphasic media", *Int J Mol Sci*, vol. 22, nº 6, p. 1–18, mar. 2021, doi: 10.3390/ijms22063066.

[81] A. H. Rather, R. S. Khan, T. U. Wani, M. A. Beigh, e F. A. Sheikh, "Overview on immobilization of enzymes on synthetic polymeric nanofibers fabricated by electrospinning", *Biotechnology and Bioengineering*, vol. 119, nº 1. John Wiley and Sons Inc, p. 9–33, 1º de janeiro de 2022. doi: 10.1002/bit.27963.

[82] J. Sun, Y. Jiang, L. Zhou, e J. Gao, "Immobilization of Candida antarctica lipase B by adsorption in organic medium", *N Biotechnol*, vol. 27, nº 1, p. 53–58, dez. 2010, doi: 10.1016/j.nbt.2009.12.001.

[83] M. Koutinas *et al.*, “Application of commercial and non-commercial immobilized lipases for biocatalytic production of ethyl lactate in organic solvents”, *Bioresour Technol*, vol. 247, p. 496–503, 2018, doi: 10.1016/j.biortech.2017.09.130.

[84] E. P. Barrett, L. G. Joyner, P. P. Halenda, “The Determination of Pore Volume and Area Distributions in Porous Substances. I. Computations from Nitrogen Isotherms”, *J. Am. Chem. Soc.*, v. 73, p. 373–380, 1951. doi: 10.1021/ja01145a126.

[85] X. Xinping, J. Jianchun, S. Kang, L. Xincheng, “Preparation and characterization of activated carbon using phosphoric acid as activator from sisal fiber”, *Chemistry and Industry of Forest Products*, v. 33, n. 3, p. 105-109, 2013.

[86] Association of Official Analytical Chemists (AOAC). *Official methods of analysis.* 18 ed. Gaithersburg: AOAC International, 2007.

[87] D. Lakshimi, M. I. Diana, P. A. Helen, P. C. Selvin, *“Functionalized Nanomaterials, Classification, Properties, and Functionalization Techniques”*, In: Hussain, C.M., Ahamed, M.B. (eds) Functionalized Nanomaterials Based Supercapacitor. Materials Horizons: From Nature to Nanomaterials. Springer, Singapore, 2024. doi: 10.1007/978-981-99-3021-0_3

CAPÍTULO 3

ARTIGO 2

Promising activated carbon functionalization for lipase immobilization: Characterization, hydrolytic activity, and ethyl lactate synthesis

---

*Manuscrito será submetido à revista Bioresource Technology (ISSN: 1873-2976) – Fator de impacto: 11.4.

ABSTRACT

This study aimed to investigate the effect of surface modification (genipin (GAC), iminodiacetic acid (IDA) + metallic particles (MAC), and genipin + metallic particles (GMAC)) on activated carbon for immobilizing lipase (Porcine pancreas lipase (PPL) and *Candida rugosa* lipase (CRL)) and their application in synthesizing ethyl lactate. The texture properties of functionalized carbons were confirmed by pore size distribution, BET surface area, and average pore diameter, indicating a valuable structure for enzyme immobilization. All the adsorbents showed high immobilization efficiency (E > 87%), with the metalized-activated carbons presenting the highest hydrolysis activity (MAC = 46.9 U and GMAC = 48.1 U for PPL and MAC = 47.3 U and GMAC = 51.6 U for CRL). The derivatives have reported promising results for the synthesis of ethyl lactate (yield > 90%). The high ester conversion after five cycles suggested that the immobilization process efficiently protected the lipase from desorption and maintained its active form, and the metalized supports had the highest yield in the last cycle (MAC = 86.16% and GMAC = 85.79% for PPL; MAC = 88.46% and GMAC = 88.14% for CRL). Therefore, the synthesized derivatives have the potential to catalyze the production of aroma esters through biotechnological tools for use in industry.

Keywords: aroma ester; functionalization; covalent bond; genipin; metallic particles.

1. Introduction

Biocatalysis is a powerful approach used in the industry to produce various chemical compounds. Enzymatic synthesis has many advantages over conventional chemical synthesis due to its selectivity, biocompatibility, biodegradability, and environmental acceptability (Monteiro et al., 2021; Sampaio et al., 2022). Hydrolases (EC 3.1.1.3) are the most commonly used biocatalysts in the market, among which lipases are known for their versatility and selectivity. They catalyze the hydrolysis of triacylglycerols but can also catalyze synthesis reactions in non-aqueous media (Nascimento et al., 2021; Pereira et al., 2022).

In recent years, lipase application for synthesizing flavor esters has become increasingly important. Flavor esters are produced by reacting short or medium-chain carboxylic acids with alcohols, resulting in fruity and floral aromas. These compounds are crucial for the food, cleaning, cosmetics, and hygiene industries as they determine the

sensorial properties of products and consumer acceptance (Bayout et al., 2020; Kovalenko et al., 2021).

Ester production through natural sources or chemical synthesis is related to several variables, such as ester concentration and bonding in the raw material, processing conditions, and toxicity (Vilas Bôas & de Castro, 2022). Consequently, the method becomes more expensive and cannot meet the current market demand since aromas, flavors, and fragrances are the world's largest field of food additives, with an estimated global market of US$12.8 billion in 2023. Therefore, the trend to efficiently and sustainably synthesize aromas using biotechnological tools is increasing (Bayramoglu et al., 2022; Santos et al., 2023).

The use of free lipases in industrial processes is often hindered due to their low long-term stability, a gradual decrease in activity during storage, and expensive and/or inefficient recovery, which makes reuse difficult. However, these disadvantages can be addressed by using an appropriate immobilization protocol (Santos et al., 2020). There are several methods of immobilization based on the interaction between the biomolecule and the matrix, such as adsorption (Gonçalves et al., 2021), covalent bonds (Brito et al., 2020), cross-linking (Guajardo et al., 2020), and encapsulation (Nadar & Rathod, 2020). Among these mechanisms, activated carbon has shown potential as an adsorptive support in enzyme immobilization.

Activated carbon (AC) is a carbon-based material suitable for different applications such as catalytic support. Nevertheless, the adsorption efficiency is affected by the diffusional effects of substrate and products, randomness, and strength of the enzyme-support interaction (Hasanzadeh et al., 2020; Rather et al., 2022). Several studies have recently been carried out to overcome these challenges by modifying surfaces to obtain heterofunctional carbonaceous support (Gonçalves et al., 2021; Santos et al., 2022). Promising agents for covalently and ionically binding lipases on activated carbon include genipin as an alternative to the conventional functionalization with glutaraldehyde and magnetic particles, respectively (Bayramoglu et al., 2022; Oliveira et al., 2022).

Genipin is a green, stable, and low-toxicity (up to 10,000 < glutaraldehyde) crosslinking agent. This is a natural compound obtained from iridoid glycoside (geniposide) commonly used in alternative medicine due to its antimicrobial, antitumor, and anti-inflammatory properties (Tacias-Pascacio et al., 2019; Yu et al., 2021). The cross-linking activity occurs in primary amines of different materials creating covalent bonds. Although

genipin use as a crosslinking agent is widely applied in enzyme immobilization in chitosan (Bayramoglu et al., 2022), gelatin (Sun et al., 2022), and collagen (Adamiak & Sionkowska, 2020), there are few works for surface modification on carbon-based materials. Before this study, the literature only reported protease immobilization using activated carbon (M. P. F. Santos et al., 2022). Therefore, lipase immobilization on genipin-functionalized activated carbon should be investigated to increase process efficiency.

On the other hand, functionalization using metallic particles is an acknowledged technique for having several advantages such as biocompatibility, low toxicity, magnetic properties, easy execution, stability in different conditions, and reusability of the solution. Among the chemicals used, magnetic iron oxide (Fe_3O_4) particles are known to bind lipases covalently. Iron oxide (II, III) is produced by the co-precipitation of Fe^{2+} and Fe^{3+} ions (Darwesh et al., 2020; Oliveira et al., 2022; Rusu et al., 2022). However, the benefits presented regarding enzyme stability and activity are limited by the iron leaching due to changes in reaction conditions (Alchouron et al., 2021). Chelating agent incorporation is an alternative as they have a strong binding ability for metal ions, such as iminodiacetic acid (IDA) (Anito et al., 2020).

Although lipolytic enzymes are widely studied, lipase immobilization on functionalized activated carbon with genipin and metallic particles has not been reported yet. Therefore, this study aimed to investigate the effect of surface modification (genipin, IDA + metallic particles, and genipin + metallic particles) on activated carbon for immobilizing lipase (Porcine pancreas lipase and *Candida rugosa* lipase) and their application in synthesizing ethyl lactate.

2. Materials and methods

2.1 Materials

Sisal waste was previously characterized regarding lignocellulosic content (w/w): 41.11% cellulose, 18.45% hemicellulose, 20.83% lignin, and 5.52% ash. Activated carbon (synthesis yield = 45.61%, Ash = 7.89% w/w, pH_{PCZ} = 5.83, Sg = 600 $m^2\ g^{-1}$, Dp = 5.68 nm, V_{meso} = 0.4738 $cm^3\ g^{-1}$, V_{micro} = 0.0888 $cm^3\ g^{-1}$, V_{total} = 0.6024 $cm^3\ g^{-1}$) was synthesized in previous studies by chemical activation method using phosphoric acid through sisal waste carbonization at 700 ºC, 86 minutes, and an impregnation ratio of 2.5:1 (activating agent mass/precursor mass). Genipin extract (70% ethyl alcohol, 6.46 mg mL^{-1}) was obtained from

the work carried out by Santos et al. (Santos et al., 2022). Lipase (CAS: 9001-62-1) from Porcine Pancreas (PPL) type II (≥ 125 units/mg protein) and Lipase from *Candida rugosa* (CRL) type VII (≥ 700 units/mg solid) were obtained from Sigma-Aldrich Corporation. All other chemicals used were of analytical grade.

2.2 Functionalization of Activated Carbon

The surface modification of activated carbon was performed through different modifying agents such as genipin and iron salts (Fe^{2+} and Fe^{3+}). The functionalization with magnetic particles was also investigated using iminodiacetic acid (IDA) as a chelating agent and genipin as a cross-linking agent.

2.2.1 Functionalization with Genipin

The surface modification using genipin was performed as described by Santos et al. (Santos et al., 2022). First, 10 g of AC was mixed in an amine solution (2.5% v/v) containing 0.85 mL of ethylenediamine (99%) and 32.5 mL of acetone. This mixture was manually stirred for 10 min and left undisturbed for 24 hours to obtain amino-functionalized activated carbon.

The amino-functionalized AC was mixed with a genipin solution containing 33.5 mL of genipin extract and 33.5 mL of acetone under magnetic stirring at 85 g force for 30 min. The sample was dried at 60 ºC for 24 h. After solvent evaporation, the functionalized activated carbon was washed with distilled water to remove any unbound chemical compounds and dried at 60 ºC for 6 h. Finally, the genipin-functionalized activated carbon (GAC) was sieved (40 mesh) and packaged in airtight packaging.

2.2.2 Functionalization with magnetic particles

The surface modification using iron salts was carried out by co-precipitating Fe^{2+} and Fe^{3+} ions to incorporate magnetic particles on the activated carbon surface and create cross-links with enzymes. For this, two methods were employed: functionalization using iminodiacetic acid (IDA) as a chelating agent and genipin as a cross-linking agent before the incorporation of metallic particles.

i. Iminodiacetic acid as a chelating agent

To incorporate iminodiacetic acid (IDA) as a chelating agent, 3 g of AC were mixed with 20 mL of 1M sodium carbonate (Na_2CO_3) under magnetic stirring for 1 h. Then, 20 mL of 0.5M iminodiacetic acid 98% ($HN(CH_2COOH)_2$) were added, and the pH was adjusted to 11 with 1M sodium hydroxide (NaOH). The mixture was kept under stirring at 10 g force and 40 ºC for 14 h in a BOD incubator. After this period, the activated carbon was washed with an acetic acid solution (1% v/v) until the washing water became neutral.

The metallic particles were synthesized following Mohan et al. (Mohan et al., 2011) and Santos et al. (Santos et al., 2022) through the co-precipitation of ferrous sulfate (Fe^{2+}) and ferric chloride (Fe^{3+}) in an alkaline solution. For this, 5 g of activated carbon were mixed with 250 mL of ultrapure water while being stirred magnetically. The iron salts solution was prepared by mixing 200 mL of a solution containing 0.067 mol of trivalent iron ($FeCl_3.6H_2O$), 200 mL of a solution with 0.033 mol of bivalent iron ($FeSO_4.7H_2O$), and 2.5 mL of 37% HCl. The ferrous sulfate and ferric chloride solutions were added to the AC and stirred at 70 ºC for 15 min. After this step, 500 mL of 4M sodium hydroxide (NaOH) was added to the solution to precipitate the particles under magnetic stirring for 2 h. The precipitate was collected in Falcon tubes, washed 10 times with 40 mL of ultrapure water, and centrifuged at 2285 g force for 5 min. Once washed, the magnetic activated carbon with iminodiacetic acid as a chelating agent (MAC) was dried at 60 ºC for 24 h.

ii. Genipin as a cross-linking agent

The activated carbon cross-linked with genipin and functionalized with magnetic particles (GMAC) was prepared according to the methods described in 2.2.1 and 2.2.2 (i), respectively.

2.3 Supports characterization

The supports were characterized by Fourier Transform Infrared Spectroscopy (FTIR), point of zero charge (pH_{PZC}), Scanning Electron Microscopy (SEM), Porosity, and BET surface area.

The functional groups were evaluated through Fourier Transform Infrared Spectroscopy (FTIR). The sample was directly analyzed using the attenuated total reflectance (ATR) technique in the 4000-600 cm^{-1} infrared region in an Agilent Cary 630

FTIR spectrophotometer (Agilent Technologies Inc., Santa Clara, CA, USA). The point of zero charge (pH_{PZC}) was obtained as described by Kuśmierek et al. (Kuśmierek et al., 2016). Scanning Electron Microscopy (SEM) determined the surface morphology (QUANTA 250, FEI COMPANY, Waltham, MA, USA). The support samples were placed in stubs and metalized with a thin layer of gold. Subsequently, the samples were observed under the microscope. The specific surface area was measured by the Brunauer–Emmett–Teller (BET) equation (Brunauer et al., 1938). The pore size distribution was obtained through the desorption isotherm using the Barrett–Joyner–Halenda (BJH) method (Barrett et al., 1951) and the micropore volume was achieved from the t-plot analysis according to the adsorption isotherms (Lippens et al., 1964) on a Micrometrics ASAP 2420 equipment (Georgia, USA) using approximately 0.20 g of sample at -196.15 ºC.

2.4 Enzyme immobilization

Lipase from Porcine Pancreas (PPL) and *Candida Rugosa* (CRL) were immobilized on functionalized activated carbons. First of all, 0.1 g of support and 5 mL of lipase solution (6000 mg L^{-1} for PPL or 2000 mg L^{-1} for CRL) in sodium acetate buffer (0.1M, pH 5.0) were stirred on an orbital shaker at 10 g force and 30 ºC for 2 h (Brito et al., 2020a). The samples were centrifugated (2000 g force, 5 min), and the supernatant was collected to measure the protein concentration (Bradford, 1976). The immobilization capacity was calculated by Equation 1, and the immobilization efficiency (E%) was determined according to the ratio between the immobilized and initial lipase mass.

$$C_{imo} = \frac{v\,(C_i - C)}{m_a} \quad (1)$$

Where: C_{Imo} is the immobilization capacity (mg g^{-1}); v is the volume of lipase solution (mL); C_i is the initial lipase concentration (mg L^{-1}); C is the lipase concentration at equilibrium (mg L^{-1}); m_a is the adsorbent mass (g).

2.5 Hydrolytic activity

The hydrolysis of olive oil emulsion determined the lipolytic activity according to Soares et al. (Soares et al., 1999) with modifications. One unit of activity was defined as the amount of enzyme that releases 1 μmol of fatty acid per minute of reaction under the assay

conditions. The Enzyme Activity Yield (%) was calculated by the ratio between the immobilized and free enzyme activities.

2.6 Ethyl lactate synthesis

The esterification of ethyl lactate was carried out following the method described by Oliveira et al. (2022), with slight modifications. The substrate was prepared by mixing lactic acid (100 mM) and ethanol (300 mM) in hexane solvent. The reaction was carried out in a shaker bath at 40 ºC and 115 g force for 4 hours using 5 mL of the reaction mixture and 0.5 g of the derivative. The lactic acid content was determined after the reaction by titration (30 mM NaOH) until pH 11 was reached. The results were presented based on the yield of esterification (Y%).

2.7 Operational stability

The operational stability of the derivatives was evaluated using the reuse cycles method through esterification reactions between lactic acid and ethyl alcohol as mentioned in 2.6. After each cycle, the biocatalysts were washed using sodium acetate buffer (0.1M, pH 5.0) followed by hexane before beginning a new reaction.

2.8 Statistical analysis

The data was evaluated by analysis of variance (ANOVA) with the F test and Tukey test for comparison between means ($p < 0.05$) using SAS Studio and Sigmaplot software. All assays were performed in triplicate.

3. Results and discussion

3.1. Characterization of activated carbons

3.1.1. Fourier transform infrared spectroscopy (FTIR)

Fourier transform infrared spectroscopy (FTIR) was used to determine the functional groups present in sisal waste, activated carbon (AC), and AC modified with genipin (GAC), IDA + metal (MAC), and genipin + metal (GMAC) as shown in Figure 1.

Sisal waste presented functional groups related to the lignocellulosic content. These include a band at 3283 cm^{-1} referred as the hydroxyl group (OH) in the cellulose structure; the band at 2922 cm^{-1}, which represents the vibration of methyl group (C–H) from cellulose,

hemicellulose, and lignin; 1597 cm^{-1} is attributed to the C=O bond in carboxymethyl cellulose; 1241 cm^{-1} is associated to the guaiacyl groups; and the wavelength at 1027 cm^{-1} is related to the stretching of the glycosidic bonds (C–O and C–O–C) of lignin, cellulose and hemicellulose (Lu et al., 2022; Zhuang et al., 2020).

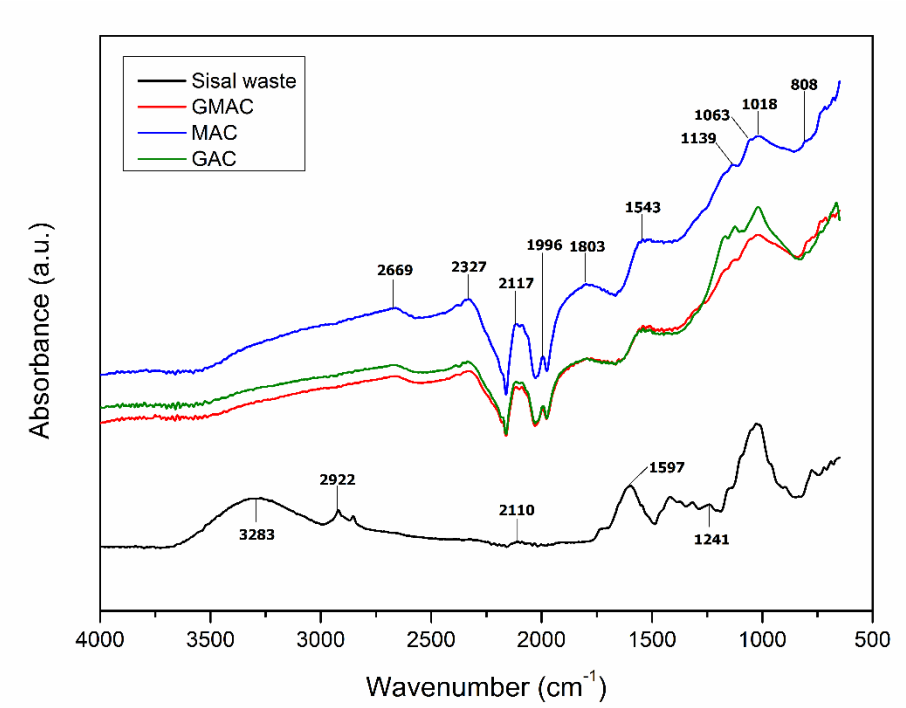

Figure 1. FTIR of sisal waste and activated carbon functionalized with genipin (GAC), IDA + metal (MAC), and genipin + metal (GMAC).

During activated carbon synthesis, chemical activation and pyrolysis caused some functional groups to thermally decompose (3283 cm^{-1}, 2922 cm^{-1}, and 1241 cm^{-1}) while new ones emerged. It was verified that the band at 2330 cm^{-1} corresponds to the methyl group; 2110 cm^{-1} is assigned to the stretching of C–O bond from ketone groups; the wavelength at 1996 cm^{-1} is associated to the carboxylic acid anhydrides groups; 1794 cm^{-1} is attributed to C=O vibrations of ketone, aldehyde, lactone or carboxylic groups; the band at 1162 cm^{-1} is related to the C–O vibrations in tertiary alcohols; and 1070 cm^{-1} represents the phosphate ester bonds from the activation with phosphoric acid (P^{+}–O^{-} and P–O–P) (Bhandari & Gogate, 2018; Mistar et al., 2020).

The spectra of modified supports verified an increase in peak intensity when compared to the unmodified support, especially the metallic activated carbon (MAC). Additionally, new vibrations were observed for all functionalized matrices such as the bands

at 2669 cm^{-1} and 1543 cm^{-1} referred to the methyl and amine groups, respectively. Regarding the adsorbents modified with magnetic particles, the incorporation of metal and IDA (MAC) showed greater peak intensity than metal and genipin (GMAC) due to the greater interaction between the functional groups and Fe_3O_4 through a chelating agent. This may be due to the strong binding ability of iminodiacetic acid functional groups for most metal ions (Anito et al., 2020; Aryee et al., 2020).

3.1.2. Point of zero charge (pH_{PCZ})

The surface charge of carbon materials was measured through the point of zero charge (pH_{PCZ}). Activated carbon (AC) from sisal waste had pH_{PCZ} = 5.83 due to the acid groups obtained from chemical activation with phosphoric acid and dissociating acidic surface oxygen complexes, such as carboxyl and phenolic groups (Brito et al., 2020a). According to the FTIR spectra (Figure 1), the functional groups related to the low pHpcz were C-O-C (1997 cm^{-1}), C=O (1563 cm^{-1}), C–O (1162 cm-^{1}), P+–O- and P–O–P (1070 cm^{-1}).

The pHpcz of the supports modified with genipin (GAC), IDA + metal (MAC), and genipin + metal (GMAC) was higher than pHpcz of unmodified biochar (6.54, 8.13, and 7.94, respectively). The increase in pHpcz of GAC (pHpcz = 6.54) might be attributed to the surface amination for genipin incorporation. On the other hand, the higher pHpcz values of MAC (pHpcz = 8.13) and GMAC (pHpcz = 7.94 no GMAC) may be due to the basic solution (NaOH) used to include the metallic particles and the resulting increase in surface alkalinity (Delgadillo-Velasco et al., 2021). Among the metal-functionalized adsorbents, IDA + metal (MAC) presented the highest point of zero charge and it can be related to the higher content of iron oxide inserted on the activated carbon surface due to the chelation by iminodiacetic acid (Anito et al., 2020). Furthermore, genipin acidic groups may have reduced the pHpcz of GMAC (Hong et al., 2021).

The point of zero charge (pH_{PCZ}) or charge density determines the pH at which a material has zero surface electrical charge density. If the pH of the solution is lower than the pH_{PCZ}, the surface will be positively charged and adsorb anions more efficiently. On the other hand, for solutions with a pH higher than the pH_{PCZ}, the carbonaceous surface will be negatively charged and present greater efficiency in adsorbing cations (Fernandez-Sanroman et al., 2020). The findings of this work indicate that the modified supports are positively charged at the pH of enzyme immobilization (pH = 5.0). As the isoelectric point of porcine pancreas lipase (PPL) is around 4.9 (Gonçalves et al., 2021) and *Candida rugosa* lipase is

4.2 (Geluk et al., 1992), its surface has a negative charge at the pH of immobilization. Therefore, the immobilization process occurs through specific forces such as electrostatic interactions.

3.1.3. Texture properties

Figure 2 shows the nitrogen (N_2) adsorption-desorption isotherms and pore size distribution of activated carbon functionalized with genipin (GAC), IDA + metal (MAC), and genipin + metal (GMAC).

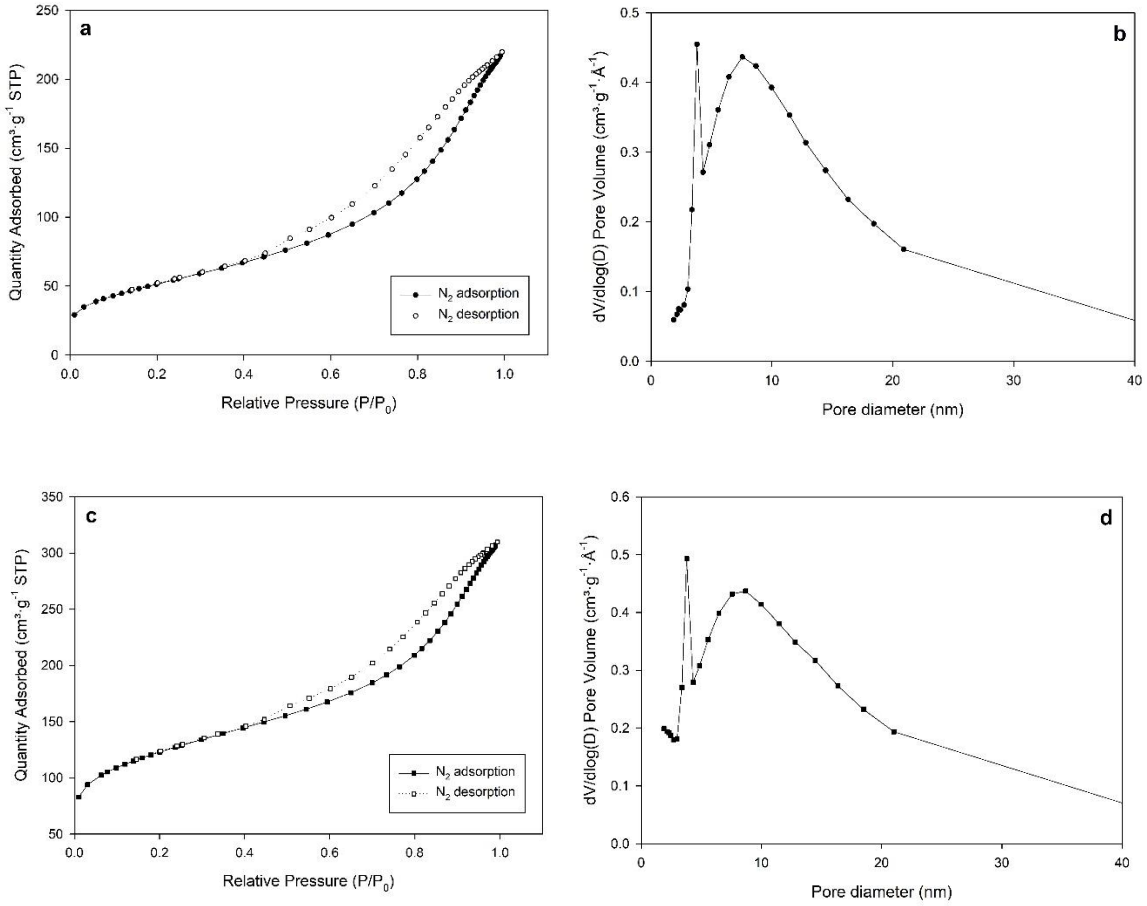

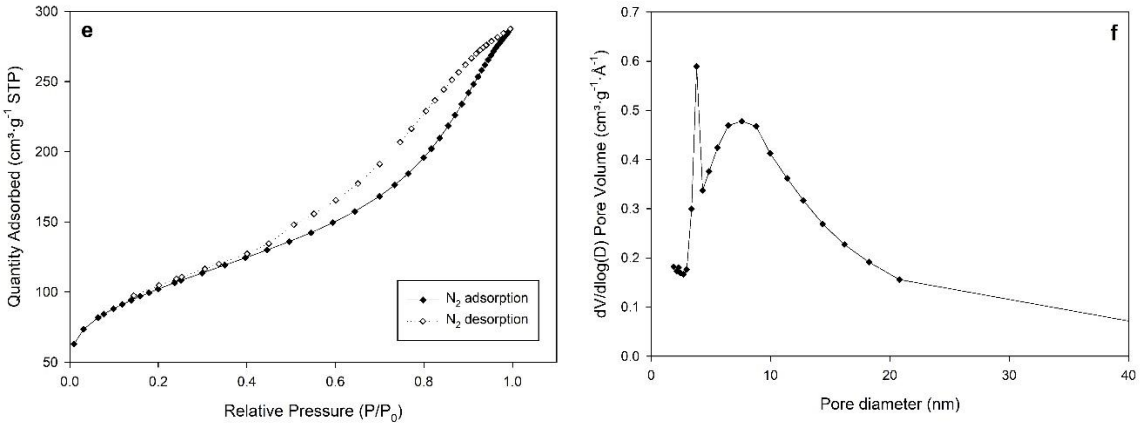

Figure 2. Nitrogen adsorption-desorption isotherms and pore distribution of activated carbon functionalized with genipin (GAC) (a and b), IDA + metal (MAC) (c and d), and genipin + metal (GMAC) (e and f).

All the functionalized supports demonstrated hysteresis loop characteristics (Type IV isotherm) according to the IUPAC classification (1985). Hysteresis refers to the capillary condensation in mesopore structures, and it may exhibit a wide variety of shapes such as Type I of hysteresis loop. This type of loop is often associated with porous materials that have agglomerates or compacts of regular array and narrow pore size distributions. The first nitrogen slope was observed in the low-pressure region ($P/P_0 < 0.5$), which is attributed to the monolayer coverage. On the other hand, at $P/P_0 > 0.5$ the multilayer adsorption began. It was also verified that MAC adsorbed the highest N_2 volume (309.89 cm^3 g^{-1} STP) when compared to the other matrices, except for the unmodified activated carbon (395.63 cm^3 g^{-1} STP), suggesting a greater pore volume and surface area available for adsorption. These observations can be confirmed by analyzing the pore size distribution (Figure 2 b, d, and f) and texture properties of the adsorbents (Table 1).

The modified activated carbons have a pore distribution that indicates peaks at 3.8 and 10 nm in diameter, classifying these adsorbents as micro-mesoporous. In addition to the standard AC (0.769 cm^3 g^{-1} $Å^{-1}$), GMAC presented the highest value for pore volume (0.589 cm^3 g^{-1} $Å^{-1}$). The adsorption phenomenon is influenced by the good relationship between the mesopores and micropores of materials since the mesopore allows for the diffusion of compounds to the micropores, where the adsorption is carried out (Gonçalves et al., 2021; Peng et al., 2022). Additionally, Table 1 shows the texture properties of supports functionalized with genipin (GAC), IDA + metal (MAC), and genipin + metal (GMAC).

Table 1. Texture properties of activated carbon functionalized with genipin (GAC), IDA + metal (MAC), and genipin + metal (GMAC).

Sample	Sg (m^2 g^{-1})	Dp (nm)[a]	V_{meso} (cm^3 g^{-1})	V_{micro} (cm^3 g^{-1})	V_{total} (cm^3 g^{-1})
GAC	187	6.82	0.3317	0.0026	0.3393
MAC	433	6.04	0.3850	0.0602	0.4694
GMAC	366	5.79	0.3847	0.0257	0.4369

Sg – BET surface area; Dp – average pore diameter; a – maximum pore size distribution; Vmeso – mesopore volume; Vmicro – micropore volume; Vtotal – total pore volume.

Regarding the activated carbon properties (Section 2.1), all modified supports verified a decrease in surface area and pore volume, which confirms the surface changes. This behavior may be due to the insertion of the chelating/crosslinking agent and magnetic particles into the pores during the functionalization process, leading to pore blockage (Bonyadi et al., 2022). These findings show that the BET area depends on pore characteristics, especially the micropores. As the pore volume decreases, the surface area will also decrease. However, the modifications led to an increase in the pore diameter and it can be related to the smaller pores being obstructed by the functionalizing agents resulting in a higher average pore diameter (Santos et al., 2022).

Genipin-functionalized AC demonstrated the lowest BET area and pore volume among the modified adsorbents. This demonstrates a 68.8% reduction in the surface area compared to unmodified activated carbon. Genipin is a crosslinking agent that creates stable cross-linked structures, which can lead to self-crosslinking and higher pore clogging (Yu et al., 2021). This can be verified by observing the genipin-iron oxide interaction in GMAC that resulted in lower pore obstruction and higher surface area (39% reduction compared to the original matrix).

Although the BET area was reduced by 27.8%, the highest surface area and pore volume between the functionalized activated carbons was observed for MAC. The higher values for both metal-functionalized adsorbents suggest that most iron particles were incorporated into the surface, and the chelating agent (MAC) was more effective in retaining iron oxide on the surface than the crosslinking agent (GMAC). The greater the texture parameters, the more efficient lipase immobilization tends to be since it provides a greater area available for bonding between the enzyme and support (Brito et al., 2020b).

The texture changes on functionalized activated carbons were also observed through Scanning Electron Microscope (SEM) (Figure 3). The surface morphology of modified supports has a spongy appearance and porous structure with different pore sizes and shapes, containing both micropores and mesopores. This statement agrees with the area and pore distribution analyses. Figure 3 also confirms that the functionalization was successful as the structure became smoother with smaller pores due to obstruction by the modifying agents.

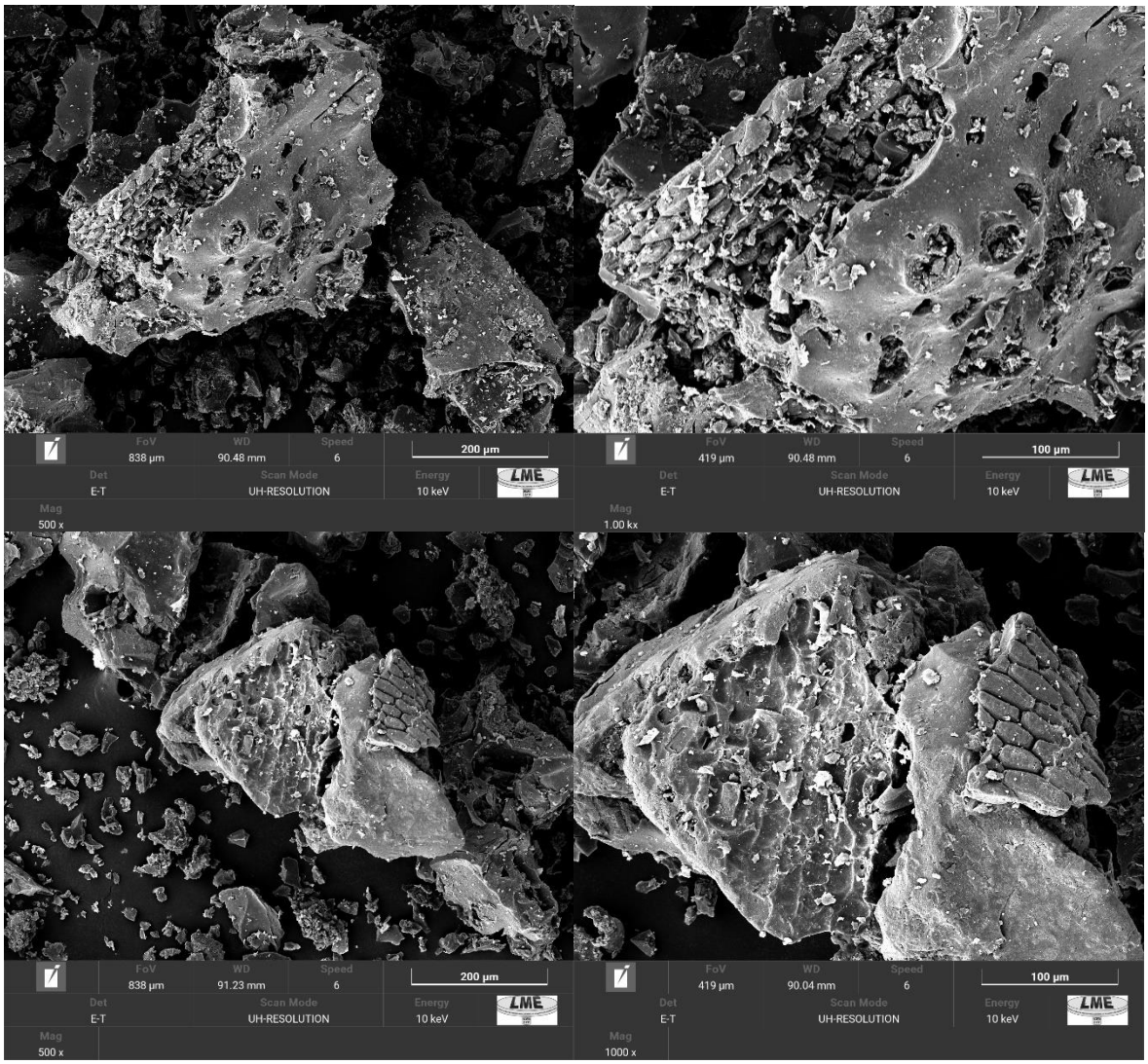

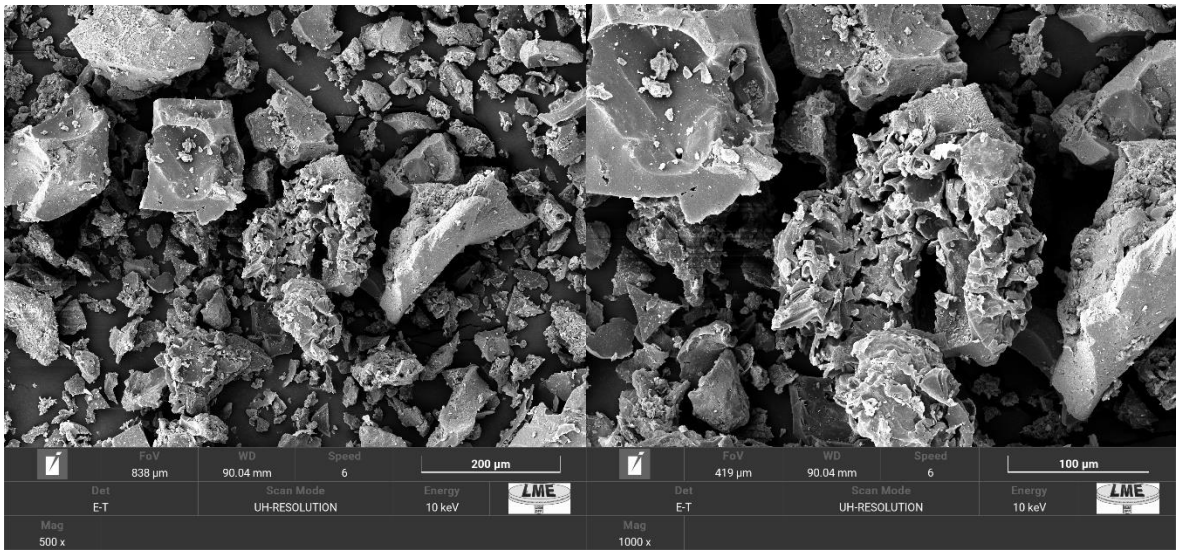

Figure 3. Scanning Electron Microscopy (SEM) of activated carbon functionalized with genipin (GAC) (a), IDA + metal (MAC) (b), and genipin + metal (GMAC) (c).

3.2. Lipase immobilization

3.2.1. Effect of lipase source on immobilization

The effect of lipase source for immobilization on different activated carbons was investigated based on their Immobilization Efficiency (%), Enzyme Activity (U), and Enzyme Activity Yield (%) as shown in Table 2.

Table 2. Effect of activated carbon functionalization on lipase immobilization.

Sample	Porcine Pancreas Lipase (PPL)			*Candida rugosa* Lipase (CRL)		
	Immobilization Efficiency (%)	Enzyme Activity (U)	Enzyme Yield (%)	Immobilization Efficiency (%)	Enzyme Activity (U)	Enzyme Yield (%)
GAC	89.32 ± 0.0117 ^{B,b}	31.3 ± 2.851 ^{A,b}	53.64 ± 4.887 ^{A,b}	98.17 ± 0.0018 ^{A,a}	32.2 ± 0.917 ^{A,b}	54.67 ± 1.556 ^{A,c}
MAC	99.43 ± 0.0015 ^{A,a}	46.9 ± 1.652 ^{A,a}	80.38 ± 2.832 ^{A,a}	98.76 ± 0.0021 ^{A,a}	47.3 ± 0.346 ^{A,a}	80.30 ± 0.588 ^{A,b}
GMAC	87.41 ± 0.0176 ^{B,b}	48.1 ± 3.822 ^{A,a}	82.43 ± 6.551 ^{B,a}	97.90 ± 0.0021 ^{A,a}	51.6 ± 0.520 $^{A.a}$	87.61 ± 0.882 ^{A,a}

*Means followed by the same lowercase letter in the support type and uppercase letter in the lipase source do not differ significantly from each other according to Tukey's test ($P < 0.05$).

Lipase from porcine pancreas had the highest Immobilization Efficiency for MAC (E% = 99.43) while the highest Enzyme Activity (U = 48.1) and Enzyme Yield (Y% = 82.43) were found for GMAC. However, there was no significant difference between GMAC and MAC, which showed an activity of 46.9 U and a yield of 80.38%. Similarly to PPL, lipase

from *Candida rugosa* found the highest E% = 98.76 for MAC, U = 51.6, and R% = 87.61 for GMAC.

The differences between immobilization and activity parameters for different supports may be due to the strength and orientation with which the lipase was attached to the support. Although the immobilization is suitable for all materials, the biocatalyst can bind with an orientation in which the active site is blocked or the substrate diffusion is restricted. Lipase has a specific catalytic property called interfacial activation that occurs in the oil-water interface, which allows the enzyme to have two configurations: the closed, inactive conformation and the open, active conformation. This mechanism has a mobile hydrophobic α-helix polypeptide chain that acts as a "lid" and blocks the active site from the reaction medium. However, the lid opens in the presence of a hydrophobic interface and aids the substrate-active site interaction. Thus, the biocatalyst activity is influenced by the immobilization on hydrophobic surfaces such as activated carbon (Remonatto et al., 2022; Zhang et al., 2022). Furthermore, the functionalizing agents tend to incorporate the enzyme through strong bonds, changing the lipase conformational structure and decreasing its flexibility (Al-sareji et al., 2023; Hasanzadeh et al., 2020).

Comparing both enzyme sources, *Candida rugosa* lipase showed significantly higher efficiency values (> 97% for all supports). Since the molecular weight of PPL is around 50 kDa (Mendes et al., 2012) and CRL is around 60 kDa (De María et al., 2006), the immobilization process of CRL was probably more influenced by interactions on the activated carbon surface than inside the pores. For the other parameters, CRL also had the highest values but they did not differ significantly from each other. This can be attributed to the higher purity level of CRL since PPL is supplied via a crude extract of porcine pancreas composed of other hydrolases as contaminants, such as esterases, amylases, and proteases (Majd et al., 2022). For instance, the experiments were carried out with different protein concentrations (PPL = 6000 mg L^{-1} and CRL = 2000 mg L^{-1}) to achieve similar lipolytic activity.

Moreover, each source has its specificity and selectivity to the substrate. Regarding regiospecificity, PPL is sn-1,3 specific and hydrolyzes ester bonds at the sn-1 and sn-3 positions, which releases free fatty acids and 2-monoacylglycerol. On the other hand, CRL is nonspecific and randomly hydrolyzes all triglyceride positions. This results in a mixture of products, including free fatty acids, monoacylglycerols, diacylglycerols, and glycerol (Monteiro et al., 2021). Lipases also show selectivity for different types of fatty acids, such

as *Candida rugosa* lipase, which preferentially recognizes substrates containing oleic acids (Remonatto et al., 2022). The olive oil employed in our work as substrate has a high oleic acid content (56-84 % of total fatty acids), making it suitable for the CRL catalytic mechanism (Lopez et al., 2020).

3.2.2. Effect of surface modification on lipase immobilization

As reported in Table 2, the effect of surface functionalization on activated carbon for different lipase sources was also evaluated based on their Immobilization Efficiency (%), Enzyme Activity (U), and Enzyme Activity Yield (%). The highest immobilization efficiency was observed for MAC, followed by GAC and GMAC. On the other hand, the highest enzymatic variables were found by GMAC, MAC, and GAC, respectively.

Among the modified matrices, genipin-functionalized support achieved the lowest immobilization parameters for both enzymes and the immobilization efficiency was the only variable that had a significant difference between them. Even with a low surface area, genipin-carbon presented a high immobilization efficiency and this suggests that immobilization occurred through the spacer arms inserted into the surface. The functionalization method involves the carbon surface amination followed by genipin incorporation through the amino group attack on the carbonyl from the ester group of genipin (C-11), developing a stable amide bond. Due to its bifunctional properties, genipin can also bind to proteins through ion exchange, covalent, or hydrophobic interactions. Under low pH conditions, the primary amines of the amino acid side chains (such as lysine, hydroxylysine, and arginine) make a nucleophilic attack on the C-3 of genipin. This attack promotes an opening in the genipin dihydropyranic ring and creates an intermediate aldehyde group in the molecule. Subsequently, the intermediate aldehyde group undergoes an aldol condensation with the secondary amines, resulting in a new heterocyclic compound (Flores et al., 2019; Tacias-Pascacio et al., 2019).

Regarding the low enzyme activity, the low enzyme yield indicates that the decreased biocatalyst mobility following immobilization may have increased restrictions on the substrate. Since this is a novel immobilization method for lipases, it is very likely that the potential of this chemical is not yet fully exploited. Therefore, further studies should be carried out by evaluating the optimal modification and immobilization conditions to increase

process efficiency. Furthermore, tests can be performed by incorporating pure genipin to enhance surface properties (Khan et al., 2020).

Metal-functionalized carbon (MAC) was significantly efficient in immobilization (E > 98%) with a significant difference for Porcine Pancreas Lipase. Since the molecular weight of PPL is lower than CRL, the high surface area and pore volume of this support may favor PPL adsorption within the pores. Furthermore, MAC activity and yield did not differ significantly from GMAC even though the enzymatic values were not the highest. The interaction mechanism between magnetic particles and enzymes is mainly influenced by electrostatic, van der Waals, and hydrophobic forces, followed by covalent bonding between epoxy groups of iron oxide and amino acids (amino, thiol, or hydroxyl groups) of lipase (Esmi et al., 2021; Moreira et al., 2020).

GMAC showed the lowest immobilization efficiency despite having an intermediate surface area. This may be due to a hysterical hindrance caused by adding large molecules into the activated carbon surface, such as the spacer arm and metal particles (Ouyang et al., 2020). As a result, lipase did not bind as easily. However, the binding enzyme concentration showed the highest activity and yield compared to the free enzyme. This suggests that the biocatalyst has bound tightly with preserved activity since the high point of zero charge of the metalized supports enhanced the electrostatic interactions between the adsorbent (positively charged) and enzyme (negatively charged) at the immobilization pH (Oliveira et al., 2022).

Although influenced by different factors, both iminodiacetic acid and genipin proved to be effective in retaining magnetic particles on the AC surface when used as a chelating and cross-linking agent, respectively. However, GMAC offers a green approach by eliminating a chemical compound from the process and reducing costs through the use of genipin extract in the modification method. Therefore, genipin has the potential to replace IDA as a binding agent.

For all modified activated carbons, high immobilization efficiency was observed even with different texture properties. These findings are attributed to the difference in charges on the supports and enzyme under the immobilization conditions. Therefore, immobilization was favored by electrostatic interactions, especially for adsorbents that have surface groups that intensify these interactions (MAC and GMAC) (Santos et al., 2022). GMAC was influenced by crosslinking (genipin) and electrostatic interactions (iron oxide).

3.3. Ethyl lactate synthesis

Once lipolytic immobilization proved to be efficient, the derivative was evaluated for the synthesis of aroma esters. The esterification of ethyl lactate using different lipase sources and modified activated carbons regarding Yield of Esterification (Y%) is presented in Table 3, which was greater than 90% for all variables investigated.

Among the modified supports, GMAC had the highest yield compared to free enzyme (FE) for porcine pancreas lipase and similar significance to GAC and MAC for *Candida rugosa* lipase. This is attributed to the strong binding of the biocatalyst in a favorable orientation, leading to higher esterification activity of this derivative.

Despite the low hydrolytic activity value, GAC achieved high ester conversion, indicating a high specificity of the enzymes for esterification reactions and protection of the active site even after the immobilization process (Gamayurova et al., 2021). As previously mentioned, genipin is a cost-effective and low-toxicity crosslinking agent. Therefore, it can be used as an alternative to conventional functionalization methods such as glutaraldehyde, as it proves to be effective for the synthesis of ethyl lactate.

Table 3. Conversion of ethyl lactate ester catalyzed by PPL and CRL (FE) immobilized on activated carbon functionalized with genipin (GAC), IDA + metal (MAC), and genipin + metal (GMAC).

Sample	Conversion (Y%)	
	Porcine Pancreas Lipase (PPL)	*Candida rugosa* Lipase (CRL)
FE	94.968 ± 0.959 ^{B,a}	96.571 ± 0.222 ^{A,a}
GAC	91.917 ± 0.691 ^{A,b}	91.477 ± 0.070 ^{A,b}
MAC	91.444 ± 0.064 ^{A,b}	92.880 ± 0.831 ^{A,b}
GMAC	94.213 ± 0.756 ^{A,a}	92.299 ± 0.039 ^{B,b}

*Means followed by the same lowercase letter in the column and uppercase letter in the row do not differ significantly from each other according to Tukey's test ($P < 0.05$).

When comparing both biocatalyst sources applied, CRL showed the highest yield for FE despite having no significant difference concerning PPL. On the other hand, PPL reached the highest significant conversion for immobilized enzyme using GMAC, similar to Y% of free enzyme. High activity for the free enzyme is expected since it has greater mobility and access to the substrate (Santos et al., 2020). The high yield for both lipases can be attributed

to their specificity for short- and medium-chain compounds, such as ethyl alcohol and lactic acid (Gamayurova et al., 2016).

This is a promising result for commercial purposes as it offers effective support options for lipolytic immobilization and its application in the synthesis of aroma esters. Ethyl lactate is widely applied due to its low toxicity, and its use as a flavoring agent is highlighted by the buttery notes to dairy products and wines (Cong et al., 2019). Previous work reported ester conversion of 87.32% using *Aspergillus fumigatus* lipase (Mehta et al., 2020), 83.3% using immobilized *Candida antarctica* lipase B (CALB) (Sun et al., 2010), and 88% using Novozym 435 (Koutinas et al., 2018). These findings show the potential of these derivatives for use in the food, cosmetic, and pharmaceutical industries.

3.4. Operational stability

The main feature of the industrial application of immobilized enzymes is their operational stability, as reusing the biocatalyst reduces process costs (Maghraby et al., 2023). To illustrate this point, Figure 4 presents the cycles of use for lipase from porcine pancreas (a) and *Candida rugosa* (b) using the modified activated carbons based on Ethyl lactate conversion (%).

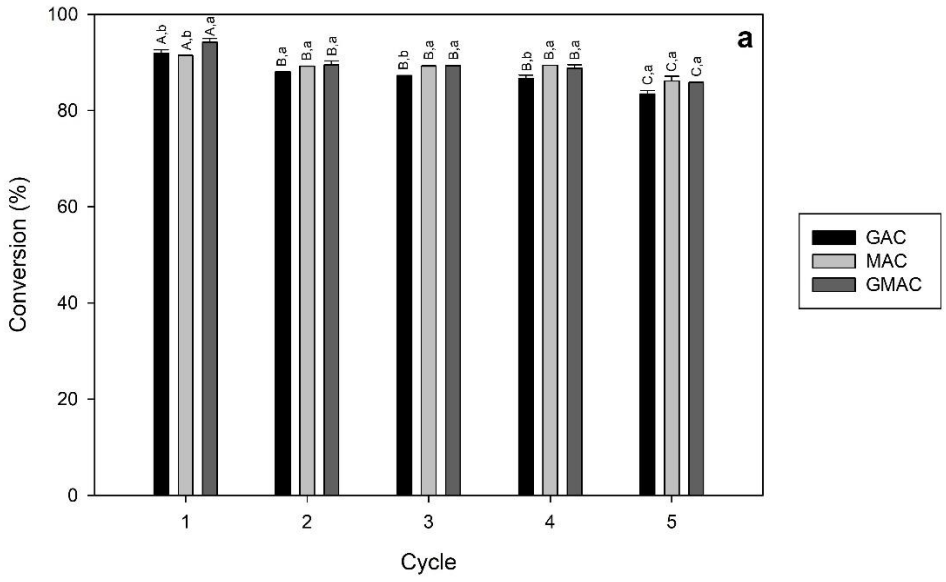

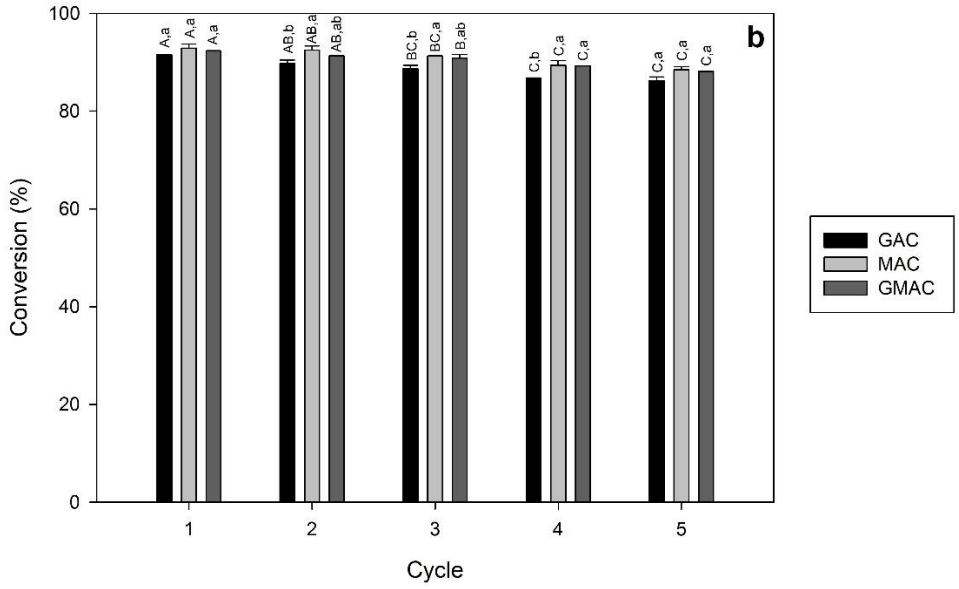

*Means followed by the same lowercase letter in the sample and uppercase letter in the cycle of reuse for the same sample do not differ significantly from each other according to Tukey's test ($P < 0.05$).

Figure 4. Conversion of ethyl lactate ester catalyzed by PPL (a) and CRL (b) immobilized on activated carbon functionalized with genipin (GAC), IDA + metal (MAC), and genipin + metal (GMAC) as a function of the number of use cycles (T = 40 ºC, t = 4 h).

All derivatives exhibited stability during reuse for both enzymes, and the metalized supports had the highest yield in the last cycle (MAC = 86.16 ± 0.947% and GMAC = 85.79 ± 0.117% for PPL; MAC = 88.46 ± 0.657% and GMAC = 88.14 ± 0.073% for CRL). This may be due to the strong interactions between the lipase structure and the functionalized supports such as covalent bonds and electrostatic interactions, mitigating biocatalyst losses via desorption (Al-sareji et al., 2023). Moreover, these results suggest that using genipin and iminodiacetic acid as crosslinking and chelating agents were efficient methods in preventing the leaching of metal ions from the carbon surface (Long et al., 2021).

Both lipase sources achieved great results in the reuse cycles, although PPL was less stable in the last cycle. The high ester conversion after 5 cycles (> 83%) suggests that the immobilization process efficiently protected the biocatalyst from denaturation during its successive use through the synthesis of a rigid derivative (Liang et al., 2020). Koutinas et al. (Koutinas et al., 2018) found 85% of ethyl lactate after 5 cycles using the commercial lipase Novozym 435. Furthermore, Brito et al. (Brito et al., 2020) state that washing the derivative with hexane after each cycle may have contributed to maintaining its activity since this non-

polar solvent removes any product around the enzyme that may reduce its activity and limit the substrate and product diffusion.

3.5. Effect of terc-butanol as solvent

The polarity of the esterification solvent was investigated by using terc-butanol as a solvent based on the ethyl lactate yield. The study found Y(%) = 73.25 ± 0.622 for free PPL and Y(%) = 70.60 ± 2.971 for PPL-GMAC. On the other hand, it was reported Y(%) = 77.49 ± 0.916 for free CRL and Y(%) = 75.17 ± 2.446 for CRL-GMAC. These findings are lower than those obtained using hexane as a solvent, but this is expected as lipase-mediated esterification occurs mainly in a hydrophobic medium (isooctane > petroleum ether > n-hexane > terc-butanol > terc-amyl alcohol). According to Subroto et al. (Subroto et al., 2020), it is caused by a strong deformation due to the essential interactions between water and protein. Hydrophilic solvents influence the water content surrounding the lipase microenvironment on the active site, which affects its conformation structure and activity. Further studies are needed, but the method may have a similar potential (Y > 70%) to hexane as a less toxic solvent in the ethyl lactate synthesis using immobilized lipase on activated carbon.

4. Conclusion

The surface modification of activated carbon from sisal waste through gepinin, iminodiacetic acid and metallic particles, and genipin and metallic particles was successfully applied to immobilize lipase from porcine pancreas and *Candida rugosa* for ethyl lactate synthesis. The texture properties of derivatives were confirmed by pore size distribution, BET surface area, and average pore diameter, indicating a valuable structure for enzyme immobilization. All the supports showed high immobilization efficiency, with the metalized-activated carbons presenting the highest hydrolysis activity. The derivatives have reported promising results for the synthesis of ethyl lactate. The high ester conversion after five cycles suggested that the immobilization process efficiently protected the lipase from desorption and enzyme denaturation. Therefore, the synthesized derivatives have the potential to catalyze the production of aroma esters through biotechnological tools for use in industry.

Acknowledgments

The authors gratefully acknowledge the financial support provided for this work by the National Council for Scientific and Technological Development (CNPq) and Coordination for the Improvement of Higher Education Personnel (CAPES). We are also thankful for the support in analyses by CETENE and LME (UFLA).

References

1. Adamiak, K., & Sionkowska, A. (2020). Current methods of collagen cross-linking: Review. In *International Journal of Biological Macromolecules* (Vol. 161, pp. 550–560). Elsevier B.V. https://doi.org/10.1016/j.ijbiomac.2020.06.075

2. Alchouron, J., Navarathna, C., Rodrigo, P. M., Snyder, A., Chludil, H. D., Vega, A. S., Bosi, G., Perez, F., Mohan, D., Pittman, C. U., & Mlsna, T. E. (2021). Household arsenic contaminated water treatment employing iron oxide/bamboo biochar composite: An approach to technology transfer. *Journal of Colloid and Interface Science*, *587*, 767–779. https://doi.org/10.1016/j.jcis.2020.11.036

3. Al-sareji, O. J., Meiczinger, M., Somogyi, V., Al-Juboori, R. A., Grmasha, R. A., Stenger-Kovács, C., Jakab, M., & Hashim, K. S. (2023). Removal of emerging pollutants from water using enzyme-immobilized activated carbon from coconut shell. *Journal of Environmental Chemical Engineering*, *11*(3). https://doi.org/10.1016/j.jece.2023.109803

4. Anito, D. A., Wang, T. X., Liu, Z. W., Ding, X., & Han, B. H. (2020). Iminodiacetic acid-functionalized porous polymer for removal of toxic metal ions from water. *Journal of Hazardous Materials*, *400*. https://doi.org/10.1016/j.jhazmat.2020.123188

5. Aryee, A. A., Mpatani, F. M., Zhang, X., Kani, A. N., Dovi, E., Han, R., Li, Z., & Qu, L. (2020). Iron (III) and iminodiacetic acid functionalized magnetic peanut husk for the removal of phosphate from solution: Characterization, kinetic and equilibrium studies. *Journal of Cleaner Production*, *268*. https://doi.org/10.1016/j.jclepro.2020.122191

6. Barrett, E.P., Joyner, L.G., Halenda, P.P. (1951). The Determination of Pore Volume and Area Distributions in Porous Substances. I. Computations from Nitrogen Isotherms. *Journal of the American Chemical Society*, 73, 373–380. https://doi.org/10.1021/ja01145a126.

7. Bayout, I., Bouzemi, N., Guo, N., Mao, X., Serra, S., Riva, S., & Secundo, F. (2020). Natural flavor ester synthesis catalyzed by lipases. *Flavour and Fragrance Journal*, *35*(2), 209–218. https://doi.org/10.1002/ffj.3554

8. Bayramoglu, G., Celikbicak, O., Kilic, M., & Yakup Arica, M. (2022). Immobilization of Candida rugosa lipase on magnetic chitosan beads and application in flavor esters synthesis. *Food Chemistry*, *366*. https://doi.org/10.1016/j.foodchem.2021.130699

9. Bhandari, P. S., & Gogate, P. R. (2018). Kinetic and thermodynamic study of adsorptive removal of sodium dodecyl benzene sulfonate using adsorbent based on thermo-chemical activation of coconut shell. *Journal of Molecular Liquids*, *252*, 495–505. https://doi.org/10.1016/j.molliq.2017.12.018

10. Bonyadi, E., Ashtiani, F. Z., Ghorabi, S., & Niknejad, A. S. (2022). Bio-inspired hybrid coating of microporous polyethersulfone membranes by one-step deposition of polydopamine embedded with amino-functionalized SiO2 for high-efficiency oily wastewater treatment. *Journal of Environmental Chemical Engineering*, *10*(1). https://doi.org/10.1016/j.jece.2021.107121

11. Bradford, M. M. (1976). A Rapid and Sensitive Method for the Quantitation of Microgram Quantities of Protein Utilizing the Principle of Protein-Dye Binding. In *ANALYTICAL BIOCHEMISTRY* (Vol. 72).

12. Brito, M. J., Bauer, L. C., Flores Santos, M. P., Santos, L. S., Ferreira Bonomo, R. C., da Costa Ilhéu Fontan, R., & Veloso, C. M. (2020). Lipase immobilization on activated and functionalized carbon for the aroma ester synthesis. *Microporous and Mesoporous Materials*, *309*. https://doi.org/10.1016/j.micromeso.2020.110576

13. Brito, M. J., Flores Santos, M. P., Souza Júnior, E. C. De, Santos, L. S., Ferreira Bonomo, R. C., Da Costa Ilhéu Fontan, R., & Veloso, C. M. (2020a). Development of activated carbon from pupunha palm heart sheaths: Effect of synthesis conditions and its application in lipase immobilization. *Journal of Environmental Chemical Engineering*, *8*(5). https://doi.org/10.1016/j.jece.2020.104391

14. Brito, M. J., Flores Santos, M. P., Souza Júnior, E. C. De, Santos, L. S., Ferreira Bonomo, R. C., Da Costa Ilhéu Fontan, R., & Veloso, C. M. (2020b). Development of activated carbon from pupunha palm heart sheaths: Effect of synthesis conditions and its application in lipase immobilization. *Journal of Environmental Chemical Engineering*, *8*(5). https://doi.org/10.1016/j.jece.2020.104391

15. Brunauer, S., Emmett, P. H., & Teller, E. (1938). *Adsorption of Gases in Multimolecular Layers*. https://pubs.acs.org/sharingguidelines

16. Cong, S., Tian, K., Zhang, X., Lu, F., Singh, S., Prior, B., & Wang, Z. X. (2019). Synthesis of flavor esters by a novel lipase from Aspergillus niger in a soybean-solvent system. *3 Biotech*, *9*(6). https://doi.org/10.1007/s13205-019-1778-5

17. Darwesh, O. M., Ali, S. S., Matter, I. A., Elsamahy, T., & Mahmoud, Y. A. (2020). Enzymes immobilization onto magnetic nanoparticles to improve industrial and environmental applications. In *Methods in Enzymology* (Vol. 630, pp. 481–502). Academic Press Inc. https://doi.org/10.1016/bs.mie.2019.11.006

18. Delgadillo-Velasco, L., Hernández-Montoya, V., Ramírez-Montoya, L. A., Montes-Morán, M. A., del Rosario Moreno-Virgen, M., & Rangel-Vázquez, N. A. (2021). Removal of phosphate and aluminum from water in single and binary systems using iron-modified carbons. *Journal of Molecular Liquids*, *323*. https://doi.org/10.1016/j.molliq.2020.114586

19. De María, P. D., Sánchez-Montero, J. M., Sinisterra, J. V., & Alcántara, A. R. (2006). Understanding Candida rugosa lipases: An overview. In *Biotechnology*

Advances (Vol. 24, Issue 2, pp. 180–196). https://doi.org/10.1016/j.biotechadv.2005.09.003

20. Esmi, F., Nematian, T., Salehi, Z., Khodadadi, A. A., & Dalai, A. K. (2021). Amine and aldehyde functionalized mesoporous silica on magnetic nanoparticles for enhanced lipase immobilization, biodiesel production, and facile separation. *Fuel*, *291*. https://doi.org/10.1016/j.fuel.2021.120126

21. Fernandez-Sanroman, A., Acevedo-García, V., Pazos, M., Sanromán, M. A., & Rosales, E. (2020). Removal of sulfamethoxazole and methylparaben using hydrocolloid and fiber industry wastes: Comparison with biochar and laccase-biocomposite. *Journal of Cleaner Production*, *271*. https://doi.org/10.1016/j.jclepro.2020.122436

22. Flores, E. E. E., Cardoso, F. D., Siqueira, L. B., Ricardi, N. C., Costa, T. H., Rodrigues, R. C., Klein, M. P., & Hertz, P. F. (2019). Influence of reaction parameters in the polymerization between genipin and chitosan for enzyme immobilization. *Process Biochemistry*, *84*, 73–80. https://doi.org/10.1016/j.procbio.2019.06.001

23. Gamayurova, V. S., Zinov'eva, M. E., Shnaider, K. L., & Davletshina, G. A. (2021). Lipases in Esterification Reactions: A Review. *Catalysis in Industry*, *13*(1), 58–72. https://doi.org/10.1134/S2070050421010025

24. Geluk, M. A., Norde, W., Kaisbeek, H. K. A. I. Van, & Van 't Riet, K. (1992). *Adsorption of lipase from Candida rugosa on cellulose and its influence on lipolytic activity*.

25. Gonçalves, G. R. F., Gandolfi, O. R. R., Brito, M. J. P., Bonomo, R. C. F., Fontan, R. C. I., & Veloso, C. M. (2021). Immobilization of porcine pancreatic lipase on activated carbon by adsorption and covalent bonding and its application in the synthesis of butyl butyrate. *Process Biochemistry*, *111*, 114–123. https://doi.org/10.1016/j.procbio.2021.10.027

26. Guajardo, N., Ahumada, K., & Domínguez de María, P. (2020). Immobilized lipase-CLEA aggregates encapsulated in lentikats® as robust biocatalysts for continuous processes in deep eutectic solvents. *Journal of Biotechnology*, *310*, 97–102. https://doi.org/10.1016/j.jbiotec.2020.02.003

27. Hasanzadeh, M., Simchi, A., & Shahriyari Far, H. (2020). Nanoporous composites of activated carbon-metal organic frameworks for organic dye adsorption: Synthesis, adsorption mechanism and kinetics studies. *Journal of Industrial and Engineering Chemistry*, *81*, 405–414. https://doi.org/10.1016/j.jiec.2019.09.031

28. Hong, J., Jung, D., Park, S., Oh, Y., Oh, K. K., & Lee, S. H. (2021). Immobilization of laccase via cross-linked enzyme aggregates prepared using genipin as a natural cross-linker. *International Journal of Biological Macromolecules*, *169*, 541–550. https://doi.org/10.1016/j.ijbiomac.2020.12.136

29. Khan, N., Maseet, M., & Basir, S. F. (2020). Synthesis and characterization of biodiesel from waste cooking oil by lipase immobilized on genipin cross-linked

chitosan beads: A green approach. *International Journal of Green Energy*, *17*(1), 84–93. https://doi.org/10.1080/15435075.2019.1700122

30. Koutinas, M., Yiangou, C., Osório, N. M., Ioannou, K., Canet, A., Valero, F., & Ferreira-Dias, S. (2018). Application of commercial and non-commercial immobilized lipases for biocatalytic production of ethyl lactate in organic solvents. *Bioresource Technology*, *247*, 496–503. https://doi.org/10.1016/j.biortech.2017.09.130

31. Kovalenko, G., Perminova, L., Pykhtina, M., & Beklemishev, A. (2021). Lipase-active heterogeneous biocatalysts for enzymatic synthesis of short-chain aroma esters. *Biocatalysis and Agricultural Biotechnology*, *36*. https://doi.org/10.1016/j.bcab.2021.102124

32. Kuśmierek, K., Szala, M., & Świątkowski, A. (2016). Adsorption of 2,4-dichlorophenol and 2,4-dichlorophenoxyacetic acid from aqueous solutions on carbonaceous materials obtained by combustion synthesis. *Journal of the Taiwan Institute of Chemical Engineers*, *63*, 371–378. https://doi.org/10.1016/j.jtice.2016.03.036

33. Liang, S., Wu, X. L., Xiong, J., Zong, M. H., & Lou, W. Y. (2020). Metal-organic frameworks as novel matrices for efficient enzyme immobilization: An update review. In *Coordination Chemistry Reviews* (Vol. 406). Elsevier B.V. https://doi.org/10.1016/j.ccr.2019.213149

34. Lippens, B. C., Linsen, B. G., & De Boer, J. H. (1964). Studies on Pore Systems in Catalysts I. The Adsorption of Nitrogen; Apparatus and Calculation. In *JOURNAL OF CATALYSIS* (Vol. 3).

35. Long, Y., Li, S., Su, Y., Wang, S., Zhao, S., Wang, S., Zhang, Z., Huang, W., Liu, Y., & Zhang, Z. (2021). Sulfur-containing iron nanocomposites confined in S/N co-doped carbon for catalytic peroxymonosulfate oxidation of organic pollutants: Low iron leaching, degradation mechanism and intermediates. *Chemical Engineering Journal*, *404*. https://doi.org/10.1016/j.cej.2020.126499

36. Lopez, S., Bermudez, B., Montserrat-de la Paz, S., Pacheco, Y. M., Ortega-Gomez, A., Varela, L. M., Lemus-Conejo, A., Millan-Linares, M. C., Rosillo, M. A., Abia, R., & Muriana, F. J. G. (2020). Oleic acid-the main component of olive oil on postprandial metabolic processes. In *Olives and Olive Oil in Health and Disease Prevention* (pp. 639–649). Elsevier. https://doi.org/10.1016/B978-0-12-819528-4.00034-1

37. Lu, S., Ma, T., Hu, X., Zhao, J., Liao, X., Song, Y., & Hu, X. (2022). Facile extraction and characterization of cellulose nanocrystals from agricultural waste sugarcane straw. *Journal of the Science of Food and Agriculture*, *102*(1), 312–321. https://doi.org/10.1002/jsfa.11360

38. Maghraby, Y. R., El-Shabasy, R. M., Ibrahim, A. H., & Azzazy, H. M. E. S. (2023). Enzyme Immobilization Technologies and Industrial Applications. In *ACS Omega* (Vol. 8, Issue 6, pp. 5184–5196). American Chemical Society. https://doi.org/10.1021/acsomega.2c07560

39. Mehta, A., Grover, C., Bhardwaj, K. K., & Gupta, R. (2020). Application of lipase purified from aspergillus fumigatus in the syntheses of ethyl acetate and ethyl lactate. *Journal of Oleo Science*, *69*(1), 23–29. https://doi.org/10.5650/jos.ess19202

40. Mendes, A. A., Oliveira, P. C., & De Castro, H. F. (2012). Properties and biotechnological applications of porcine pancreatic lipase. In *Journal of Molecular Catalysis B: Enzymatic* (Vol. 78, pp. 119–134). https://doi.org/10.1016/j.molcatb.2012.03.004

41. Mistar, E. M., Alfatah, T., & Supardan, M. D. (2020). Synthesis and characterization of activated carbon from Bambusa vulgaris striata using two-step KOH activation. *Journal of Materials Research and Technology*, *9*(3), 6278–6286. https://doi.org/10.1016/j.jmrt.2020.03.041

42. Mohan, D., Sarswat, A., Singh, V. K., Alexandre-Franco, M., & Pittman, C. U. (2011). Development of magnetic activated carbon from almond shells for trinitrophenol removal from water. *Chemical Engineering Journal*, *172*(2–3), 1111–1125. https://doi.org/10.1016/j.cej.2011.06.054

43. Monteiro, R. R. C., Arana-Peña, S., da Rocha, T. N., Miranda, L. P., Berenguer-Murcia, Á., Tardioli, P. W., dos Santos, J. C. S., & Fernandez-Lafuente, R. (2021). Liquid lipase preparations designed for industrial production of biodiesel. Is it really an optimal solution? In *Renewable Energy* (Vol. 164, pp. 1566–1587). Elsevier Ltd. https://doi.org/10.1016/j.renene.2020.10.071

44. Moreira, K. da S., de Oliveira, A. L. B., Júnior, L. S. de M., Monteiro, R. R. C., da Rocha, T. N., Menezes, F. L., Fechine, L. M. U. D., Denardin, J. C., Michea, S., Freire, R. M., Fechine, P. B. A., Souza, M. C. M., & dos Santos, J. C. S. (2020). Lipase From Rhizomucor miehei Immobilized on Magnetic Nanoparticles: Performance in Fatty Acid Ethyl Ester (FAEE) Optimized Production by the Taguchi Method. *Frontiers in Bioengineering and Biotechnology*, *8*. https://doi.org/10.3389/fbioe.2020.00693

45. Mozaffari Majd, M., Kordzadeh-Kermani, V., Ghalandari, V., Askari, A., & Sillanpää, M. (2022). Adsorption isotherm models: A comprehensive and systematic review (2010−2020). In *Science of the Total Environment* (Vol. 812). Elsevier B.V. https://doi.org/10.1016/j.scitotenv.2021.151334

46. Nadar, S. S., & Rathod, V. K. (2020). Immobilization of proline activated lipase within metal organic framework (MOF). *International Journal of Biological Macromolecules*, *152*, 1108–1112. https://doi.org/10.1016/j.ijbiomac.2019.10.199

47. Nascimento, P. A., Alves, A. N., dos Santos, K. A., Veloso, C. M., Santos, L. S., da Costa Ilhéu Fontan, R., dos Santos Sampaio, V., & Bonomo, R. C. F. (2021). Optimization of lipase extraction from pequi seed (Caryocar brasiliense Camb.). *Journal of Food Processing and Preservation*, *45*(7). https://doi.org/10.1111/jfpp.15616

48. Oliveira, T. P., Santos, M. P. F., Brito, M. J. P., & Veloso, C. M. (2022). Incorporation of metallic particles in activated carbon used in lipase immobilization for production of isoamyl acetate. *Journal of Chemical Technology and Biotechnology*, *97*(7), 1736–1746. https://doi.org/10.1002/jctb.7043

49. Ouyang, J., Pu, S., Wang, J., Deng, Y., Yang, C., Naseer, S., & Li, D. (2020). Enzymatic hydrolysate of geniposide directly acts as cross-linking agent for enzyme immobilization. *Process Biochemistry*, *99*, 187–195. https://doi.org/10.1016/j.procbio.2020.09.006

50. Peng, S., Huang, B., Lin, Y., Pei, G., & Zhang, L. (2022). Effect of Surface Functionalization and Pore Structure Type on the Release Performance of Mesoporous Silica Nanoparticles. *Microporous and Mesoporous Materials*, *336*. https://doi.org/10.1016/j.micromeso.2022.111862

51. Pereira, A. da S., de Souza, A. H., Fraga, J. L., Villeneuve, P., Torres, A. G., & Amaral, P. F. F. (2022). Lipases as Effective Green Biocatalysts for Phytosterol Esters' Production: A Review. In *Catalysts* (Vol. 12, Issue 1). MDPI. https://doi.org/10.3390/catal12010088

52. Rather, A. H., Khan, R. S., Wani, T. U., Beigh, M. A., & Sheikh, F. A. (2022). Overview on immobilization of enzymes on synthetic polymeric nanofibers fabricated by electrospinning. In *Biotechnology and Bioengineering* (Vol. 119, Issue 1, pp. 9–33). John Wiley and Sons Inc. https://doi.org/10.1002/bit.27963

53. Remonatto, D., Miotti, R. H., Monti, R., Bassan, J. C., & de Paula, A. V. (2022). Applications of immobilized lipases in enzymatic reactors: A review. In *Process Biochemistry* (Vol. 114, pp. 1–20). Elsevier Ltd. https://doi.org/10.1016/j.procbio.2022.01.004

54. Rusu, A. G., Chiriac, A. P., Nita, L. E., Balan, V., Serban, A. M., & Croitoriu, A. (2022). Synthesis and Comparative Studies of Glucose Oxidase Immobilized on Fe3O4 Magnetic Nanoparticles Using Different Coupling Agents. *Nanomaterials*, *12*(14). https://doi.org/10.3390/nano12142445

55. Sampaio, C. S., Angelotti, J. A. F., Fernandez-Lafuente, R., & Hirata, D. B. (2022). Lipase immobilization via cross-linked enzyme aggregates: Problems and prospects – A review. In *International Journal of Biological Macromolecules* (Vol. 215, pp. 434–449). Elsevier B.V. https://doi.org/10.1016/j.ijbiomac.2022.06.139

56. Santos, M. M. O., de Menezes, L. H. S., do Espirito Santo, E. L., de Carvalho, M. S., Gonçalves, M. S., de Carvalho Tavares, I. M., Mendes, A. A., Ruiz, H. A., Salay, L. C., Franco, M., & de Oliveira, J. R. (2023). Synthesis of hexyl butyrate (apple and citrus aroma) by Candida rugosa lipase immobilized on Diaion HP-20 using the Box-Behnken design. *Food Science and Biotechnology*, *32*(5), 689–696. https://doi.org/10.1007/s10068-022-01200-1

57. Santos, M. P. F., Porfírio, M. C. P., Junior, E. C. S., Bonomo, R. C. F., & Veloso, C. M. (2022). Pepsin immobilization: Influence of carbon support functionalization. *International Journal of Biological Macromolecules*, *203*, 67–79. https://doi.org/10.1016/j.ijbiomac.2022.01.135

58. Santos, M. M. O., Gama, R. S., Tavares, I. M. C., Santos, P. H., Gonçalves, M. S., Carvalho, M. S., Vilas Boas, E. V. B., Oliveira, J. R., Mendes, A. A., Franco, M. (2020). *Application of lipase immobilized on a hydrophobic support for the synthesis of aromatic esters running title: lipase immobilized in aroma esters synthesis*. https://doi.org/10.1002/bab.1959_AM_COPY

59. Sing, K. S. W., Everett, D. H., Haul, R. A. W., Moscou, L., Pierotti, R. A., Rouquérol, J., Siemieniewska, T. (1985). Reporting physisorption data for gas/solid systems-with special reference to the determination of surface area and porosity. *International Union of Pure and Applied Chemistry*, *57*(4), 603–619.

60. Soares, C. M. F., De Castro, H. F., De Moraes, F. F., & Zanin, G. M. (1999). *Characterization and Utilization of Candida rugosa Lipase Immobilized on Controlled Pore Silica*.

61. Subroto, E., Indiarto, R., Pangawikan, A. D., Huda, S., & Yarlina, V. P. (2020). Characteristics, immobilization, and application of Candida rugosa lipase: A review. In *Food Research* (Vol. 4, Issue 5, pp. 1391–1401). Rynnye Lyan Resources. https://doi.org/10.26656/fr.2017.4(5).060

62. Sun, G., Huang, Z., Zhang, Z., Liu, Y., Li, J., Du, G., Lv, X., & Liu, L. (2022). A Two-Step Cross-Linked Hydrogel Immobilization Strategy for Diacetylchitobiose Deacetylase. *Catalysts*, *12*(9). https://doi.org/10.3390/catal12090932

63. Sun, J., Jiang, Y., Zhou, L., & Gao, J. (2010). Immobilization of Candida antarctica lipase B by adsorption in organic medium. *New Biotechnology*, *27*(1), 53–58. https://doi.org/10.1016/j.nbt.2009.12.001

64. Tacias-Pascacio, V. G., García-Parra, E., Vela-Gutiérrez, G., Virgen-Ortiz, J. J., Berenguer-Murcia, Á., Alcántara, A. R., & Fernandez-Lafuente, R. (2019). Genipin as an emergent tool in the design of biocatalysts: Mechanism of reaction and applications. In *Catalysts* (Vol. 9, Issue 12). MDPI. https://doi.org/10.3390/catal9121035

65. Vilas Bôas, R. N., & de Castro, H. F. (2022). A review of synthesis of esters with aromatic, emulsifying, and lubricant properties by biotransformation using lipases. In *Biotechnology and Bioengineering* (Vol. 119, Issue 3, pp. 725–742). John Wiley and Sons Inc. https://doi.org/10.1002/bit.28024

66. Gamayurova, V. S., Shnaider, K. L., Zaripova, S. K., Mataz, J. J. (2016). Enzymatic Synthesis of Fatty Esters by Lipase from Porcine Pancreas. *Journal of Thermodynamics & Catalysis*, *07*(01). https://doi.org/10.4172/2157-7544.1000161

67. Yu, Y., Xu, S., Li, S., & Pan, H. (2021). Genipin-cross-linked hydrogels based on biomaterials for drug delivery: A review. In *Biomaterials Science* (Vol. 9, Issue 5, pp. 1583–1597). Royal Society of Chemistry. https://doi.org/10.1039/d0bm01403f

68. Zhang, J., Wang, Z., Zhuang, W., Rabiee, H., Zhu, C., Deng, J., Ge, L., & Ying, H. (2022). Amphiphilic Nanointerface: Inducing the Interfacial Activation for Lipase. *ACS Applied Materials and Interfaces*, *14*(34), 39622–39636. https://doi.org/10.1021/acsami.2c11500

69. Zhuang, J., Li, M., Pu, Y., Ragauskas, A. J., & Yoo, C. G. (2020). Observation of potential contaminants in processed biomass using fourier transform infrared spectroscopy. *Applied Sciences (Switzerland)*, *10*(12). https://doi.org/10.3390/app10124345

CAPÍTULO 4

ARTIGO 3

Synthesis and microencapsulation of acylglycerols rich in omega-3 PUFAs by glycerolysis using lipase immobilized on activated carbon

---

*Manuscrito será submetido à revista Food Research International (ISSN: 1873-7145) – Fator de impacto: 8.1.

ABSTRACT

This work aimed to explore the potential of immobilized lipase (*Rhizomucor miehei*) on activated carbon to convert the high Free Fatty Acid (FFA) content of squid waste oil into acylglycerols (MAG and DAG) rich in n-3 PUFAs in a solvent-free system. The product was microencapsulated by complex coacervation, and stability studies were investigated. The effect of glycerolysis conditions was evaluated according to enzyme concentration, derivative concentration, substrate molar ratio, and reaction time, with the conversion of Free Fatty Acid as the response variable. The optimal parameters were 15 mg g^{-1} support, 8% of derivative (w/v of the reaction mixture), 1:5 of glycerol:oil, and 24 h. The lipid class of squid waste oil in the optimal conditions was EE(%) = 2.63, TAG(%) = 17.91, FFA(%) = 8.08, and MDG(%) = 71.38. The fatty acid composition analysis confirmed that squid waste oil had a high content of omega-3 PUFAs (ω-3 = 42.28%). The enzyme-treated oil was microencapsulated by complex coacervation between gelatin and sodium hexametaphosphate to protect the oil against oxidation. Microscope and Scanning Electron Microscopy (SEM) confirmed the microcapsule formation. The microencapsulation process achieved an Encapsulation Efficiency (%) of 99.79, Payload of 65.71 %, and Encapsulation Yield of 98.82 %. The microcapsules showed unexpectedly high oxidative stability (OSI = 52.35 h) compared to untreated (OSI = 0.04 h) and lipase-treated oil (OSI = 2.46 h). Therefore, immobilized lipase on activated carbon has the potential to efficiently synthesize acylglycerol without solvents, making it a fast and reusable enzymatic technology for creating omega-3-rich functional ingredients. Furthermore, the microencapsulation by complex coacervation can stabilize the omega-3 oil structure against oxidation for incorporation in food products.

Keywords: Enzyme; Esterification; Free fatty acid; Immobilization; Squid oil.

1. Introduction

Lipases catalyze triacylglycerol hydrolysis in diacylglycerols, monoacylglycerols, and free fatty acids. However, they also have a mechanism for working on esterification, transesterification, and interesterification reactions under non-aqueous conditions (Pereira et al., 2022; Sampaio et al., 2022; Verma et al., 2021). This interfacial property gives the enzyme versatility and selectivity, making them an important tool in different fields, such as

food (Chen et al., 2023), pharmaceuticals (Balogh-Weiser et al., 2023), detergents (Safdar et al., 2023), pulp and paper (Dixit et al., 2022), cosmetics (Liu et al., 2022), textiles (Taleb et al., 2022), biofuels (Wancura et al., 2023), and effluent treatment (Nimkande et al., 2023).

The high cost associated with lipase separation and reuse has been identified as the most significant issue to their use in large-scale and continuous industrial processes (Monteiro et al., 2021; Sousa et al., 2021). To overcome this limitation, the immobilized enzyme has been employed due to its benefits against the free enzyme, including activity, stability, substrate specificity, resistance to inhibitors, and greater control over reaction conditions (Almeida et al., 2022; Rodrigues et al., 2021).

There are several methods of immobilization based on the interaction between the biomolecule and the support, such as adsorption (Ferreira Gonçalves et al., 2021), covalent bonds (Oliveira et al., 2022), cross-linking (Guajardo et al., 2020), and encapsulation (Nadar & Rathod, 2020). The activity of the immobilized enzyme is influenced by the reaction conditions, surface area, porosity, and hydrophobicity of the support. For lipases, hydrophobic matrices allow biomolecule interaction in an open form through interfacial activation (Remonatto et al., 2022; Zhang et al., 2022). Among these mechanisms, activated carbon has shown potential as support in enzyme immobilization.

Lipase immobilization enhances its application as a catalyst for industrial processes. Recently, it has been used in marine oil processing to concentrate omega-3 polyunsaturated fatty acids (n-3 PUFAs) for nutritional supplements since omega-3 is an essential nutrient that cannot be produced by the human body (Innes & Calder, 2020; Magoni et al., 2022). Among marine organisms, squid viscera are an alternative source for obtaining PUFAs. Squid is an economical seafood with high protein and nutritional quality that can benefit human physiological functions. For instance, Park (2017) observed a significant content of EPA (20.23%) and DHA (35.50%) for squid oil. However, squid processing generates a large number of by-products that represent 35% of the total mass caught, including head, viscera, and skin (Wang et al., 2019a). Studies have been developed to reuse such components, where Aubourg et al., (Aubourg et al., 2023) reported high levels of EPA (17.73%) and DHA (34.67%) for a squid waste mixture. To our knowledge, the reuse of squid gut oil to obtain concentrated n-3 PUFAs has not been reported in the literature.

The most common forms of omega-3 concentrates are triacylglycerol (TAG) and ethyl ester (EE). However, recent studies have shown that monoacylglycerol (MAG) and diacylglycerol (DAG) are more easily digested and absorbed than TAG and EE due to

differences in absorption, digestion, and stereospecificity (Chen et al., 2022; Gunathilake et al., 2021). Furthermore, MAG and DAG are partial acylglycerols widely used as emulsifiers in the food, pharmaceutical, and cosmetic industries. They are produced through glycerolysis reactions between glycerol and free fatty acids. Lipase-catalyzed glycerolysis is an alternative to the high-temperature chemical process usually applied on an industrial scale for MAG and DAG synthesis due to the mild conditions needed for enzymatic processes, making the production of these heat-sensitive PUFAs suitable (Awadallak et al., 2020; Palacios et al., 2022). The reaction yield can be influenced by modifying glycerolysis conditions such as enzyme concentration, substrate molar ratio, solvent addition, and reaction time (Li et al., 2023; Palacios et al., 2019). Accordingly, it is important to evaluate the effect of glycerolysis parameters on lipase-treated oil.

The unsaturated structure of PUFAs makes omega-3 oils more susceptible to oxidative deterioration and gives undesirable organoleptic properties to products (Garcia-Oliveira et al., 2021). Thus, microencapsulation techniques can protect the active compound against oxidation during storage, processing, or incorporation into foods and drugs (Mu et al., 2022; Šavikin et al., 2021). Among the encapsulation methodologies, complex coacervation has been used in recent years for having unique characteristics such as high stability, compacted structure, high load density, and processing under moderate conditions (Xia et al., 2020).

Although enzymatic glycerolysis has been widely studied, the treatment of omega-3-rich oil using lipase immobilized on activated carbon has not been reported yet. Therefore, this study aimed to explore the potential of immobilized lipase (*Rhizomucor miehei*) on activated carbon to convert the high Free Fatty Acid (FFA) content of squid waste oil into acylglycerols (MAG and DAG) rich in n-3 PUFAs in a solvent-free system. The product was microencapsulated by complex coacervation, and stability studies were investigated.

2. Materials and methods

2.1 Materials

Activated carbon was synthesized in previous studies by chemical activation method using phosphoric acid through sisal waste carbonization at 700 ºC, 86 minutes, and an impregnation ratio of 2.5:1 (activating agent mass/precursor mass) (Yield = 45.61%, Ash = 7.89%, pH_{PCZ} = 5.83, Sg = 600 $m^2\ g^{-1}$, Dp = 5.68 nm, V_{meso} = 0.4738 $cm^3\ g^{-1}$, V_{micro} = 0.0888 $cm^3\ g^{-1}$, V_{total} = 0.6024 $cm^3\ g^{-1}$). Crude squid gut oil from arrow squid was provided by Mantzaris Fisheries Pty Ltd, North Geelong, Australia. Lipase from *Rhizomucor miehei*

(Palatase 20,000 L, Activity ≥ 20,000 U/g) was purchased from Sigma-Aldrich Corporation. All other chemicals were of analytical grade.

2.2 Enzyme immobilization

Rhizomucor miehei lipase was immobilized on activated carbon (AC) by adsorption following previous tests. For this, 0.1 g of activated carbon was suspended in 5 mL of sodium phosphate buffer solution (25 mM pH 7.0) containing RML (enzymatic load: 10 mg/g support) (Moreira et al., 2020). The system was placed under constant agitation at 10 g force for 2 hours at 30 ºC. Samples were centrifugated at 2000g for 5 min, washed with the immobilization buffer to remove non-adsorbed molecules, and dried in an oven at 40 ºC for 8 h. The biocatalyst synthesized was characterized by Circular Dichroism Spectroscopy.

2.3 Enzymatic glycerolysis

Glycerolysis of squid waste oil was carried out in a glass bottle (300 mL) at 50 ºC with magnetic stirring at 170 g force. The effect of reaction parameters on Free Fatty Acid (FFA) reduction was investigated, such as enzyme concentration (5–20 mg g^{-1} of support), derivative concentration (2–8% of derivative (w/v of the reaction mixture)), substrate molar ratio (1:2–1:5 of glycerol: oil molar ratio), and reaction time (1–24 h). Each of the factors was varied while others were kept constant. Aliquots of the sample (500 µL) were periodically withdrawn from the reaction mixture for lipid class analysis by Thin Layer Chromatography-Flame Ionization Detector (Iatroscan-FID).

2.4 Analysis of Fatty Acid Compositions by Gas Chromatography

Fatty acids in squid oil samples were converted to methyl esters as earlier described (Akanbi et al., 2013). The samples were analyzed using an Agilent 6890 gas chromatograph equipped with a BPX70 SGE column (30 m, 0.25 mm i.d., 0.25 µm film thickness) and a flame ionization detector (FID). The oven's temperature was programmed to increase from 140 °C (5 min hold) to 240 °C (5 min hold) at a rate of 4 °C/min and a total run time of 30 minutes. A split ratio of 50:1 was used to inject 1 µL of the solution (injector temperature = 250 °C). Helium was used as the carrier gas, with a constant flow of 1.5 mL/min. The detector gases were defined as 30 mL/min hydrogen, 300 mL/min air, and 30 mL/min nitrogen. ChemStation software was used to integrate peak areas, which were corrected by theoretical relative FID response factors (Craske and Bannon, 1987). Fatty acid standards

for the GC were a mixture of saturated, monounsaturated, and polyunsaturated fatty acids ranging from carbon 4 to 24 (C4-24) (Gunathilake et al., 2021).

2.5 Microencapsulation using complex coacervation

Microcapsules of acylglycerol concentrate from squid waste oil were prepared using the complex coacervation method based on the procedure described by Xia et al. (2020), with minor modifications. For this methodology, 15 g of squid oil under enzymatic treatment was mixed with gelatin dispersion (6%, w/w). The mixture was mechanically stirred for 5 min at 400 g force and emulsified for 15 minutes at 8570 g force using a homogenizer followed by adding sodium hexametaphosphate solution (0.6%, w/v) at 340 g force. The emulsion pH was adjusted to 4.7 by dropwise 1% phosphoric acid while coacervate synthesis was monitored by microscope. The procedure was carried out at 50 ºC, followed by cooling down to 5 ºC (8 ºC/h) through a refrigerating water bath. The sample was kept at 5 ºC for an hour, after which a transglutaminase dispersion (5%, w/w) was added to it. The temperature was then raised gradually to 25 ºC (5 ºC/h) and maintained for 5 hours, allowing the enzyme to be activated and create cross-links. Finally, the microcapsules obtained were freeze-dried to achieve a final powdered product. Microcapsule morphology was observed by Scanning Electron Microscopy (SEM) using a Zeiss LEO EVO 40 XVP (Germany) with a secondary electron (SE) detector and accelerating voltage of 20 kV. Samples were gold coated with a sputter coating technique.

2.6 Physicochemical properties of microcapsules

The properties of the coacervate microcapsules were determined as follows. The moisture content was determined gravimetrically by drying the solid microcapsules at 105 °C for 12 h. The surface oil content was determined using Liu et al. (2010) method with minor modifications. Briefly, 3 g of dried microcapsule powder was dispersed in 30 mL hexane and vortexed for 60 s. The solvent containing the extracted oil was centrifuged at 18,514 g force and 20 °C for 15 min. The solvent was removed by evaporation under a fume hood for 12 h. The extracted oil was further heated to 80 °C for 1 h to remove any residual hexane and was finally cooled down to room temperature. The mass of the extracted oil was measured by weighing.

Total oil (i.e., both surface oil and encapsulated oil within the coacervates) was determined according to Wang et al. (2014). In this protocol, 3 g microcapsules were

dispersed in 90 mL 4 N hydrochloric acid and vortexed for 60 s. Then 45 mL hexane was added followed by vortexing for another 60 s and incubating at room temperature for 12 h at 228 g force. After this, it was centrifuged at 18,514 g force for 30 min at 20 °C. The solvent phase was recovered and dried at 80 °C in an inert atmosphere to remove the residual solvent. The encapsulation efficiency (EE), payload (PL), and encapsulation yield (EY) were calculated using Equations 1-3.

$$EE = \frac{w_t - w_s}{w_t}\ x\ 100\% \quad (1)$$

$$PL = \frac{w_t}{w_m}\ x\ 100\% \quad (2)$$

$$EY = \frac{w_t}{w_i}\ x\ 100\% \quad (3)$$

Where w_t is the total oil mass (g) of microcapsules, w_s is the surface oil mass (g) of microcapsules, w_i is the mass (g) of oil added during microencapsulation and w_m is the mass (g) of the resulting microcapsules.

2.7 Oxidative stability analysis

Accelerated oxidation tests were carried out for squid oil and microcapsules using Rancimat (Herison 743 model). For this, oil (3 mL) or microcapsules (1.5 g) samples were heated at 110 ºC under purified air with a flow rate of 20 L/h. The induction time of samples was determined and used as the oxidative stability index (OSI).

2.8 Statistical analysis

All assays were performed in triplicate. The data was evaluated through analysis of variance (ANOVA) with F test and Tukey test for comparison between means ($p < 0.05$) using SAS Studio and Sigmaplot software.

3. Results and Discussion

3.1 Circular Dichroism

The Circular Dichroism spectra for activated carbon, lipase, and immobilized lipase on activated carbon are presented in Figure 1.

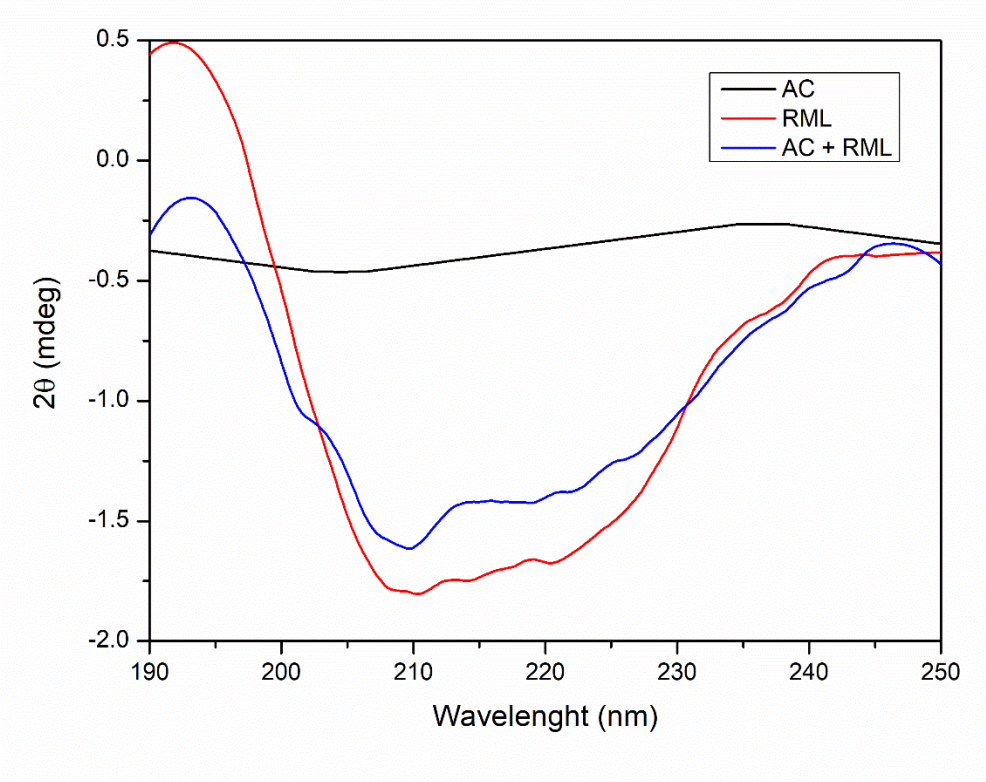

Figure 1. The Circular Dichroism spectra for activated carbon (AC), lipase (RML), and immobilized lipase (AC-RML).

CD spectroscopy was employed to investigate the conformational changes related to RML immobilization. In the far-UV region (190-240 nm), which corresponds to the peptide bond absorption, the CD spectrum can be analyzed. This analysis can give information about the content of regular secondary structural features, such as α-helix and, β-sheet (Miles et al., 2021). The spectra presented minima at 208 nm and maxima at 192 nm, indicating a general excess of α-helical content. A decrease in ellipticity at 208 nm was observed between the free and immobilized enzymes, suggesting a decrease in α-helical content. This information can be explained by the bond built between the hydrophobic lipase lid and the hydrophobic surface of activated carbon, resulting in changes in the enzyme conformational structure (Mathesh et al., 2016). Although the conformational changes can improve immobilization yield, they may reduce enzyme activity due to the decreased enzyme flexibility, the active site blockage, and diffusional restrictions between substrate and enzyme within the porous structure (Al-sareji et al., 2023).

3.2 Optimization of glycerolysis conditions

The effect of glycerolysis conditions was performed using lipase from *Rhizomucor miehei* based on its broad usage in esterification and transesterification reactions, with results presented in Figures 2-5. The initial lipid class of squid waste oil was 3.07% Ethyl Ester (EE), 38.14% Triacylglycerol (TAG), 44.25% Free Fatty Acid (FFA), and 14.54% Mono-Diacylglycerol (MDG).

The impact of enzyme concentration on converting free fatty acids in omega-3 mono and diacylglycerol was investigated. Figure 2 shows that increasing enzyme load enhances glycerolysis efficiency, reaching the lowest Free Fatty Acid content (27.14%) and the highest Mono-Diacylglycerol content (35.30%) at the lipase immobilization of 15 mg g^{-1} support, before decreasing in 20 mg g^{-1} support. As adsorption is a physical phenomenon, an excessive enzyme may lead to pore clogging and protein aggregation on the activated carbon surface, limiting the mass transfer of substrate to the active site of the biocatalyst and the reaction rate (Saikia et al., 2021). Ghide et al. [42] studies presented the same behavior with immobilized RML on magnetic multiwalled carbon nanotubes. Thus, 15 mg g^{-1} support was selected as the optimum enzyme amount for immobilization.

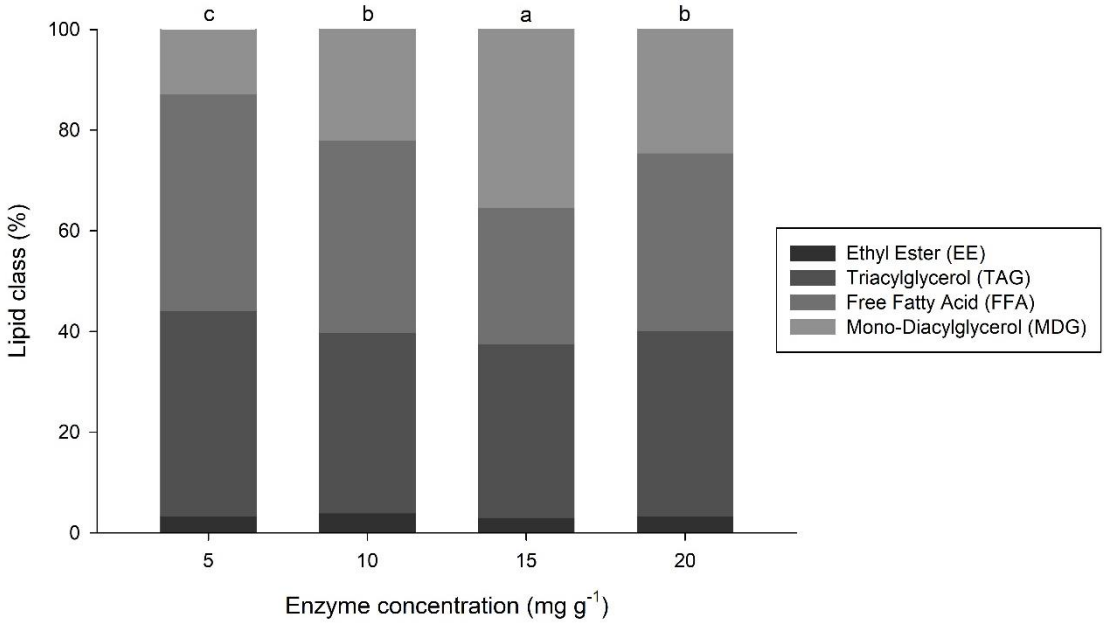

Figure 2. Effect of enzyme concentration on squid oil's lipid class (%) using immobilized lipase on activated carbon as enzymatic treatment.

As shown in Figure 3, the significance of derivative concentration was studied. We observed that esterification yield is increased as the concentration percentage increases. The lowest FFA (FFA = 14.21%) and MDG (MDG = 52.83%) were found by the derivative concentration of 8% w/v. Similar results were reported by Palacios et al. (2022), achieving the optimal condition at a concentration of 7.31% (Lipozyme RM-IM). Therefore, 8% of the derivative concentration was the condition used for subsequent experiments.

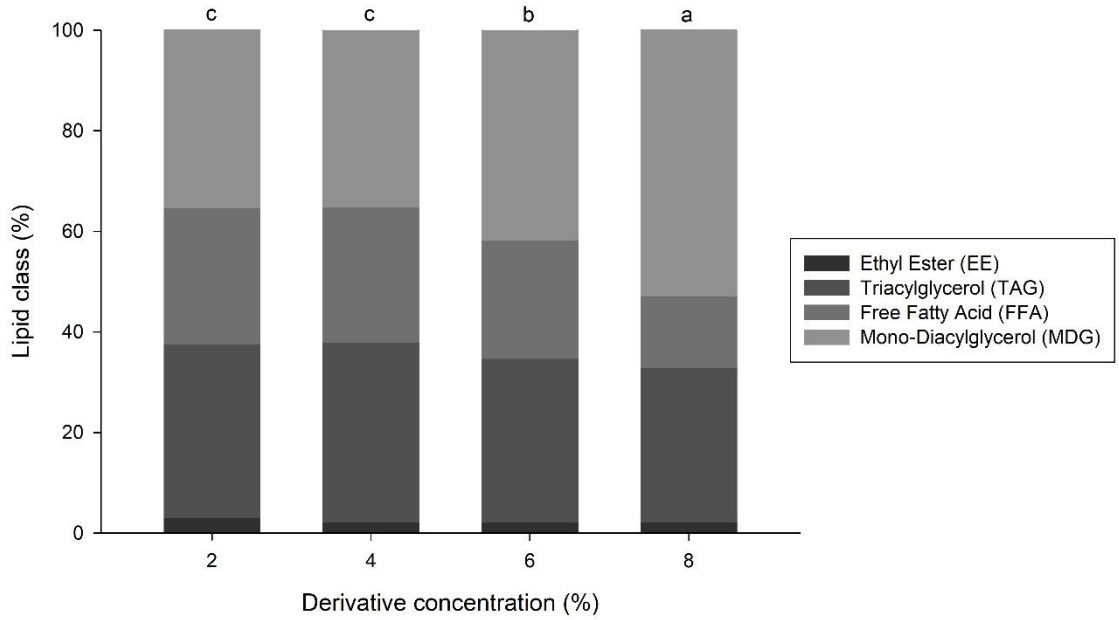

Figure 3. Effect of derivative concentration on squid oil's lipid class (%) using immobilized lipase on activated carbon as enzymatic treatment.

The effect of modifying the molar ratios of substrate (glycerol and oil) was verified by adjusting oil concentration while maintaining glycerol levels constant (Figure 4). The results showed that changing the substrate ratio did not significantly affect glycerolysis conversion, although a trend of decreasing FFA and increasing MDG was observed as the oil amount increased. The lowest FFA and highest MDG percentages were 24.73% and 39.91%, respectively. This can be explained by the lower viscosity resulting from the decrease in glycerol concentration, which could compromise homogeneity in viscous mixtures and lead to the entrapment of the immobilized enzyme particles. Furthermore, glycerol is a hydrophilic molecule with low solubility in organic solvents (95-96% insolubility for fats and oils), limiting the enzyme access to both substrates simultaneously.

Therefore, reducing glycerol content will increase solubility (Gunathilake et al., 2021). Accordingly, the substrate molar ratio was determined to be 1:5 of glycerol:oil.

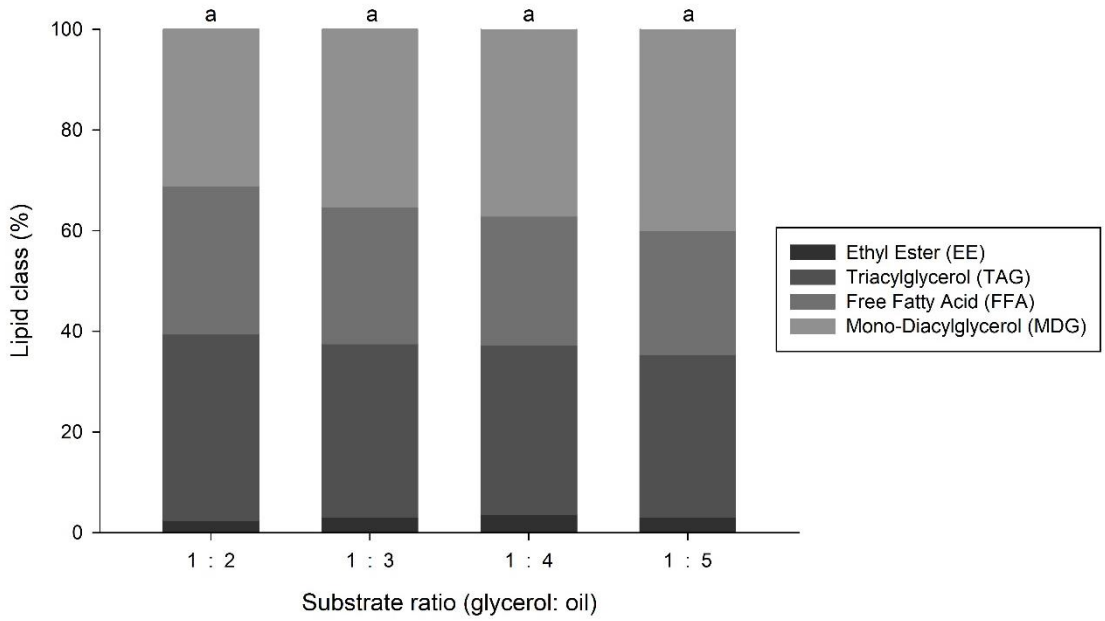

Figure 4. Effect of substrate ratio on squid oil's lipid class (%) using immobilized lipase on activated carbon as enzymatic treatment.

Figure 5 displays the study on the appropriate reaction time for MDG synthesis through FFA consumption. It was observed that FFA content decreased from 44.25% to 8.08% after 24 hours, while the MDG increased from 14.54% to 71.38% after 24 hours. In the reaction conditions tested, a small amount of free fatty acids was converted in the final reaction products (about 6% between 9 and 24 h), indicating a rapid esterification process. Similarly, Feltes et al. (2012) obtained the equilibrium after 10 h at 55 °C using the immobilized lipase Novozym 435 in another solvent-free system. Therefore, the non-aqueous mixture used is suitable for achieving good glycerolysis while limiting hydrolysis. Glycerol is also a suitable acyl group acceptor in lipase-catalyzed reactions, allowing for greater conversion of free fatty acids to MAG and DAG (Zhou et al., 2022).

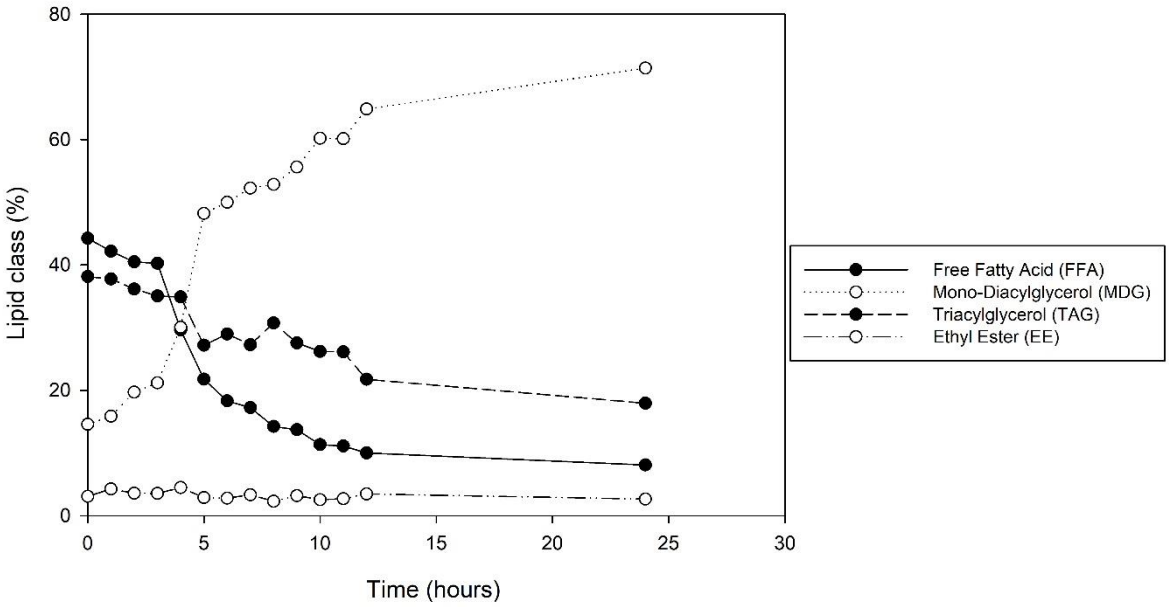

Figure 5. Effect of glycerolysis time on squid oil's lipid class (%) using immobilized lipase on activated carbon as enzymatic treatment.

However, the MDG esterification continued to increase significantly over time (about 16% between 9 and 24 h), which can be attributed to the decrease in triacylglycerol content from 27.53% to 17.91%. This process, known as interesterification (IE), can modify TAG properties through initial lysis and subsequent esterification reactions, resulting in the redistribution or exchange of fatty acids between acyglycerol molecules (Z. Zhang et al., 2020). Xia et al. (2019) used Lipozyme RMIM to optimize interesterification and remove palmitic acid from palm oil while incorporating ALA and EPA in a reaction time between 18 and 24 h. Therefore, 24 h was selected as the reaction time capable of providing the ideal lipid class for this research purpose.

The optimized conditions for the glycerolysis of Free Fatty Acids into omega-3 MDG were: immobilized lipase (*Rhizomucor miehei*) on activated carbon (15 mg g^{-1} support; 8% of derivative (w/v of reaction mixture)), molar ratio of substrates (1:5; glycerol: oil), and a reaction time of 24 h. This method uses the biocatalyst to efficiently synthesize acylglycerol without solvents, making it a fast and reusable enzymatic technology for creating omega-3-rich functional ingredients such as emulsifiers and stabilizers for the food industry.

3.3 Fatty acids composition

The fatty acid content of raw oil and oil treated with immobilized lipase (*Rhizomucor miehei*) on activated carbon were analyzed using Gas Chromatography and the results are reported in Table 1.

Table 1. Fatty acid composition determined by Gas Chromatography of raw squid waste oil and immobilized lipase-treated oil.

Fatty Acid		**Squid oil (%)**	**Lipase-treated oil (%)**
C14:0	Myristic acid	4.88 ± 0.01 [a]	4.62 ± 0.01 [a]
C16:0	Palmitic acid	14.19 ± 0.11 [a]	14.30 ± 0.06 [a]
C16:1	Palmitoleic acid	5.21 ± 0.04 [a]	5.24 ± 0.00 [a]
C18	Stearic acid	1.88 ± 0.00 [a]	1.89 ± 0.02 [a]
C18:1	Oleic acid	15.71 ± 0.04 [a]	15.75 ± 0.14 [a]
C18:2 n-6	Linoleic acid	2.27 ± 0.03 [a]	2.32 ± 0.03 [a]
C18:3 n-3	α-Linolenic acid (ALA)	1.70 ± 0.02 [a]	1.72 ± 0.02 [a]
C20:0	Arachidic acid	4.41 ± 0.00 [a]	4.42 ± 0.03 [a]
C20:1		4.22 ± 0.01 [a]	4.28 ± 0.05 [a]
C20:4 n-6	Arachidonic acid	1.33 ± 0.00 [a]	1.37 ± 0.05 [a]
C20:5 n-3	Eicosapentaenoic acid (EPA)	19.68 ± 0.04 [a]	19.90 ± 0.15 [a]
C22:6 n-3	Docosahexaenoic acid (DHA)	20.19 ± 0.01 [a]	20.39 ± 0.12 [a]
Saturated fatty acids		26.63 ± 0.08 [a]	26.53 ± 0.13 [a]
Monounsaturated fatty acids (MUFAs)		27.06 ± 0.11 [a]	26.34 ± 0.21 [a]
Polyunsaturated fatty acids (PUFAs)		46.31 ± 0.03 [a]	46.89 ± 0.42 [a]
n-6		4.49 ± 0.06 [a]	4.61 ± 0.12 [a]
n-3		41.82 ± 0.03 [a]	42.28 ± 0.30 [a]
n-6/n-3 ratio		0.11 ± 0.00 [a]	0.11 ± 0.00 [a]

According to Table 1, the fatty acid composition was not significantly modified after glycerolysis reactions of squid waste oil, showing the effectiveness of the method in

changing only the availability and stability of lipid molecules by converting FFA into MDG. The main % of fatty acids were Docosahexaenoic acid (DHA), Eicosapentaenoic acid (EPA), Oleic acid, and Palmitic acid. Similar results were found by Sun et al. (2023) for the raw oil.

Marine species are known as nutrient-rich and balanced foods due to their high content of valuable constituents, especially omega-3 compounds. However, processing these species produces significant amounts of by-products. According to the Food and Agriculture Organization (FAO), annual seafood production contributes to more than 180 million tonnes, but roughly a quarter of the total marine catch is discarded (Özyurt & Özkütük, 2020). Squid processing also generates many by-products, representing 35% of the total mass caught and including the head, viscera, and skin (Wang et al., 2019b). Recently, there has been a lot of discussion about the valorization of discarded marine species and by-products from the seafood industry because they have a similar constituent composition to commercial and edible marine tissues (Aubourg et al., 2023).

Therefore, the development of new technologies and strategies for recovering and purifying high-added-value compounds, such as ω-3 PUFAs, can promote better utilization of discards, and they could be incorporated into nutraceutical, functional food formulation or pharmaceutical applications (Ahmad et al., 2019). The percentage of PUFAs in the current work represents 46.89% of total fatty acids, and it is mainly composed of omega-3 compounds (ω-3 = 42.28% against ω-6 = 4.61%), which confirms the omega-3-rich content of squid gut oil from arrow squid. Indeed, this approach can be considered an eco-friendly strategy to convert marine wastes to high-added-value compounds while offsetting environmental pollution and disposal problems.

3.4 Microencapsulation by Complex Coacervation

The morphologies of the complex coacervates and microcapsules were studied using optical microscopy. The agglomeration of O/W emulsion droplets occurred at pH 4.7 upon the formation of complex coacervates in the aqueous phase (Figure 6A), which led to the formation of "multi-core" microcapsules in the cooling step (Figure 6B). The gelatin-SHMP complex coacervate was formed surrounding these O/W emulsion droplet agglomerates resulting in the synthesis of microcapsules with multiple oil-in-water droplets, which are stabilized as "cores." This structure is referred to as a “multi-core” structure. The coacervate layers coating the oil droplets within the microcapsules are crosslinked when transglutaminase is added, and the "multi-core" microcapsules can no longer redissolve (Xia et al., 2020).

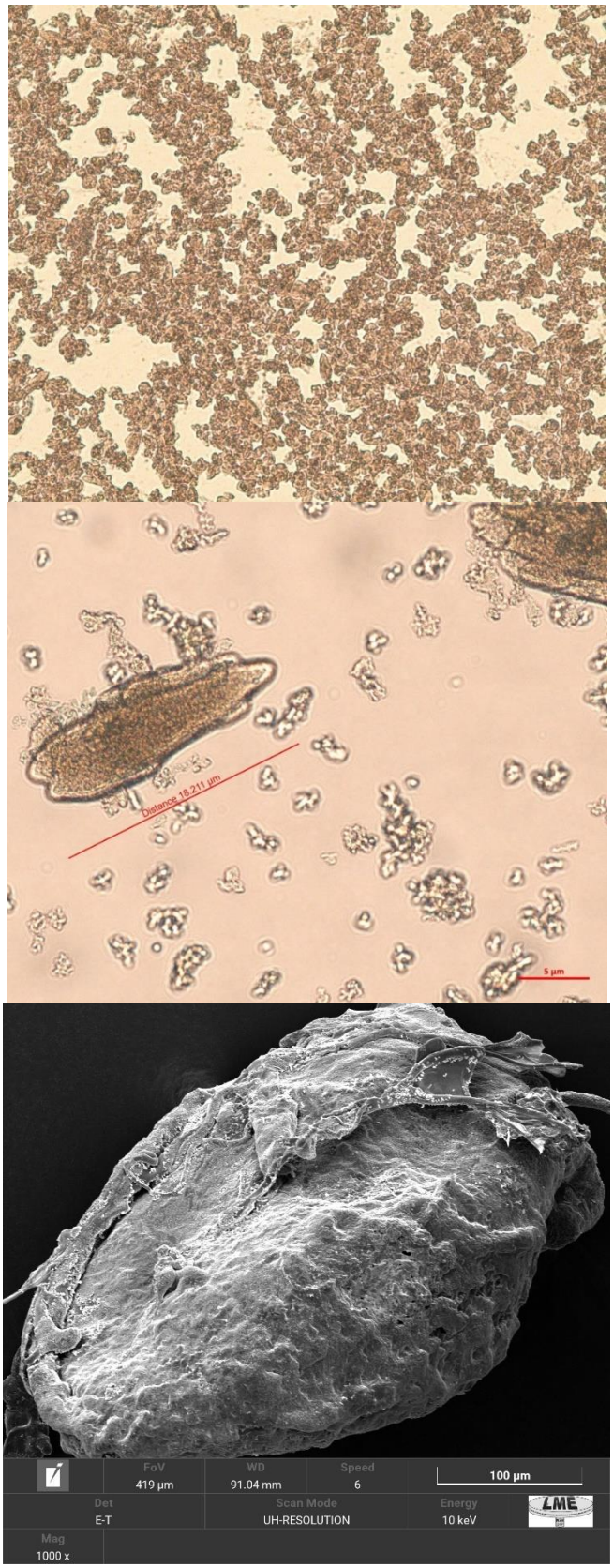

Figure 6. Morphological structure of complex coacervates (A) and microcapsules from squid waste oil observed by microscope (B) and SEM (C).

This microencapsulation method has been particularly successful in stabilizing unsaturated lipids and providing an ingredient with a sensory shelf-life consistent with the food products. It has not been used successfully to deliver unsaturated lipids into food products until the development of multicore products, though. For the preparation of multicore microcapsule, oil-in-water emulsion is produced; hence, the sizes of its inner single oil droplet cores are defined. Thereafter, the oil droplets are coated by the complex coacervate and tend to agglomerate to form multicore microcapsules with a size of 30–50 μm. However, the size of multicore microcapsules is greater than the oral sensory threshold, which is usually considered to be 10–25 μm, and therefore it can be easily perceived by the mouth (Ma et al., 2019). Figure 6B shows that the microcapsules of the present study had sizes of 18.21 μm, showing agreement with the sensory threshold for incorporation in food products.

The SEM observation confirmed the formation of microcapsules coated by complex coacervation, as shown in Figure 6C. Similarly to those observed under light microscopy, the microcapsules observed by SEM had oval morphologies with aggregated oil droplets inside and a smooth gelatin–SHMP coacervate coating layer as the outer shell. Furthermore, no holes or cracks were found on the surface of complete microcapsules in the current study, indicating an effective protective barrier.

3.5 Physicochemical properties of microcapsules

The Surface Oil, Encapsulation Efficiency, Payload, Encapsulation Yield, and Moisture of squid waste oil microencapsulated by complex coacervation are reported in Table 2.

Table 2. Physicochemical properties of microcapsules.

Sample	Surface oil (%)	Encapsulation Efficiency (%)	Payload (%)	Encapsulation Yield (%)	Moisture (%)
Microcapsule	0.13 ± 0.58	99.79 ± 0.37	65.71 ± 0.74	98.82 ± 0.81	3.38 ± 0.24

The microcapsule powder exhibited 3.38% moisture, which falls within the recommended range of 4-6% for dry food ingredients (Šavikin et al., 2021). The encapsulation efficiency attained a high value, and the powders had low surface oil content with a high encapsulation yield. Wang et al. (2019) states that the encapsulation efficiency

is related to the presence of free oil on the surface of the particles within the powder and the degree to which the shell matrix can prevent the extraction of internal oil through a leaching process. The high encapsulation efficiency observed here indicates that most squid oil would be well-protected from oxidation (Mu et al., 2022; Wang et al., 2019). Furthermore, the high encapsulation yield suggests that the oil loss during the microencapsulation is negligible.

3.6 Oxidative stability

Lipid oxidation is a complex process related to undesirable chemical reactions that reduce oil quality, resulting in organoleptic rancidity in the finished products and other degrading effects such as discoloration, vitamin destruction, nutritional losses, and polymerization (Garcia-Oliveira et al., 2021). The oxidation progresses at different rates due to different factors, such as temperature, light, oxygen, moisture, storage time, and lipid composition (Qiu et al., 2019). Therefore, the oxidative stability of raw squid oil, enzyme-treated oil, and microcapsules was investigated and the oxidative stability index (OSI) is shown in Figure 7.

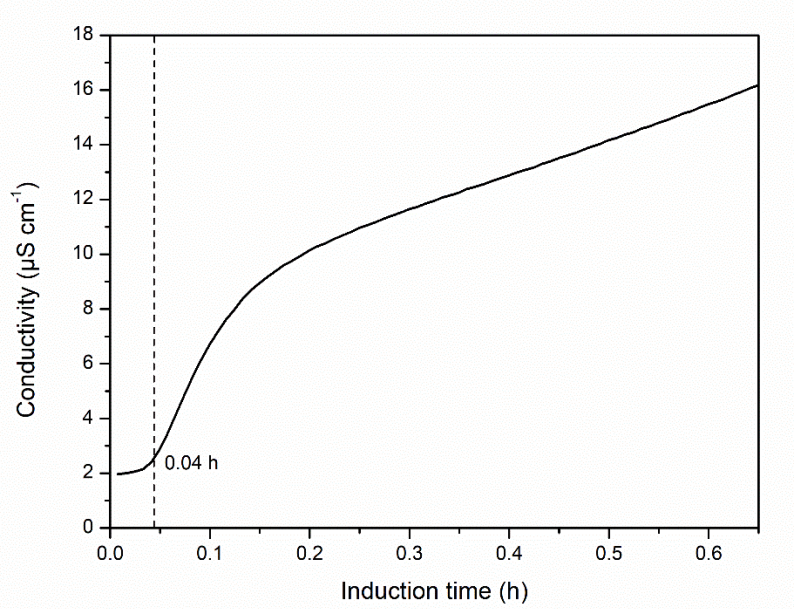

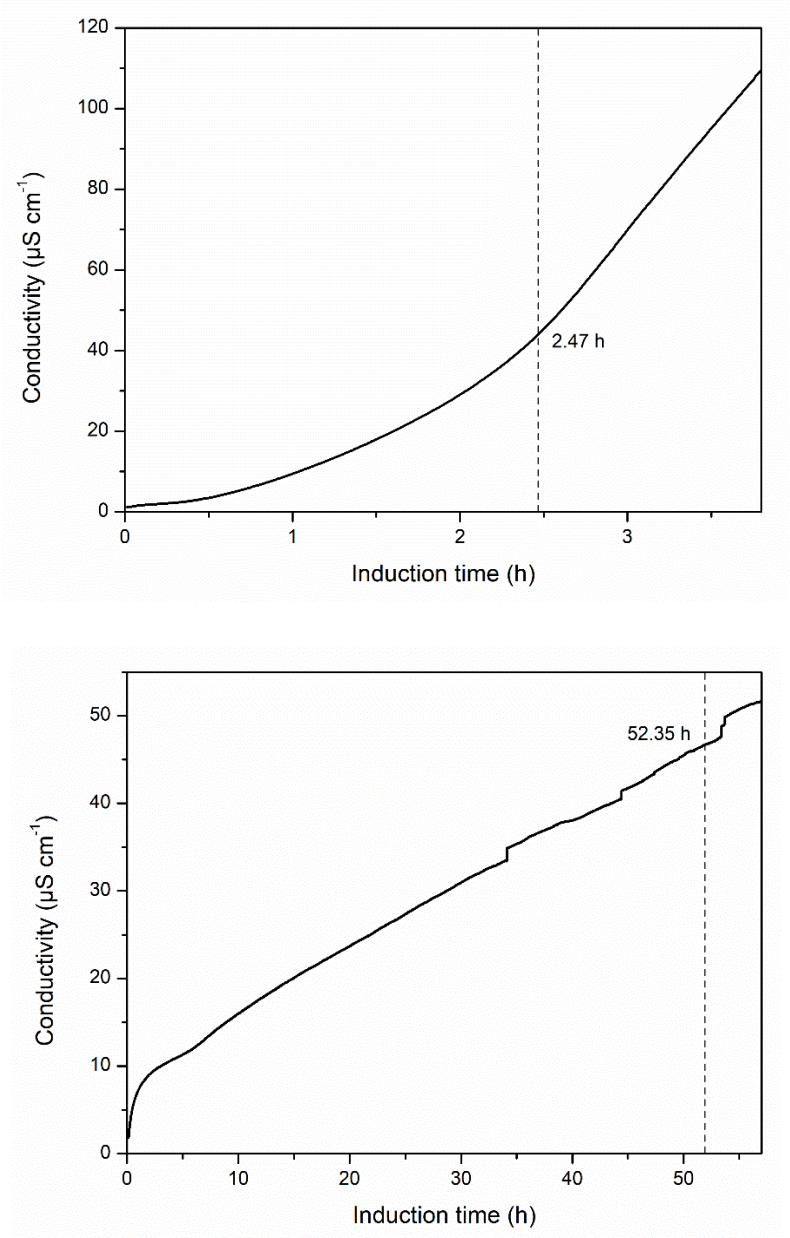

Figure 7. Oxidative stability index (OSI) of raw squid waste oil, lipase-treated oil, and microcapsules.

The oil treatment with immobilized lipases significantly enhanced the oxidative stability index (OSI = 2.46 ± 0.01 ^{b} h) of squid oil (OSI = 0.04 ± 0.0 ^{c} h) after reducing its Free Fatty Acids content from 44.25% to 8.08% after 24 h. This behavior is observed due to the susceptibility to oxidation by the long-chain polyunsaturated fatty acids (PUFAs), making omega-3 oils highly vulnerable (Du et al., 2022). Furthermore, the microcapsules showed an unexpectedly high oxidation stability of 52.35 ± 0.01 ^{a} h under high-temperature conditions (110 ºC), confirming the effective protection of the complex coacervates without

any antioxidants added to the microencapsulation process. Wang et al. (2019) reported a maximum oxidative stability index of 33.6 h in their studies with anchovy oil microcapsules, while Wang et al. (2014) reached the highest OSI = 40.2 h working with tuna oil microencapsulation. Xia et al. (2020) achieved 62 h of induction time, although their Rancimat tests were performed at 90 ºC, and the microencapsulated tuna oil was mixed with varying amounts of additives. Therefore, the current work shows potential for stabilizing the omega-3 oil structure against oxidation for incorporation in food products.

4. Conclusion

In this study, omega-3 MDG oils were produced in a solvent-free system by reacting squid waste oil and glycerol in the presence of lipase from *Rhizomucor miehei* immobilized on activated carbon. The glycerolysis conditions were optimized according to enzyme concentration, derivative concentration, substrate molar ratio, and reaction time. The fatty acid composition analysis confirmed that squid waste oil had a high content of omega-3 PUFAs. The enzyme-treated oil was microencapsulated by complex coacervation between gelatin and sodium hexametaphosphate to protect the oil against oxidation. The microcapsules showed unexpectedly high oxidative stability compared to untreated and lipase-treated oil. Therefore, immobilized lipase on activated carbon has the potential to efficiently synthesize acylglycerol without solvents, making it a fast and reusable enzymatic technology for creating omega-3-rich functional ingredients. Furthermore, the microencapsulation by complex coacervation can stabilize the omega-3 oil structure against oxidation for incorporation in food products.

Acknowledgments

The authors gratefully acknowledge the Sandwich Doctorate Program Abroad (PDSE) and the Coordination for the Improvement of Higher Education Personnel (CAPES, finance code 001) for funding. The authors also recognize the support of Deakin University, Australia, and LME–UFLA.

References

Ahmad, T. B., Rudd, D., Kotiw, M., Liu, L., & Benkendorff, K. (2019). Correlation between fatty acid profile and anti-inflammatory activity in common Australian seafood by-products. *Marine Drugs*, *17*(3). https://doi.org/10.3390/md17030155

Akanbi, T. O., Adcock, J. L., & Barrow, C. J. (2013). Selective concentration of EPA and DHA using Thermomyces lanuginosus lipase is due to fatty acid selectivity and not regioselectivity. *Food Chemistry*, *138*(1), 615–620. https://doi.org/10.1016/j.foodchem.2012.11.007

Almeida, F. L. C., Prata, A. S., & Forte, M. B. S. (2022). Enzyme immobilization: what have we learned in the past five years? Em *Biofuels, Bioproducts and Biorefining* (Vol. 16, Número 2, p. 587–608). John Wiley and Sons Ltd. https://doi.org/10.1002/bbb.2313

Al-sareji, O. J., Meiczinger, M., Somogyi, V., Al-Juboori, R. A., Grmasha, R. A., Stenger-Kovács, C., Jakab, M., & Hashim, K. S. (2023). Removal of emerging pollutants from water using enzyme-immobilized activated carbon from coconut shell. *Journal of Environmental Chemical Engineering*, *11*(3). https://doi.org/10.1016/j.jece.2023.109803

Aubourg, S. P., Rodríguez, A., Trigo, M., & Medina, I. (2023). Yield Enhancement of Valuable Lipid Compounds from Squid (Doryteuthis gahi) Waste by Ethanol/Acetone Extraction. *Foods*, *12*(14), 2649. https://doi.org/10.3390/foods12142649

Awadallak, J. A., da Silva, E. A., & da Silva, C. (2020). Production of linseed diacylglycerol-rich oil by combined glycerolysis and esterification. *Industrial Crops and Products*, *145*. https://doi.org/10.1016/j.indcrop.2019.111937

Balogh-Weiser, D., Molnár, A., Tóth, G. D., Koplányi, G., Szemes, J., Decsi, B., Katona, G., Salamah, M., Ender, F., Kovács, A., Berkó, S., Budai-Szűcs, M., & Balogh, G. T. (2023). Combined Nanofibrous Face Mask: Co-Formulation of Lipases and Antibiotic Agent by Electrospinning Technique. *Pharmaceutics*, *15*(4). https://doi.org/10.3390/pharmaceutics15041174

Camino Feltes, M. M., Villeneuve, P., Baréa, B., Barouh, N., De Oliveira, J. V., De Oliveira, D., & Ninow, J. L. (2012). Enzymatic production of monoacylglycerols (MAG) and diacylglycerols (DAG) from fish oil in a solvent-free system. *JAOCS, Journal of the American Oil Chemists' Society*, *89*(6), 1057–1065. https://doi.org/10.1007/s11746-011-1998-2

Chen, J., Zhang, Y., Zhong, H., Zhu, H., Wang, H., Goh, K. L., Zhang, J., & Zheng, M. (2023). Efficient and sustainable preparation of cinnamic acid flavor esters by immobilized lipase microarray. *LWT*, *173*. https://doi.org/10.1016/j.lwt.2022.114322

Chen, W., He, L., Song, W., Huang, J., & Zhong, N. (2022). Encapsulation of lipases by nucleotide/metal ion coordination polymers: enzymatic properties and their applications in glycerolysis and esterification studies. *Journal of the Science of Food and Agriculture*, *102*(10), 4012–4024. https://doi.org/10.1002/jsfa.11749

de Oliveira, T. P., Santos, M. P. F., Brito, M. J. P., & Veloso, C. M. (2022). Incorporation of metallic particles in activated carbon used in lipase immobilization for production of isoamyl acetate. *Journal of Chemical Technology and Biotechnology*, *97*(7), 1736–1746. https://doi.org/10.1002/jctb.7043

Dixit, M., Gupta, G. K., Pathak, P., Bhardwaj, N. K., & Shukla, P. (2022). An efficient endoglucanase and lipase enzyme consortium (ELEC) for deinking of old newspaper and ultrastructural analysis of deinked pulp. *Biomass Conversion and Biorefinery*. https://doi.org/10.1007/s13399-022-03310-6

Du, Q., Zhou, L., Li, M., Lyu, F., Liu, J., & Ding, Y. (2022). Omega-3 polyunsaturated fatty acid encapsulation system: Physical and oxidative stability, and medical applications. Em *Food Frontiers* (Vol. 3, Número 2, p. 239–255). John Wiley and Sons Inc. https://doi.org/10.1002/fft2.134

Ferreira Gonçalves, G. R., Ramos Gandolfi, O. R., Brito, M. J. P., Bonomo, R. C. F., da Costa Ilhéu Fontan, R., & Veloso, C. M. (2021). Immobilization of porcine pancreatic lipase on activated carbon by adsorption and covalent bonding and its application in the synthesis of butyl butyrate. *Process Biochemistry*, *111*, 114–123. https://doi.org/10.1016/j.procbio.2021.10.027

Garcia-Oliveira, P., Jimenez-Lopez, C., Lourenço-Lopes, C., Chamorro, F., Pereira, A. G., Carrera-Casais, A., Fraga-Corral, M., Carpena, M., Simal-Gandara, J., & Prieto, M. A. (2021). Evolution of flavors in extra virgin olive oil shelf-life. Em *Antioxidants* (Vol. 10, Número 3, p. 1–20). MDPI. https://doi.org/10.3390/antiox10030368

Ghide, M. K., Li, K., Wang, J., Abdulmalek, S. A., & Yan, Y. (2022). Immobilization of Rhizomucor miehei lipase on magnetic multiwalled carbon nanotubes towards the synthesis of structured lipids rich in sn-2 palmitic acid and sn-1,3 oleic acid (OPO) for infant formula use. *Food Chemistry*, *390*. https://doi.org/10.1016/j.foodchem.2022.133171

Guajardo, N., Ahumada, K., & Domínguez de María, P. (2020). Immobilized lipase-CLEA aggregates encapsulated in lentikats® as robust biocatalysts for continuous processes in deep eutectic solvents. *Journal of Biotechnology*, *310*, 97–102. https://doi.org/10.1016/j.jbiotec.2020.02.003

Gunathilake, T., Akanbi, T. O., & Barrow, C. J. (2021). Lipase-produced omega-3 acylglycerols for the fortification and stabilization of extra virgin olive oil using hydroxytyrosyl palmitate. *Future Foods*, *4*. https://doi.org/10.1016/j.fufo.2021.100045

Innes, J. K., & Calder, P. C. (2020). Marine omega-3 (N-3) fatty acids for cardiovascular health: An update for 2020. Em *International Journal of Molecular Sciences* (Vol. 21, Número 4). MDPI AG. https://doi.org/10.3390/ijms21041362

Li, L., Zhou, Y., Huang, C., Jian, L., Lin, Z., Lin, L., Li, C., & Ye, Y. (2023). Insight into the influence of plant oils on the composition of diacylglycerol fabricated by glycerolysis and esterification. *Industrial Crops and Products*, *204*. https://doi.org/10.1016/j.indcrop.2023.117324

Liu, S., Low, N. H., & Nickerson, M. T. (2010). Entrapment of flaxseed oil within gelatin-gum Arabic capsules. *JAOCS, Journal of the American Oil Chemists' Society*, *87*(7), 809–815. https://doi.org/10.1007/s11746-010-1560-7

Liu, Y. Q., WeiZhuo, X., & Wei, X. (2022). A review on lipase-catalyzed synthesis of geranyl esters as flavor additives for food, pharmaceutical and cosmetic applications. Em *Food Chemistry Advances* (Vol. 1). Elsevier Ltd. https://doi.org/10.1016/j.focha.2022.100052

Ma, T., Zhao, H., Wang, J., & Sun, B. (2019). Effect of processing conditions on the morphology and oxidative stability of lipid microcapsules during complex

coacervation. *Food Hydrocolloids*, *87*, 637–643. https://doi.org/10.1016/j.foodhyd.2018.08.053

Magoni, C., Bertacchi, S., Giustra, C. M., Guzzetti, L., Cozza, R., Ferrari, M., Torelli, A., Marieschi, M., Porro, D., Branduardi, P., & Labra, M. (2022). Could microalgae be a strategic choice for responding to the demand for omega-3 fatty acids? A European perspective. Em *Trends in Food Science and Technology* (Vol. 121, p. 142–155). Elsevier Ltd. https://doi.org/10.1016/j.tifs.2022.01.030

Mathesh, M., Luan, B., Akanbi, T. O., Weber, J. K., Liu, J., Barrow, C. J., Zhou, R., & Yang, W. (2016). Opening Lids: Modulation of Lipase Immobilization by Graphene Oxides. *ACS Catalysis*, *6*(7), 4760–4768. https://doi.org/10.1021/acscatal.6b00942

Miles, A. J., Janes, R. W., & Wallace, B. A. (2021). Tools and methods for circular dichroism spectroscopy of proteins: A tutorial review. Em *Chemical Society Reviews* (Vol. 50, Número 15, p. 8400–8413). Royal Society of Chemistry. https://doi.org/10.1039/d0cs00558d

Monteiro, R. R. C., Arana-Peña, S., da Rocha, T. N., Miranda, L. P., Berenguer-Murcia, Á., Tardioli, P. W., dos Santos, J. C. S., & Fernandez-Lafuente, R. (2021). Liquid lipase preparations designed for industrial production of biodiesel. Is it really an optimal solution? Em *Renewable Energy* (Vol. 164, p. 1566–1587). Elsevier Ltd. https://doi.org/10.1016/j.renene.2020.10.071

Moreira, K. da S., de Oliveira, A. L. B., Júnior, L. S. de M., Monteiro, R. R. C., da Rocha, T. N., Menezes, F. L., Fechine, L. M. U. D., Denardin, J. C., Michea, S., Freire, R. M., Fechine, P. B. A., Souza, M. C. M., & dos Santos, J. C. S. (2020). Lipase From Rhizomucor miehei Immobilized on Magnetic Nanoparticles: Performance in Fatty Acid Ethyl Ester (FAEE) Optimized Production by the Taguchi Method. *Frontiers in Bioengineering and Biotechnology*, *8*. https://doi.org/10.3389/fbioe.2020.00693

Mu, H., Song, Z., Wang, X., Wang, D., Zheng, X., & Li, X. (2022). Microencapsulation of algae oil by complex coacervation of chitosan and modified starch: Characterization and oxidative stability. *International Journal of Biological Macromolecules*, *194*, 66–73. https://doi.org/10.1016/j.ijbiomac.2021.11.168

Nadar, S. S., & Rathod, V. K. (2020). Immobilization of proline activated lipase within metal organic framework (MOF). *International Journal of Biological Macromolecules*, *152*, 1108–1112. https://doi.org/10.1016/j.ijbiomac.2019.10.199

Nimkande, V. D., Krishnamurthi, K., & Bafana, A. (2023). Potential of Antarctic lipase from Acinetobacter johnsonii Ant12 for treatment of lipid-rich wastewater: screening, production, properties and applications. *Biodegradation*. https://doi.org/10.1007/s10532-023-10041-6

Özyurt, G., & Özkütük, S. (2020). *Advances in discard and by-product processing.* Boca Raton: Taylor and Francis Group.

Palacios, D., Busto, M. D., Albillos, S. M., & Ortega, N. (2022). Synthesis and oxidative stability of monoacylglycerols containing polyunsaturated fatty acids by enzymatic glycerolysis in a solvent-free system. *LWT*, *154*. https://doi.org/10.1016/j.lwt.2021.112600

Palacios, D., Ortega, N., Rubio-Rodríguez, N., & Busto, M. D. (2019). Lipase-catalyzed glycerolysis of anchovy oil in a solvent-free system: Simultaneous optimization of monoacylglycerol synthesis and end-product oxidative stability. *Food Chemistry*, *271*, 372–379. https://doi.org/10.1016/j.foodchem.2018.07.184

Park, J. H. (2017). Quality Characteristics of Refined Squid (Todarodes pacificus) Oil as an Alternative Resource for Omega-3 Fatty Acids. *Journal of Food Processing and Preservation*, *41*(2). https://doi.org/10.1111/jfpp.12780

Pereira, A. da S., de Souza, A. H., Fraga, J. L., Villeneuve, P., Torres, A. G., & Amaral, P. F. F. (2022). Lipases as Effective Green Biocatalysts for Phytosterol Esters' Production: A Review. Em *Catalysts* (Vol. 12, Número 1). MDPI. https://doi.org/10.3390/catal12010088

Qiu, X., Chen, S., & Lin, H. (2019). Oxidative Stability of Dried Seafood Products during Processing and Storage: A Review. Em *Journal of Aquatic Food Product Technology* (Vol. 28, Número 3, p. 329–340). Taylor and Francis Inc. https://doi.org/10.1080/10498850.2019.1581317

Remonatto, D., Miotti, R. H., Monti, R., Bassan, J. C., & de Paula, A. V. (2022). Applications of immobilized lipases in enzymatic reactors: A review. Em *Process Biochemistry* (Vol. 114, p. 1–20). Elsevier Ltd. https://doi.org/10.1016/j.procbio.2022.01.004

Rodrigues, R. C., Berenguer-Murcia, Á., Carballares, D., Morellon-Sterling, R., & Fernandez-Lafuente, R. (2021). Stabilization of enzymes via immobilization: Multipoint covalent attachment and other stabilization strategies. Em *Biotechnology Advances* (Vol. 52). Elsevier Inc. https://doi.org/10.1016/j.biotechadv.2021.107821

Safdar, A., Ismail, F., & Imran, M. (2023). Characterization of Detergent-Compatible Lipases from *Candida albicans* and *Acremonium sclerotigenum* under Solid-State Fermentation. *ACS Omega*. https://doi.org/10.1021/acsomega.3c03644

Saikia, K., Rathankumar, A. K., Vaithyanathan, V. K., Cabana, H., & Vaidyanathan, V. K. (2021). Preparation of highly diffusible porous cross-linked lipase B from Candida antarctica conjugates: Advances in mass transfer and application in transesterification of 5-Hydroxymethylfurfural. *International Journal of Biological Macromolecules*, *170*, 583–592. https://doi.org/10.1016/j.ijbiomac.2020.12.178

Sampaio, C. S., Angelotti, J. A. F., Fernandez-Lafuente, R., & Hirata, D. B. (2022). Lipase immobilization via cross-linked enzyme aggregates: Problems and prospects – A review. Em *International Journal of Biological Macromolecules* (Vol. 215, p. 434–449). Elsevier B.V. https://doi.org/10.1016/j.ijbiomac.2022.06.139

Šavikin, K., Nasti´cnasti´c, N., Jankovi´c, T. J., Bigovi´cbigovi´c, D., Miličevi´c, B. M., Vidovi´cvidovi´c, S., Menkovi´c, N. M., & Vladi´cvladi´c, J. (2021). *Effect of Type and Concentration of Carrier Material on the Encapsulation of Pomegranate Peel Using Spray Drying Method*. https://doi.org/10.3390/foods

Sousa, R. R., Silva, A. S. A., Fernandez-Lafuente, R., & Ferreira-Leitão, V. S. (2021). Solvent-free esterifications mediated by immobilized lipases: A review from thermodynamic and kinetic perspectives. Em *Catalysis Science and Technology* (Vol. 11, Número 17, p. 5696–5711). Royal Society of Chemistry. https://doi.org/10.1039/d1cy00696g

Sun, Q., Wang, T., Zhan, X., Hong, S., Lin, L., Tan, P., Xiong, Y., Zhao, H., Zheng, Z., Bi, R., Liu, W., Wang, S., & Khim, J. S. (2023). Legacy and novel perfluoroalkyl substances in raw and cooked squids: Perspective from health risks and nutrient benefits. *Environment International*, *177*. https://doi.org/10.1016/j.envint.2023.108024

Taleb, M. A., Gomaa, S. K., Wahba, M. I., Zaki, R. A., El-Fiky, A. F., El-Refai, H. A., & El-Sayed, H. (2022). Bioscouring of wool fibres using immobilized thermophilic lipase. *International Journal of Biological Macromolecules*, *194*, 800–810. https://doi.org/10.1016/j.ijbiomac.2021.11.128

Verma, S., Meghwanshi, G. K., & Kumar, R. (2021). Current perspectives for microbial lipases from extremophiles and metagenomics. Em *Biochimie* (Vol. 182, p. 23–36). Elsevier B.V. https://doi.org/10.1016/j.biochi.2020.12.027

Wancura, J. H. C., Brondani, M., dos Santos, M. S. N., Oro, C. E. D., Wancura, G. C., Tres, M. V., & Oliveira, J. V. (2023). Demystifying the enzymatic biodiesel: How lipases are contributing to its technological advances. Em *Renewable Energy* (Vol. 216). Elsevier Ltd. https://doi.org/10.1016/j.renene.2023.119085

Wang, B., Adhikari, B., & Barrow, C. J. (2014). Optimisation of the microencapsulation of tuna oil in gelatin-sodium hexametaphosphate using complex coacervation. *Food Chemistry*, *158*, 358–365. https://doi.org/10.1016/j.foodchem.2014.02.135

Wang, B., Adhikari, B., Mathesh, M., Yang, W., & Barrow, C. J. (2019). Anchovy oil microcapsule powders prepared using two-step complex coacervation between gelatin and sodium hexametaphosphate followed by spray drying. *Powder Technology*, *358*, 68–78. https://doi.org/10.1016/j.powtec.2018.07.034

Wang, C. H., Doan, C. T., Nguyen, V. B., Nguyen, A. D., & Wang, S. L. (2019a). Reclamation of fishery processing waste: A mini-review. Em *Molecules* (Vol. 24, Número 12). MDPI AG. https://doi.org/10.3390/molecules24122234

Wang, C. H., Doan, C. T., Nguyen, V. B., Nguyen, A. D., & Wang, S. L. (2019b). Reclamation of fishery processing waste: A mini-review. Em *Molecules* (Vol. 24, Número 12). MDPI AG. https://doi.org/10.3390/molecules24122234

Xia, Q., Akanbi, T. O., Li, R., Wang, B., Yang, W., & Barrow, C. J. (2019). Lipase-catalysed synthesis of palm oil-omega-3 structured lipids. *Food and Function*, *10*(6), 3142–3149. https://doi.org/10.1039/c9fo00668k

Xia, Q., Akanbi, T. O., Wang, B., Li, R., Liu, S., & Barrow, C. J. (2020). Investigation of enhanced oxidation stability of microencapsulated enzymatically produced tuna oil concentrates using complex coacervation. *Food and Function*, *11*(12), 10748–10757. https://doi.org/10.1039/d0fo02350g

Zhang, J., Wang, Z., Zhuang, W., Rabiee, H., Zhu, C., Deng, J., Ge, L., & Ying, H. (2022). Amphiphilic Nanointerface: Inducing the Interfacial Activation for Lipase. *ACS Applied Materials and Interfaces*, *14*(34), 39622–39636. https://doi.org/10.1021/acsami.2c11500

Zhang, Z., Lee, W. J., & Wang, Y. (2020). Evaluation of enzymatic interesterification in structured triacylglycerols preparation: a concise review and prospect. Em *Critical*

Reviews in Food Science and Nutrition (p. 1–15). Taylor and Francis Inc. https://doi.org/10.1080/10408398.2020.1793725

Zhou, J., Lee, Y. Y., Mao, Y., Wang, Y., & Zhang, Z. (2022). Future of Structured Lipids: Enzymatic Synthesis and Their New Applications in Food Systems. Em *Foods* (Vol. 11, Número 16). MDPI. https://doi.org/10.3390/foods11162400

CAPÍTULO 5

Considerações finais

O resíduo do processamento do sisal foi utilizado como fonte precursora de carbono para a síntese de carvão ativado. Os parâmetros texturais demonstraram a formação de uma estrutura com área superficial e porosidade adequadas para a imobilização enzimática. Além disso, realizou-se a modificação de superfície através da incorporação de genipina, partículas metálicas utilizando o ácido iminodiacético como agente quelante e partículas metálicas utilizando genipina como agente reticulante. A modificação foi confirmada a partir de análises texturais, ponto de carga zero, Microscopia Eletrônica de Varredura e Espectroscopia no Infravermelho por Transformada de Fourier, onde observou-se uma redução na área superficial e porosidade em relação ao carvão ativado. Os materiais foram utilizados como suportes para a imobilização de lipases (Lipase do Pâncreas do Porco e *Candida rugosa*) e apresentaram alta eficiência de imobilização. Os biocatalisadores também demonstraram resultados promissores para a síntese de lactato de etila, onde o suporte metalizado apresentou os maiores valores para atividade de hidrólise e esterificação. Os derivados se mostraram viáveis comercialmente uma vez que apresentaram elevada estabilidade operacional a partir dos ciclos de reutilização. Além disso, a lipase imobilizada em carvão ativado foi aplicada com sucesso na produção de acilgliceróis de ômega-3 em um sistema livre de solventes por reação de glicerólise do óleo residual de lula. A microencapsulação por coacervação complexa do óleo enzimaticamente tratado mostrou elevada estabilidade oxidativa quando comparada ao óleo sem tratamento. Portanto, o carvão ativado do resíduo do sisal funcionalizado por diferentes métodos de modificação tem potencial para imobilização de lipase como um adsorvente sustentável de baixo custo através do reaproveitamento de resíduos agroindustriais para aplicação na obtenção de ingredientes alimentícios, como o lactato de etila e acilgliceróis de ômega-3.